Supplementary Information

Supplementary Discussion

One caveat of using Akt activator as a drug for neurological disorders is that hyperactivation of Akt signaling may induce cancer. Nevertheless, induction of cancer by elevating PtdIns(3,4,5)P3/Akt signaling is a progressive process and usually takes several months or even years. For example, in myeloid-specific PTEN knockout mice, we could not find any tumor until 3 months after the birth. When used as a suppressor of neuronal death caused by glutamate-excitotoxicity, Akt activator will only be given for several days, even several hours; thus it is unlikely that this type of treatment will lead to tumorigenesis. Interestingly, it was recently reported that activation of Akt1 decreases mammary epithelial cell migration, and Akt1 prevents an epithelial-to-mesenchymal transition that resembles events required for metastasis (1, 2). Another report showed that in some acute myeloid leukemia (AML), activation of Akt surprisingly reduced leukemic cell growth by inhibiting FOXO (3), suggesting that Akt activator can even potentially be used to treat certain cancers.

Akt is also a key enzyme involved in other processes such as cell migration, immune cell activation, embryonic development, hematopoetic and mesenchymal differentiation, and glucose homeostasis, thus SC79 may potentially be used to modulate cell function in other physiological and pathological situations such as wound healing, host defense, and blood glucose control in diabetes. For example, SC79 may have a potential benefit in regulating glucoregulatory responses and insulin sensitivity in type 1 and 2 diabetes. Phosphorylation and deactivation of GSK3b promotes glycogen synthesis resulting in decreased blood glucose. Akt-mediated GLUT4 translocation mediates glucose transport. GSK3b and FOXO also play a role in expression of genes in gluconeogenesis like G6Pase and PEPCK(4). In innate immunity, activating neutrophil functions by elevating PI3K/Akt pathway using PTEN inhibitor has been previously reported (5). SC79 may also offer similar effect by directly activating Akt. In addition, SC79 may also be effective in preventing myocardial infarction in heart attack, in which the acquired resistance to apoptosis is mediated at least in part by the sustained activation of Akt. Use of SC79 could exert a wide range of cardio-protective effects in myocardial ischemia/reperfusion-induced injury, myocardial hypertrophy, hypertension and vascular diseases by suppressing cell death and inducing angiogenesis by regulating eNOS.

Supplementary Methods

A cell-based screening system for detection of Akt plasma membrane translocation.
Activation of PtdIns(3,4,5)P3/Akt pathway relies on PtdIns(3,4,5)P3-mediated plasma membrane translocation of Akt. To visualize the Akt membrane translocation in intact cells, we used the PH-domain of Akt (PH_{Akt}) fused with green fluorescent protein (PH_{Akt}-GFP) as a marker for this event. The 120 amino acids PH domain is from human Akt1 and specifically bind to PtdIns(3,4,5)P3. Overnight starvation in serum-free medium abolished PH_{Akt}-GFP membrane localization in unstimulated cells (Figure S1). Subsequent PH_{Akt}-GFP membrane translocation was triggered by the addition of insulin growth factor (IGF) (100 ng/ml). In the experiment described in Figure S1, we utilized transient transfection to deliver PH_{Akt}-GFP construct. Although we were able to detect robust membrane translocation of PH_{Akt}-GFP, variable transfection efficiency and levels of recombinant protein expression could be problematic for high-throughput screening. To circumvent this problem, we generated a stable cell line expressing PH_{Akt}-GFP fusion protein. These cells were healthy and IGF-elicited PH_{Akt}-GFP membrane translocation could be easily detected as described in Figure S1 (Figure S2). More

importantly, the expression level of PH_{Akt}-GFP fusion protein was almost the same in each individual cell, thus making the automatic imaging analysis feasible.

Screening for inhibitors of Akt plasma membrane translocation.

To validate our cell based assay for high throughput screening, we first conducted a pilot screening using a bioactive compound library (approximately 3000 compounds). The screening was performed at the Institute for Chemistry and Cell Biology (ICCB) at Harvard Medical School. Every step of the experiment was handled in a high throughput mode (Figure S3). Based on our preliminary data, we incubated cells which have been serum-starved (0.1% serum) for overnight with chemical compounds for 30 min before inducing PH_{Akt}-GFP membrane translocation with IGF. Our goal is to identify compounds which directly inhibit PtdIns(3,4,5)P3/Akt signaling pathway. Thus, we chose to use short incubation time to exclude compounds which indirectly block GFP-PH membrane translocation (e.g. via affecting transcription or translation). From the pilot screening, we identified 21 positive hit compounds (Figure S4 and Table S1). As expected, several known PI3 kinase inhibitors and compounds that nonspecifically inhibit PI3 kinase activity were identified as positive hit compounds, validating our strategy and method for high throughput screening.

We then carried out the high throughput screening using several synthetic compound libraries. The ICCB compounds are from a variety of sources including commercial libraries from ChemBridge, ChemDiv, Bionet, Maybridge, Peakdale, and CEREP, NIH-NCI collections, libraries that result from diversity-oriented organic synthesis (DOS), known bioactive compounds, and historic collections of compounds resulting from different synthetic strategies. When ICCB purchased compound libraries, they selected collections that are enriched for complex heterocyclic compounds and compounds of higher molecular weight (an average mw of ~350-400 Daltons) because these types of compounds are more likely to provide interesting hits in high throughput screens. In addition, they sought to minimize the number of potentially "bad" compounds, those with groups that might make them unstable or toxic. In particular, they eliminated unstable imines, compounds with free carboxyl groups, and compounds with building block elements that might chelate metals. Table S2 is a list of libraries used for current screening, which include more than 60,000 synthetic compounds.

The high throughput screening was performed twice to minimize the number of false positive hit compounds. From the first screening, we identified about 446 positive hit compounds and 125 of them were confirmed in the second screening (Table S3 and Figure S5). We later found that 25 of the positive compounds could generate auto-florescence and their effect on PH-Akt membrane translocation was in fact of the result of the greatly enhanced background florescence (Table S3).

Confirmation of the positive hits by time-lapse fluorescent imaging.

In this study, more than 60,000 chemical compounds were screened and it is difficult to titrate the optimal concentration of each compound. The compound stocks were stored at 5 mg/ml in DMSO. In our screen, 100 nl of compound stock was transferred into a 50 µl assay volume, resulting in a final concentration of 20 µM for a compound of 500 Daltons. This is a generally utilized concentration at ICCB. One potential problem of our screening assay is that the transferred compounds may not be able to diffuse evenly in each well due to the relatively short incubation time. Thus, the effect of some positive hit compounds on PH-Akt membrane translocation could be result of very high local concentration. In order to select the most potent compounds for further characterization, we conducted dose-ranging experiments using live cells cultured in 35-mm plate.

The initial 125 positive hit compounds identified after the second screening (**Figure S5**) were purchased from ChemBridge, ChemDiv, or Maybridge. The fresh stock solution was freshly prepared in DMSO (5 mg/ml). This stock solution was directly added to culture medium to yield three different final concentrations (4, 8, 16 µg/ml). For time-lapse live cell imaging, HeLa-PH-EGFP cells were plated into a 35-mm glass-bottom dish (MatTek) and cultured for 24 to 48 hours. Cells were serum-starved in 2 mL Leibovitz L15 medium for 1 to 2 h and the medium was replaced with 1 mL of fresh serum-free Leibovitz

L15 medium containing a desired concentration of each compound. After 30 min pre-incubation, IGF1 (5 ng/mL) was added and images were taken every 5 to 10 min under a 40× oil objective lens. The relative fluorescent intensity at the membrane versus adjacent cytoplasm was determined. The compounds that led to a greater than 75% inhibition of PH-EGFP membrane translocation at or below 16 μg/ml were identified and designated as the confirmed hits. The representative live images and structure of 55 confirmed hit compounds were shown in **Figure S6 and Figure S7.**

SC79-induced cytosolic phosphorylation of Akt analyzed by western blotting.
Hela cells were serum starved for 1 hr and treated with IGF (100ng/ml) or SC79 (4 μg/ml) for 30 minutes. Cells were lysed in Lysis buffer containing 250 mM Sucrose, 20 mM HEPES, 10 mM KCl, 1.5 mM MgCl2, 1 mM EDTA, 1 mM EGTA supplemented with protease inhibitors. Cells were passed through 25G needle several times and kept on ice for 20 minutes. Total cell lysate was taken at this point. Cell lysates were centrifuged at 100,000g for 30 minutes. Supernatant was collected as the cytosolic fraction . Pellet was washed with lysis buffer and represents the membrane fraction. Total cell lysate, cytosolic and membrane fractions were resolved by SDS-PAGE and analyzed for phospho-Akt (S473), Total Akt, Tubulin (cytosolic marker) and Orai1 (membrane marker) by western blotting.

MTT (3-(4,5-Dimethylthiazol-2-yl)-2,5-diphenyltetrazolium bromide) assay for cell viability.
HsSultan or NB4 cells (2.5×10^5) were plated in a 24-well plate in 500 μL of phenol red-free RPMI medium supplemented with 10% FBS. After incubation for 24 hours, each compound (8 μg/ml) was added and cultured for overnight (16–20 h). Fifty microliters of MTT solution (5 mg/mL in PBS) were added to each well. Following 2 hrs incubation, the purple formazan crystals were dissolved by directly adding in 500 μL of isopropanol with 0.1 M HCl to each well. After clearing the cell debris by centrifugation, the absorbance was measured at a wavelength of 570 nm.

***In silico* docking**
In silico docking calculations were carried out using AutoDock Vina (6) as described elsewhere (7). Three dimensional crystal structures of Protein Kinase B/Akt PH domain unbound form (RCSB PDB ID: 1UNR) and inositol-(1,3,4,5)-tetrakisphosphate (IP4) bound form (RCSB PDB ID: 1UNQ) were retrieved from Protein Data Bank corrected for bond order and orientation with application of proper protonation states used in docking experiments using MGLTools (v1.5.4) (8). Structural coordinates of ligand SC79 were generated using Sybyl sketcher module (9) and energy minimized using a standard Tripos forcefield (TRIPOS, St. Louis, MI) that employs Powell minimization and simplex optimization with the distance dielectric function and an energy gradient of 0.05 Kcal/Mol Å with application of Gasteiger charges. Docking of SC79 onto proteins 1UNR and 1UNQ was carried out with similar grid dimension of 100 Å × 100 Å × 100 Å. A local optimization and exhaustive search was carried out by docking algorithm to find and cluster best docked poses of SC79 onto protein structures. Similar docking parameters were applied in both the cases. The best 9 lowest-energy docked poses were identified and analyzed. Ligand IP4 was also docked onto ligand free Akt PH domain structure. As a validation to the applied parameters, native ligand IP4 was redocked onto bound PH domain structure that resulted in binding to similar pocket with a RMSD of 0.9581Å. Figures were generated using program PyMOL (DeLano Scientific, LLC, San Carlos, CA, USA).

A flexible grid-based SC79-PH domain docking protocol defined 9 clustered poses for the PH domain bound to SC79. Figure 3D illustrates best docked pose of SC79 onto unbound PH domain that possessed ΔG of -5.6 kcal/mol. This pose identified residue Arg25 within binding site which exhibits numerous interactions with the ligand SC79 including hydrogen bond interaction. Results demonstrate that SC79 binds to the similar pocket in unbound PH domain structure as was reported a IP4 binding site in bound PH domain structure. This prompted us to investigate about the IP4 binding pocket in unbound PH domain. Interestingly, IP4 binding site resembles the SC79 binding site in unbound PH domain (Figure 3D, *left panel*). The SC79 and IP4 ligands compete with each other to occupy a similar binding

site onto PH domain. SC79 docking onto IP4 bound PH domain resulted in yielding alternate binding pockets of SC79 other than noted above (Figure 3D). Taken together, these docking analyses suggest that SC79 binds to PH domain. SC79 binding to IP4 bound PH domain may result in a weaker affinity complex.

Circular Dichroism (CD)
Far-UV CD (260-195 nm) was carried out at 25 °C on a Jasco-810 spectropolarimeter (Jasco, Easton, MD) purged with nitrogen gas. Data were acquired in 1-mm quartz cuvette with 1-nm bandwidth, 2-s response time, 10 nm/min scan speed, and four scans. Pure N-terminal 6His-tagged recombinant full length Human Akt1 was purchased from Millipore (www.millipore.com/catalogue/item/14-279). Chemically synthesized and purified SC79 was purchased from ChemBridge. Protein and ligand samples were prepared in 50 mM Tris pH 7.5, 150 mM NaCl. Akt1 was incubated with SC79 at 37 °C for 30 min. Data sets were acquired in duplicate. Percent secondary structure was determined using programs K2D (http://www.embl.de/~andrade/k2d.html) and K2D2 (http://www.ogic.ca/projects/k2d2/).

Neuronal cell cultures and Cytotoxicity Primary cortical or hippocampal neuronal cultures were prepared as previously described (10). To induce excitotoxicity, the cells were prewashed with Tris-buffered control salt (CSS) solution (120 mM NaCl, 5.4 mM KCl, 1.8 mM$CaCl_2$, 25 mM Tris-HCl, pH 7.4, and 15 mM glucose) and treated with CSS containing 50 μM glutamate for 40 min, followed by 4 hr recovery in regular culture medium. SC79 (4 μg/ml) was given 15 min before and during glutamate treatment. Toxicity was assayed 4 h after glutamate exposure by microscopic examination with computer-assisted cell counting. Total and dead cells were determined by nuclei staining with Hoechst (0.5 ng/ml) and propidium iodide (1 μg/ml), respectively. After 20 min incubation, the cells were examined under a fluorescence microscope with excitation at 360 nm. Cell death was determined as the ratio of dead-to-total cell number and quantified by counting 1,000 cells.

Permanent focal cerebral ischemia model
This study was conducted in accordance with the Animal Welfare Guidelines of Tokai University School of Medicine, Japan. The permanent focal cerebral ischemia was induced by middle cerebral artery occlusion (MCAO) essentially as described previously(11). Briefly, mice (C57 Black/6) weighing 17–25 g were anesthetized with 4% isoflurane/66% N_2O/30% O_2 and maintained with 1.5% isoflurane. Permanent focal ischemia was achieved as follows: a 2-mm hole was drilled at a site superior and lateral to the left foramen ovale to expose the left middle cerebral artery. The proximal portion of the left middle cerebral artery (MCA) was permanently occluded over a 1-mm segment distal to the origin of the lenticulostriate branches through the use of a bipolar coagulator (12). SC79 was injected intraperitoneally (0.04 mg/g mouse body weight) 5 min before permanent MCAO (Figure 4E). In another experiment, extra SC79 was injected (0.04 mg/g mouse body weight, once per hour for 6 hours) (Figure 4F).

Akt activation in the brain assessed by immunohistochemistry
The mouse brains were perfused from the apex of the heart with PBS and perfusion-fixed with 4% paraformaldehyde in PBS. They were then immersion-fixed overnight at 4°C in 4% paraformaldehyde with rocking and subsequently cryoprotected in 10% (2 hours), 15% (2 hours), 20% (2 hours), and 25% (overnight) sucrose in PBS at 4°C. The slices were then embedded in OCT compound (Miles Scientific) and quickly frozen in isopentane. Coronal frozen sections (10-μm) were prepared on a cryostat and stored at -80 °C until use. The frozen sections were thawed, washed three times in PBS, permeabilized with 0.1% Triton X-100/PBS at room temperature for 5 min, and then blocked in 5% skim milk/3% BSA/PBS for 60 min. Total and phosphorylated Akt/PKB were detected using anti-Akt and anti-Phospho-Akt (Ser473) antibodies (Cell Signaling,), respectively. The slides were incubated with primary antibodies (1:200) at 4 °C overnight, and with the secondary antibodies at room temperature for 2 h, and immunoreactivity visualized by the ABC method (10).

References

1. Yoeli-Lerner M, *et al.* (2005) Akt blocks breast cancer cell motility and invasion through the transcription factor NFAT. *Mol Cell* 20(4):539-550.
2. Manning BD, *et al.* (2005) Feedback inhibition of Akt signaling limits the growth of tumors lacking Tsc2. *Genes Dev* 19(15):1773-1778.
3. Sykes SM, *et al.* (2011) AKT/FOXO Signaling Enforces Reversible Differentiation Blockade in Myeloid Leukemias. *Cell* 146(5):697-708.
4. Wymann MP & Schneiter R (2008) Lipid signalling in disease. *Nat Rev Mol Cell Biol* 9(2):162-176.
5. Li Y, *et al.* (2011) Pretreatment with phosphatase and tensin homolog deleted on chromosome 10 (PTEN) inhibitor SF1670 augments the efficacy of granulocyte transfusion in a clinically relevant mouse model. *Blood* 117(24):6702-6713.
6. Trott O & Olson AJ (AutoDock Vina: improving the speed and accuracy of docking with a new scoring function, efficient optimization, and multithreading. *J Comput Chem* 31(2):455-461.
7. Sharma AK, *et al.* (Solution structure of the guanine nucleotide-binding STAS domain of SLC26-related SulP protein Rv1739c from Mycobacterium tuberculosis. *J Biol Chem* 286(10):8534-8544.
8. Sanner MF (1999) Python: a programming language for software integration and development. *J Mol Graph Model* 17(1):57-61.
9. SYBYL 8.0 TI, 1699 South Hanley Rd., St. Louis, Missouri, 63144, USA. (SYBYL 8.0, Tripos International, 1699 South Hanley Rd., St. Louis, Missouri, 63144, USA.
10. Luo HR, *et al.* (2003) Akt as a mediator of cell death. *Proc Natl Acad Sci U S A* 100(20):11712-11717.
11. Kawada H, *et al.* (2006) Administration of hematopoietic cytokines in the subacute phase after cerebral infarction is effective for functional recovery facilitating proliferation of intrinsic neural stem/progenitor cells and transition of bone marrow-derived neuronal cells. *Circulation* 113(5):701-710.
12. Zhang F & Iadecola C (1992) Stimulation of the fastigial nucleus enhances EEG recovery and reduces tissue damage after focal cerebral ischemia. *J Cereb Blood Flow Metab* 12(6):962-970.

Table S1. Positive hit bioactive compounds identified from the pilot screening.

Plate #	Well #	Name	Target or biological activity	Molecular formula	Molar weight	Source
500	E17	Ciprofloxacin hydrochloride	Antibiotics; Inhibit bacterial DNA rewind	C17N3O3F	312.99234	NINDS
500	F15	Econazole nitrate	Antifungal drug; Inhibit fungal cell membranes	C18H15N2OCl3	380.02496	NINDS
500	H18	Miconazole nitrate	Antifungal drug; Inhibit fungal cell membranes	C18H14N2OCl4	413.98596	NINDS
500	I15	Gossypol	Polyphenols; Inhibitor of dehydrogenases	C30H30O8	518.1939	NINDS
500	M20	Tamoxifen citrate	Competitive antagonist of estrogen receptor	C26H29NO	371.2248	NINDS
500	B13	Gentian violet	Antifungal and bactericidal agent	C25H30N31+	372.2439	NINDS
500	K11	Centrimonium bromide	Antiseptic agent; Cationinc surfactants	C19H42N1+	284.33173	NINDS
500	O8	Phenylmercuric acetate	Fungicide; Herbicide	C8H8O2Hg	338.023	NINDS
1362	I17	NSC-95397	Inhibitor of Cdc25 dual specificity phosphatases	C14H14O4S2	310.03336	BIOMOL
1362	K19	BAY 11-7082	Inhibitor of NF kappa B activation	C10H9NO2S	207.0354	BIOMOL
1362	N13	Wortmannin	Inhibitor of phosphoinositide 3 kinases	C23H24O8	428.1471	BIOMOL
501	E17	Merbromin	Antiseptic agent	C20O6Br2Hg2-	695.77686	NINDS
500	E16	Hexylresorcinol	Antiseptic and antihelmintic agent	C12H18O2	194.13069	NINDS
501	B08	Cetylpyridinium chloride	Antiseptic and antibacterial agent	C21H38N1+	304.3004	NINDS
1362	E19	Ro 31-8220	Selective PKC inhibitor	C25H23N5O2S	457.15714	BIOMOL
1362	J07	Staurosporine	ATP-competitive protein kinase inhibitor	C28H26N4O3	466.53	BIOMOL
503	G17	Harmalol hydrochloride	Alkaloids from plants	C12H12N2O	200.09496	NINDS
502	D20	Celastrol	Antioxidant and anti-inflammatory agent	C28H36O4	436.2613	NINDS
1569	L10	Ellipticine	Anticancer agent;Binds to topoisomerase II	C17H14N2	246.11569	Prestwick
1362	F09	Quercetin dihydrate	Antioxidant flavonoid;Inhibitor of cAMP-phosphodiesterases	C15O7	291.9644	BIOMOL
1362	M5	LY294002	Inhibitor of phosphoinositide 3 kinases	C19H17NO3	307.343	BIOMOL

Table S2. Compound libraries used for primary and secondary screenings.

	Library name	# of Compounds	Plate Numbers	# of Plates
Bioactive	Biomol ICCB Known Bioactives	480	1361-1362	2
Compounds	NINDS Custom Collection	1,040	500-503	4
	Prestwick 1 Collection	1,120	1568-1571	4
	ChemBridge 3	19,560	1577-1606	30
Synthetic	ChemDiv 4	14,677	1607-1648	42
Compounds	Maybridge 5	3,212	1661-1670	10
	ChemDiv 3	16,544	1473-1519	47
	Maybridge 1	8,800	542-563	22
	Total number of chemicals	65433		

Table S3. Positive hit compounds identified from the primary and secondary screenings.

ID	Plate/Well #		Source	Reagent Source ID	Mol. Formula	Mol. Weight	PubChem CID	Autofluorescence	Toxicity	ID
SC1	545	H12	Maybridge	Maybridge BTB 06587	C_9NO_4	191	2799766			SC1
SC2	550	I05	Maybridge	Maybridge CD 08589	$C_9H_4N_5O_4SF_3$	335	2805154			SC2
SC3	550	O05	Maybridge	Maybridge CD 08635	$C_{16}H_{22}N_2O_2S_2$	338	2805164			SC3
SC4	554	P07	Maybridge	Maybridge KM 02595	$C_8H_{13}NO_2S_3$	251	2778657			SC4
SC5	554	P22	Maybridge	Maybridge KM 03776	$C_{12}H_{13}NO_3S_2$	283	2820297		*	SC5
SC6	558	H11	Maybridge	Maybridge RDR 03078	C6H12N2S2	176	167013; 167304; 123256; 105062; 522634; 313; 10313041			SC6
SC7	561	H02	Maybridge	Maybridge S 02113	$C_{14}H_{15}NO_2$	229	300890			SC7
SC8	561	K13	Maybridge	Maybridge RJC 03273	$C_7H_5O_2Br$	200	2729629			SC8
SC9	1476	B07	ChemDiv	ChemDiv 2548-0771	$C_{18}H_{19}NO_5$	329	4606022			SC9
SC10	1477	C02	ChemDiv	ChemDiv 3182-0185	$C_{13}H_{21}N_2S_2^{1+}$	269	5475033; 5749630; 102370; 7015549	*		SC10
SC11	1478	C16	ChemDiv	ChemDiv 3448-1880	$C_{18}H_{14}N_2O_5$	338	1917689; 703540; 1917688		*	SC11
SC12	1479	N21	ChemDiv	ChemDiv 3888-0510	$C_{17}H_{13}NO_3S$	311	5724532; 6740709; 5398661			SC12
SC13	1481	H17	ChemDiv	ChemDiv 4340-1702	$C_{21}H_{17}N_2O_3SBr$	456	1337448; 1337447		*	SC13
SC14	1481	H22	ChemDiv	ChemDiv 4379-0593	$C_{16}H_{12}N_2O_2S_4$	388	2194030	*	*	SC14
SC15	1483	O06	ChemDiv	ChemDiv 4663-0305	$C_{12}H_7O_2Br$	262	749613			SC15
SC16	1490	I04	ChemDiv	ChemDiv 6234-0158	$C_{17}H_{17}N_4S_2F$	360	7045555; 3357152; 7127443			SC16
SC17	1491	N08	ChemDiv	ChemDiv 6658-0003	$C_{23}H_{28}N_2O$	348	2952775; 961714; 961713		*	SC17
SC18	1491	N15	ChemDiv	ChemDiv 6623-0252	$C_{15}H_{17}NO$	227	781226; 2063512; 781227	*		SC18
SC19	1498	A09	ChemDiv	ChemDiv C301-2030	$C_{14}N_2OCl_2$	282	584802		*	SC19
SC20	1498	G02	ChemDiv	ChemDiv C301-3578	$C_{14}NO_2Cl$	249	768385			SC20
SC21	1498	I18	ChemDiv	ChemDiv C306-0545	$C_{25}HN_3O_2S$	407	6621759			SC21
SC22	1511	J19	ChemDiv	ChemDiv K788-0502	$C_{26}N_2O_2S$	404	4058887			SC22
SC23	1515	D07	ChemDiv	ChemDiv 7286-2245	$C_{15}H_{14}N_4O_3S$	326	970664			SC23
SC24	1515	M03	ChemDiv	ChemDiv E746-0124	$C_{18}H_{19}N_3O_2S$	337	6624952			SC24
SC25	1517	D06	ChemDiv	ChemDiv D053-0021	$C_{13}H_{11}N_3O_4SCl_2$	375	2987701		*	SC25
SC26	1577	C20	ChemBridge	5106399	$C_{13}H_9NO_4$	243	2192517			SC26
SC27	1577	D22	ChemBridge	5193093	$C_{10}H_7NOS$	189	1626686; 2832913		*	SC27
SC28	1578	B03	ChemBridge	5140994	$C_8H_8N_4$	160	6787450; 6863956; 5544086	*		SC28
SC29	1578	B09	ChemBridge	5214970	$C_{15}H_{17}NO$	227	781226; 2063512; 781227	*		SC29
SC30	1578	B15	ChemBridge	5216515	$C_{10}H_{13}O_2Br$	244	787529			SC30
SC31	1578	F19	ChemBridge	5260273	$C_{16}H_{23}NO_2$	261	792319; 792320; 2838039			SC31
SC32	1578	I07	ChemBridge	5115555	$C_{27}H_{35}N_5S$	461	6759337; 1377982; 5717379; 2828280	*		SC32
SC33	1578	N08	ChemBridge	5169046	$C_{11}H_{12}N_2O_2$	204	5569250; 6611042; 5718022			SC33
SC34	1579	C19	ChemBridge	5264570	$C_{16}H_{13}NO$	235	2177126; 2838279; 2177244			SC34
SC35	1579	E22	ChemBridge	5176963	$C_6H_5NS_3$	187	2832072		*	SC35
SC36	1579	F18	ChemBridge	5240810	$C_{10}H_8N_2O_4$	220	747593; 1911041; 1911042		*	SC36
SC37	1579	N16	ChemBridge	5240765	$C_{18}H_{14}N_2O_4$	322	6746064; 5417561; 5596031			SC37
SC38	1580	B08	ChemBridge	5317697	C_9HN_2OS	185	794582			SC38
SC39	1581	A12	ChemBridge	5431041	$C_{17}H_{18}NOF_3$	309	783606			SC39
SC40	1582	E17	ChemBridge	5710104	$C_8H_7NO_3$	165	869076; 96000; 11897671			SC40
SC41	1582	L14	ChemBridge	5459675	$C_{17}H_{21}NO_2$	271	11921442; 6456397; 11921441	*		SC41
SC42	1582	M19	ChemBridge	5718756	$C_{16}H_{13}N_5O_2S$	339	6745067; 5336479			SC42
SC43	1583	F15	ChemBridge	5735144	$C_{16}H_{12}N_2O_2$	264	869358; 869359; 2865647			SC43

SC44	1584	A21	ChemBridge	5787636	$C_{22}H_{27}NO_4$	369	5508822; 6758018; 5726290		SC44
SC45	1585	D07	ChemBridge	5809904	$C_{17}H_{12}N_2O_4$	308	1916528; 873244		SC45
SC46	1585	I05	ChemBridge	5943536	$C_{18}H_{12}N_2O_3S_2$	368	9586234; 2235899		SC46
SC47	1586	G16	ChemBridge	6274843	$C_{19}H_{14}N_3O_4S_2Cl$	447	1348278; 1348277; 2274928	*	SC47
SC48	1587	F16	ChemBridge	6598710	$C_{10}NOSCl_2$	252	759209		SC48
SC49	1588	G16	ChemBridge	6888464	$C_{18}H_{11}N_3O_6$	365	1323123		SC49
SC50	1590	I16	ChemBridge	7564073	$C_{14}H_{23}NO_3S$	285	623015		SC50
SC51	1593	E15	ChemBridge	7693384	$C_{15}H_{16}NOCl$	261	2948191; 828623; 828622		SC51
SC52	1593	O07	ChemBridge	7772407	$C_{17}H_{20}N_2O_3S$	328	2953048	*	SC52
SC53	1600	N13	ChemBridge	7992444	$C_{12}H_{16}N_2O_2$	220	2985018		SC53
SC54	1607	B19	ChemDiv	ChemDiv 0455-0021	$C_{13}H_{21}N_2O_2^{1+}$	237	4597466; 6160337	*	SC54
SC55	1607	K10	ChemDiv	ChemDiv 0149-0135	$C_{21}H_{28}O_3$	328	5239155		SC55
SC56	1607	M10	ChemDiv	ChemDiv 0157-0001	C_9O_2Cl	175	87326	*	SC56
SC57	1607	O08	ChemDiv	ChemDiv 0139-0206	$C_7H_3NO_2Cl_4$	273	676444		SC57
SC58	1614	A09	ChemDiv	ChemDiv 4767-1305	$C_{24}H_{26}N_2O_6S$	470	1009503; 1809094	*	SC58
SC59	1614	K07	ChemDiv	ChemDiv 4762-1092	$C_{20}H_{20}N_3O_2SF$	385	No ID		SC59
SC60	1617	H15	ChemDiv	ChemDiv 6383-0891	$C_{17}H_{18}N_3Cl$	299	975900	*	SC60
SC61	1617	K01	ChemDiv	ChemDiv 6177-0034	$C_{20}H_{20}N_2O_2$	320	7114457; 675011; 7114459; 5291898; 7114458; 2973216		SC61
SC62	1618	N08	ChemDiv	ChemDiv 7202-2080	$C_{20}H_{16}N_4O_4S_2$	436	22525620; 3318217; 5791770		SC62
SC63	1618	N18	ChemDiv	ChemDiv 7218-1489	$C_{13}H_{12}N_2O_2S_2$	292	22332416		SC63
SC64	1618	P08	ChemDiv	ChemDiv 7202-2246	$C_{16}H_9N_4O_3S_3$	401	24283764; 7728365		SC64
SC66	1621	D01	ChemDiv	ChemDiv C151-0032	$C_{18}H_{16}N_2O$	276	4137609; 6018993		SC66
SC67	1621	P05	ChemDiv	ChemDiv C151-0517	$C_{18}H_{17}N_3O$	291	702066; 2265242; 2265240		SC67
SC68	1621	P07	ChemDiv	ChemDiv C151-0796	$C_{15}H_{17}NO$	227	5050194		SC68
SC69	1622	C10	ChemDiv	ChemDiv C201-0114	$C_{11}N_2O_3$	208	No ID		SC69
SC70	1628	N07	ChemDiv	ChemDiv C700-1471	$C_{20}N_3O_3S$	362	20876818		SC70
SC71	1648	C05	ChemDiv	ChemDiv K906-4279	$C_{10}H_{12}N_2O$	176	20969907		SC71
SC72	1648	C13	ChemDiv	ChemDiv K939-0016	$C_{14}H_{10}N_2O$	222	5398228; 260652; 16039283		SC72
SC73	1648	M09	ChemDiv	ChemDiv K915-1566	C24H28N3O3Cl	441	3241960		SC73
SC74	1661	C05	Maybridge	Maybridge AW 00693	$C_{15}H_{14}N_4OClF_3$	358	2795918		SC74
SC75	1661	J01	Maybridge	Maybridge BTB 08680	$C_{17}H_{12}N_2O_3F_2$	330	2801021		SC75
SC76	1662	F06	Maybridge	Maybridge GK 03531	$C_{14}H_{11}N_6OF_3$	336	2809005; 9583713; 5714465		SC76
SC77	1662	J21	Maybridge	Maybridge GK 02921	$C_{14}H_{12}N_3O_2F_3$	311	2808617		SC77
SC78	1662	P03	Maybridge	Maybridge FM 00024	$C_{11}H_{15}NO_2$	193	11859264; 16100370; 2807445		SC78
SC79	1663	O19	Maybridge	Maybridge HTS 02701	$C_{17}H_{17}N_2O_5Cl$	364	6975756; 6975759; 6975757; 2810830; 6975758		SC79
SC80	1664	P13	Maybridge	Maybridge HTS 12963	C_8HN_2OS	173	173760		SC80
SC81	1668	B19	Maybridge	Maybridge SEW 03790	$C_{12}H_{12}O_4S$	252	591564		SC81
SC82	1668	D19	Maybridge	Maybridge SEW 03825	$C_8H_3N_2SCl$	194	2740505		SC82
SC83	1668	E07	Maybridge	Maybridge S 15443	$C_{11}N_2O_2$	192	2738086		SC83
SC84	1668	K16	Maybridge	Maybridge SEW 00543	$C_{10}H_9OSCl$	212	6925757; 6925758; 2739084		SC84
SC85	1669	D06	Maybridge	Maybridge SPB 05266	$C_{15}H_8N_4O_2Cl_2$	346	628891		SC85
SC86	1585	E12	ChemBridge	6082181	$C_{18}H_{16}N_4O_2S_2$	384	No ID		SC86
E1	1481	E10	ChemDiv	ChemDiv 4286-0237	$C_{18}H_{16}N_2O_2$	292	6620710; 5334000		E1
E2	1484	N01	ChemDiv	ChemDiv 4999-0666	$C_{18}H_{16}N_2O_4S$	356	16193244; 6620788	*	E2
E3	1607	N06	ChemDiv	ChemDiv 0645-0166	$C_{18}N_2O_2$	276	202512	*	E3
E4	1473	D13	ChemDiv	ChemDiv 0388-0143	$C_{18}H_{15}NO_2$	277	67273		E4

E5	1476	C14	ChemDiv	ChemDiv 2374-0075	$C_{21}H_{23}NO_2$	321	4533882; 11878901; 11878907; 11878905; 11878903	*	E5
E6	1487	A14	ChemDiv	ChemDiv 5701-0577	$C_{22}H_{25}NO_4$	367	4602281; 1854370	*	E6
E7	1624	O09	ChemDiv	ChemDiv C301-5476	C_9N_8O	236	3163523		E7
E8	1669	K04	Maybridge	Maybridge SPB 00784	$C_{20}H_{23}N_3OS$	353	2743318		E8
E9	1476	A20	ChemDiv	ChemDiv 2422-1298	$C_{18}NOS$	278	1730434; 744351	*	E9
E10	1477	M05	ChemDiv	ChemDiv 3062-0036	$C_{18}H_{23}NO_2S_2$	349	1514885; 1514884; 3071511		E10
E11	1481	I10	ChemDiv	ChemDiv 4286-0239	$C_{17}H_{14}N_2O_2$	278	14741964; 6620717	*	E11
E12	1580	H11	ChemBridge	5279826	$C_{11}O_2$	164	765984		E12
E13	1608	P13	ChemDiv	ChemDiv 1683-1038	$C_{17}N_2O_3S$	312	668008; 668009	*	E13
E14	1612	P06	ChemDiv	ChemDiv 4286-0232	$C_{16}H_{14}N_2O$	250	5339421; 5416091; 6801758	*	E14
E15	1639	B02	ChemDiv	ChemDiv E781-0267	$C_{17}H_{21}N_6OCl$	360	16456505		E15
E16	1669	O21	Maybridge	Maybridge SPB 00465	$C_{12}H_9N_2O_2SClF_2$	318	2743188		E16
E17	544	K16	Maybridge	Maybridge BTB 04176	$C_{15}H_{11}NOSCl_3F$	377	2798260		E17
E18	545	J10	Maybridge	Maybridge BTB 06548	$C_{17}H_{13}N_5O$	303	2799743		E18
E19	545	L09	Maybridge	Maybridge BTB 06196	$C_{13}H_9NOClF$	249	705916	*	E19
E20	550	M11	Maybridge	Maybridge CD 09133	$C_{10}H_{11}O_6S_3F_3$	380	2805283		E20
E21	554	A04	Maybridge	Maybridge KM 01302	C_9N_4O	180	2735244		E21
E22	1474	D07	ChemDiv	ChemDiv 1326-0389	$C_{17}H_{12}NO_2Cl$	297	598489		E22
E23	1502	O11	ChemDiv	ChemDiv C620-0170	$C_{19}H_{15}N_2O_2Br$	382	6622833		E23
E24	1517	D20	ChemDiv	ChemDiv D090-0079	$C_{14}H_{17}N_2Cl$	248	846381; 3138840; 846380		E24
E25	1577	A04	ChemBridge	5108485	$C_{17}H_{17}NO_2$	267	744328; 744324	*	E25
E26	1581	M02	ChemBridge	5406375	$C_{11}H_9NO_3$	203	5397103		E26
E27	1582	L05	ChemBridge	5402066	$C_{16}H_{11}NO_3$	265	5403890; 768328		E27
E28	1586	L12	ChemBridge	6717002	$C_{14}H_{14}NO_4S_2Br$	403	5733354; 2911684	*	E28
E29	1610	A10	ChemDiv	ChemDiv 3178-0151	$C_{17}H_{14}O_5$	298	743982		E29
E30	1624	B02	ChemDiv	ChemDiv C355-1313	$C_{21}N_4O_7S_2Cl$	519	No ID	*	E30
E31	1639	J17	ChemDiv	ChemDiv E771-0423	$C_{19}H_{23}N_3O$	309	20916544	*	E31
E32	1641	F12	ChemDiv	ChemDiv G017-4142	$C_{16}H_{22}N_2O_3S_3$	382	20937318		E32
E33	1642	I06	ChemDiv	ChemDiv G125-0751	$C_{25}H_{30}N_4O_2S$	450	20940800		E33
E34	1643	O03	ChemDiv	ChemDiv G278-0048	C17H21N3O2S	331	20947619		E34
E35	1645	D06	ChemDiv	ChemDiv K405-2825	$C_{16}H_{16}N_5Cl$	313	17017244		E35
E36	1647	M07	ChemDiv	ChemDiv K786-8481	$C_{25}N_5O_2Cl_2$	472	15994483		E36
E37	1663	E03	Maybridge	Maybridge HTS 01393	$C_{18}H_{19}N_3OF_4$	369	2810103; 7189247; 7189249		E37
E38	1669	A20	Maybridge	Maybridge SPB 02768	$C_{14}H_{15}N_2O_2SBr$	354	2744343		E38
E39	1669	K02	Maybridge	Maybridge SPB 00548	$C_{16}H_{14}N_3OSCl$	331	2743236		E39
E40	1669	P15	Maybridge	Maybridge SPB 04530	$C_{16}H_{15}N_3O_3S$	329	2745327		E40
E41	1670	C01	Maybridge	Maybridge SPB 07631	$C_{18}H_{19}NO$	265	2746994		E41

Table S4. Characterization of the confirmed positive hit compounds. [a] '+' indicates inhibition of membrane translocation greater than 75% of control.

[b] For morphological observation of adherent cells, HeLa cells were plated in 24-well culture dish and grown overnight in serum rich condition. Following chemical addition (8 μg/ml), the bright field images of live cells were taken at 30 min and 6 hr. '+' indicates chemicals that lead to morphological changes and/or detachment. For MTT-based cell viability assay for suspension cells, the readings (absorbance 570 nm) from triplicates were averaged and normalized against DMSO-treated group. The relative inhibitory activity was presented as following: +/- (0.9-1.16); + (0.75-0.90); ++ (0.60-0.75); +++ (0.45-0.60); ++++ (0.30-0.45); ++++ (0.15-0.30); ++++++ (<0.15).

ID	Membrane translocation assay [a]				Drug toxicity [b]						Effect on Akt phospharalation (-, no effect; +, inhibited)				
	PH_{Akt}-GFP			$PH_{PLC\delta}$-GFP	Cell morphology		MTT assay (16 hr treatment)				IGF-induced (4 ng/ml)			GPCR-mediated (HL60 cells)	
	High throughput screening		Live cell imaging	Live cell imaging	0.5 hr	6 hr	HsSultan cells		NB4 cells		HeLa	NB4	HsSultan	8 mg/ml	4 mg/ml
	First	Second													
SC2	+	+	+	-	-	-	0.13	++++++	0.19	+++++	+	+	+	+	-
SC3	+	+	+	-	-	-	0.76	+	0.79	+	-	+	+	-	+
SC4	+	+	+	-	-	-	0.25	+++++	0.28	+++++	+	+	+	+	+
SC5	+	+	+	-	-	+	0.12	++++++	0.20	+++++	+	+	+	+	+
SC7	+	+	+	-	-	-	0.13	++++++	0.32	++++	+	+	+	+	+
SC16	+	+	+	-	-	+	0.20	+++++	0.45	++++	+	+	+	+	+
SC17	+	+	+	-	-	+	0.12	++++++	0.19	+++++	+	+	-	-	-
SC25	+	+	+	-	-	+	0.13	++++++	0.20	+++++	+	+	+	+	-
SC26	+	+	+	-	-	-	0.13	++++++	0.84	+	+	+	-	+	-
SC30	+	+	+	-	-	-	0.73	++	0.69	++	-	+	-	+	-
SC31	+	+	+	-	-	-	1.05	+/-	1.02	+/-	+	-	-	+	+
SC33	+	+	+	-	-	-	0.89	+	1.16	+/-	-	-	-	-	-
SC35	+	+	+	-	-	+	0.14	++++++	0.33	++++	+	+	-	-	-
SC36	+	+	+	-	-	+	0.82	+	0.83	+	+	+	+	+	+
SC38	+	+	+	-	-	-	0.71	++	0.90	+/-	+	+	+	+	+
SC39	+	+	+	-	-	-	0.69	++	0.84	+	+	-	-	+	+
SC43	+	+	+	-	-	-	0.89	+	0.75	+	+	+	+	+	+
SC44	+	+	+	-	-	+	0.83	+	1.02	+/-	+	+	+	-	-
SC45	+	+	+	-	-	-	0.85	+	1.00	+/-	+	+	+	+	+
SC46	+	+	+	-	-	-	0.51	+++	0.37	++++	-	+	-	-	-
SC51	+	+	+	-	-	-	1.02	+/-	0.68	++	+	+	+	-	-
SC55	+	+	+	-	-	-	0.80	+	0.62	++	+	+	+	+	+
SC57	+	+	+	-	-	-	0.20	+++++	0.70	++	+	+	-	+	+
SC59	+	+	+	-	-	-	0.27	+++++	0.38	++++	-	-	-	+	-
SC62	+	+	+	-	-	-	0.32	+++++	0.27	+++++	+	-	-	+	+
SC64	+	+	+	-	-	-	0.27	+++++	0.25	+++++	+	-	-	-	-
SC69	+	+	+	-	-	-	0.90	+/-	0.96	+/-	+	+	+	-	-
SC74	+	+	+	-	-	-	0.74	++	0.26	+++++	+	+	+	-	-
SC75	+	+	+	-	-	-	0.97	+/-	0.99	+/-	+	+	+	-	-
SC79	+	+	+	-	-	-	0.90	+/-	0.83	+	increase	increase	increase	increase	increase
SC80	+	+	+	-	-	-	0.91	+/-	0.98	+/-	-	+	+	-	-
SC83	+	+	+	-	-	-	0.76	+	0.82	+	+	+	-	+	+
SC84	+	+	+	-	-	-	0.89	+	0.88	+	+	+	+	+	+
E7	+	+	+	-	-	-	1.02	+/-	0.96	+/-	+	+	-	+	+
E8	+	+	+	-	-	-	0.84	+	0.69	++	+	+	-	+	+
E10	+	+	+	-	-	-	0.61	++	0.44	++++	+	+	+	+	-
E12	+	+	+	-	-	-	0.36	++++	0.18	+++++	+	+	+	+	+
E17	+	+	+	-	-	-	0.80	+	0.74	++	+	+	+	+	+
E19	+	+	+	-	-	-	0.83	+	0.66	++	+	-	+	+	+
E20	+	+	+	-	-	-	0.57	+++	0.51	+++	-	-	-	+	+
E29	+	+	+	-	-	-	0.44	++++	0.35	++++	+	-	-	+	+
E40	+	+	+	-	-	-	1.05	+/-	0.94	+/-	+	+	+	+	+
SC1	+	+	+	-	-	-	0.13	++++++	0.27	+++++	-	+	+	+	+
SC11	+	+	+	-	-	+	0.27	+++++	0.41	+++	+	+	-	+	+
SC13	+	+	+	-	-	+	0.19	++++++	0.21	+++++	+	+	+	+	+
SC19	+	+	+	-	-	+	0.12	++++++	0.19	+++++	+/-	+	-	+	-
SC23	+	+	+	-	-	-	0.21	+++++	0.38	++++	+	+	-	+	-
SC27	+	+	+	-	-	+	0.14	++++++	0.35	++++	+	+	+	+	-
SC49	+	+	+	-	-	-	0.58	+++	1.08	+/-	+	+	+	+	+
SC63	+	+	+	-	-	-	0.69	++	0.83	+	+	+	+	+	+
SC66	+	+	+	-	-	-	0.15	++++++	0.40	++++	+/-	+	-	+	+
SC67	+	+	+	-	-	-	0.21	+++++	0.57	+++	-	-	-	+	+
SC86	+	+	+	-	-	-	0.55	+++	1.05	+/-	+/-	-	-	+	+
E26	+	+	+	-	-	-	0.88	+	0.92	+/-	+/-	-	+	+	+
WTM (100 nM)	+	+	+	-	-	-	0.94	+/-	0.84	+	+	+	+	+	+
DMSO	-	-	-	-	-	-	1	+/-	1	+/-	-	-	-	-	+

Table S5. The secondary structures of human Akt1 and its complex with SC79 were analyzed using circular dichroism (CD) spectroscopy.

	Akt1 (5mM)	Akt1+ SC79 (25 mM)	Akt1+ SC79 (50 mM)
% alpha-helix	30	25	26
% beta-sheets	16	19	18
% random coil	54	56	56
Sum (sec. structural content)	46	44	44
Random coil	54	56	56
% Loss in sec. structure upon SC79 binding		4.3	4.3

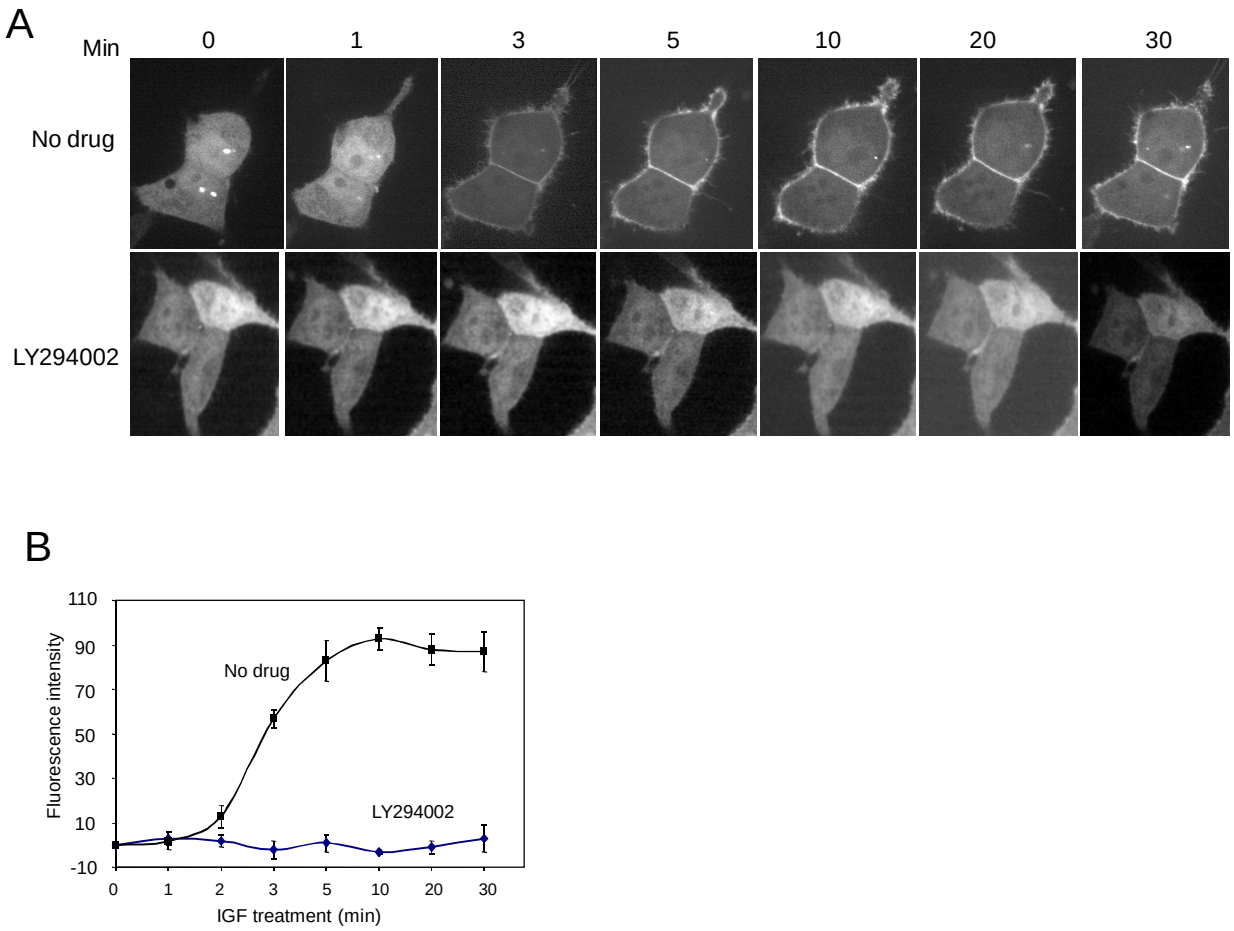

Figure S1. Insulin-like growth factor 1 -induced Akt plasma membrane translocation. Hela cells were transfected with a construct expressing the PH-domain of Akt fused with enhance green fluorescent protein (PH-EGFP). Using Lipofectamine 2000 reagent (Invitrogen), transfection efficiencies of >80% were routinely obtained. Cells were starved in serum free medium overnight and the Akt membrane translocation was triggered by IGF1 (final concentration 100 ng/ml). For LY294002 treatment, the drug (20 μM) was added to the culture medium 60 min before the IGF1 stimulation. **(A)** Confocal fluorescent images of PH-EGFP were captured at each of the indicated time points. Each experiment was repeated at least three times and virtually the same results were obtained each time. The figure shows the results of a representative experiment. **(B)** Quantitative analysis of the IGF1-elicited translocation of PH-EGFP. The average membrane fluorescence intensities in (A) were measured with IPLab software as previously described. The arbitrary number of the membrane fluorescence intensity in each individual cell was normalized to the total fluorescence intensity of the cell. Intensities from "0 min" frame was subtracted from each of the other frames and plotted as a function of time after IGF1 stimulation. The results are the means (± SD) of 20 transfected cells in three independent experiments.

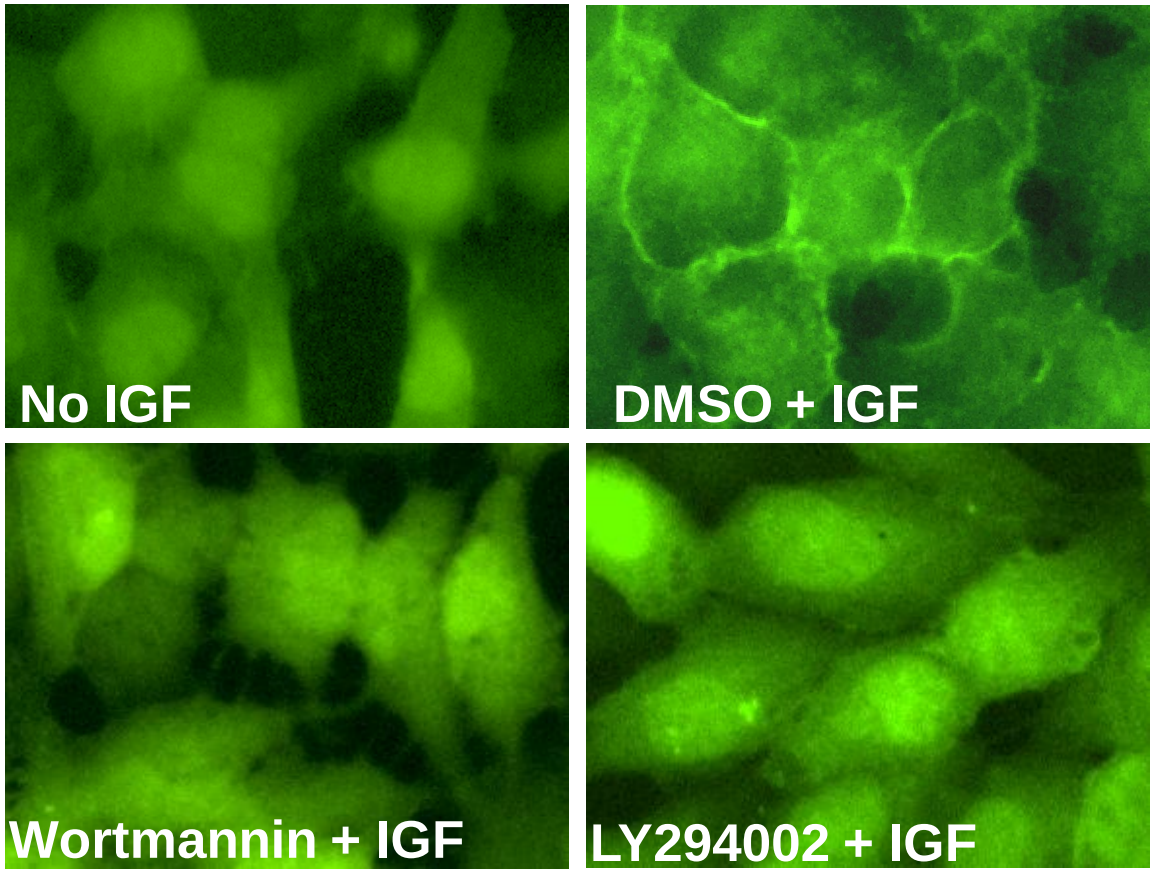

Figure S2. Generation of a stable HeLa cell line expressing Akt-PH-EGFP fusion protein. To generate a stable HeLa cell line, the plasmid containing PH-EGFP driven by chicken beta-globin promoter was co-transfected with pcDNA3.1. The transfected cells were selected in the presence of G418 (2 mg/ml) for two weeks, and the stable PH-EGFP expressing clones were isolated and maintaned in the medium containing G418 (200 mg/ml). The membrane translocation of PH-EFP, as described in Figure S1, was conducted in 384-well plate. Serum-starved cells were fixed in 3 % PFA (no IGF) or pre-treated with DMSO or PI3K inhibitors; wortmannin (200 nM) and LY294002 (20 mM) for 30 min and stimulated with IGF1 (100 ng/ml) for additional 15-30 min before fixation. Images were taken using a fully automated fluorescent microscope, Image Xpress Micro (Molecular Dynamics).

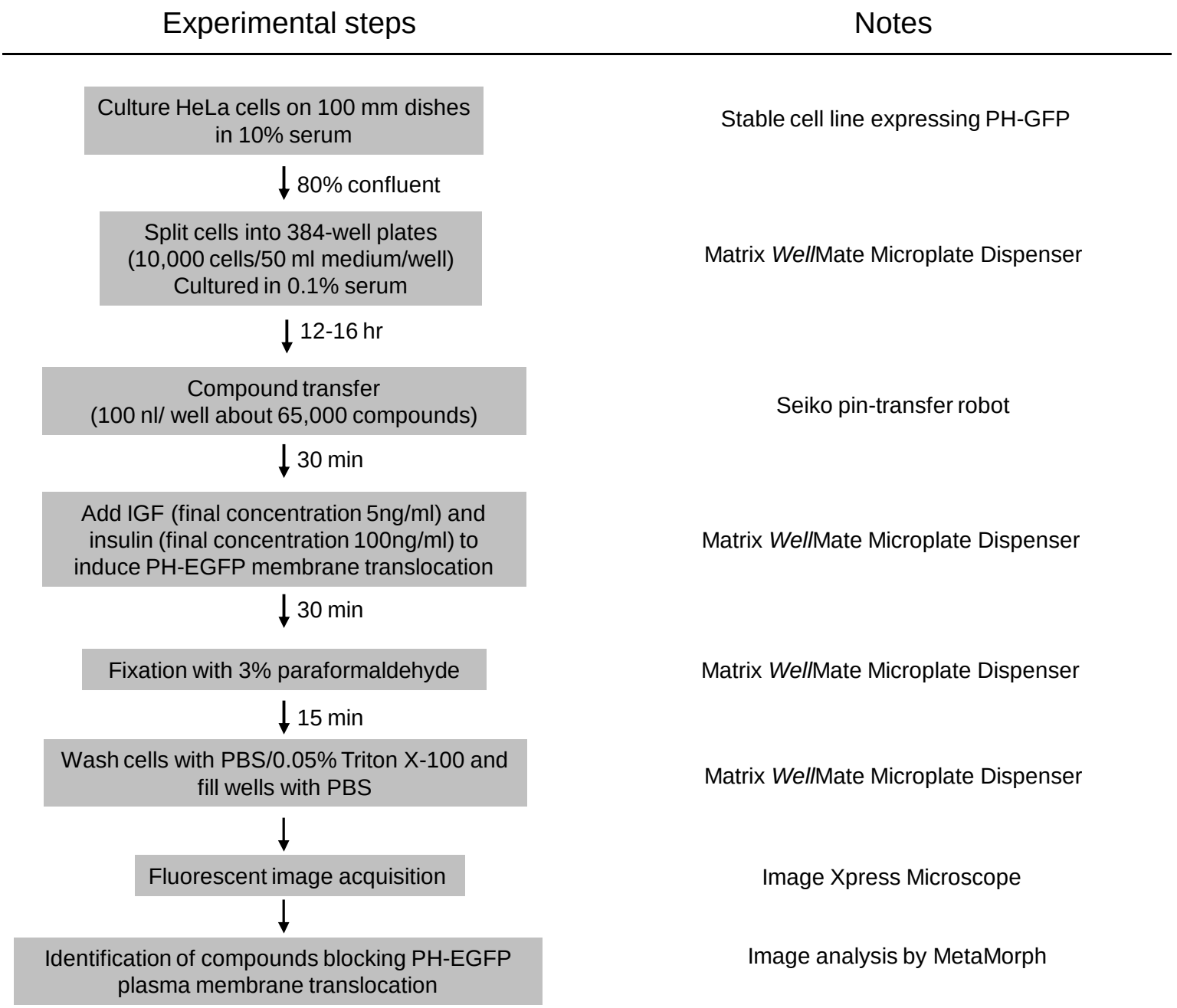

Figure S3. The flowchart of the cell-based high throughput screening for inhibitors of Akt plasma membrane translocation.

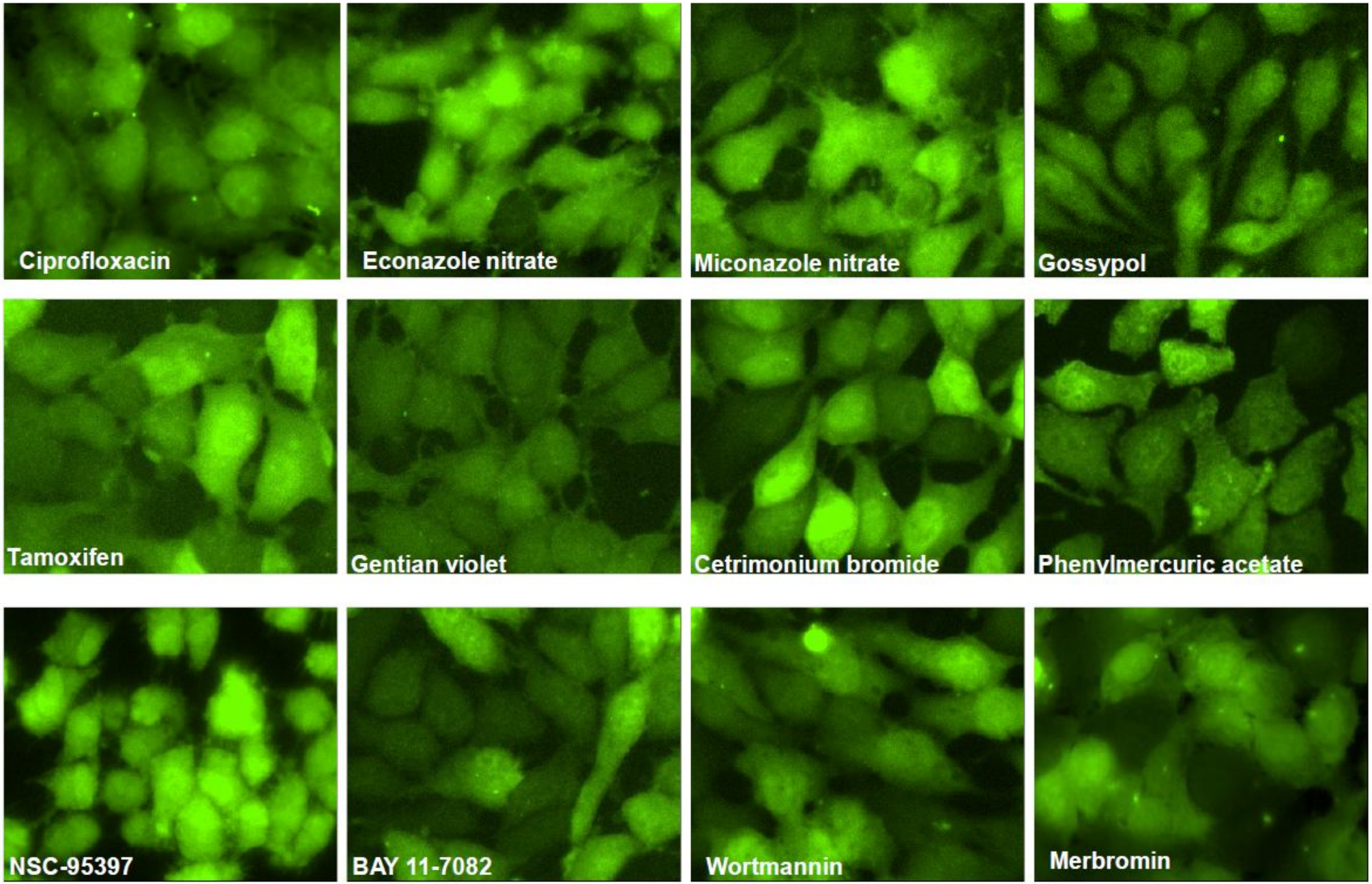
Ciprofloxacin
Econazole nitrate
Miconazole nitrate
Gossypol
Tamoxifen
Gentian violet
Cetrimonium bromide
Phenylmercuric acetate
NSC-95397
BAY 11-7082
Wortmannin
Merbromin

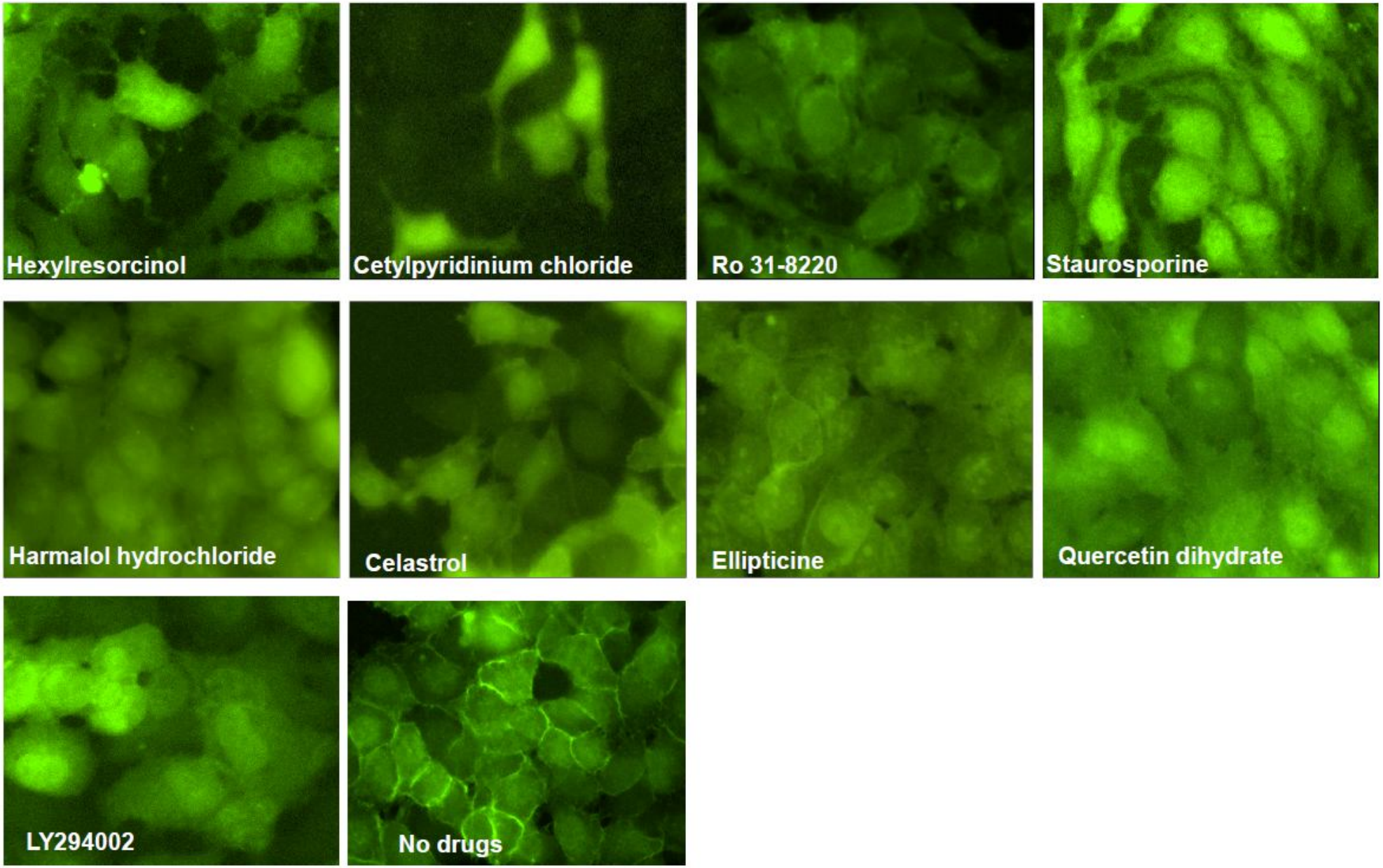

Figure S4. Pilot screening identified 21 bioactive compounds that inhibit IGF1-induced Akt-PH-EGFP membrane translocation.

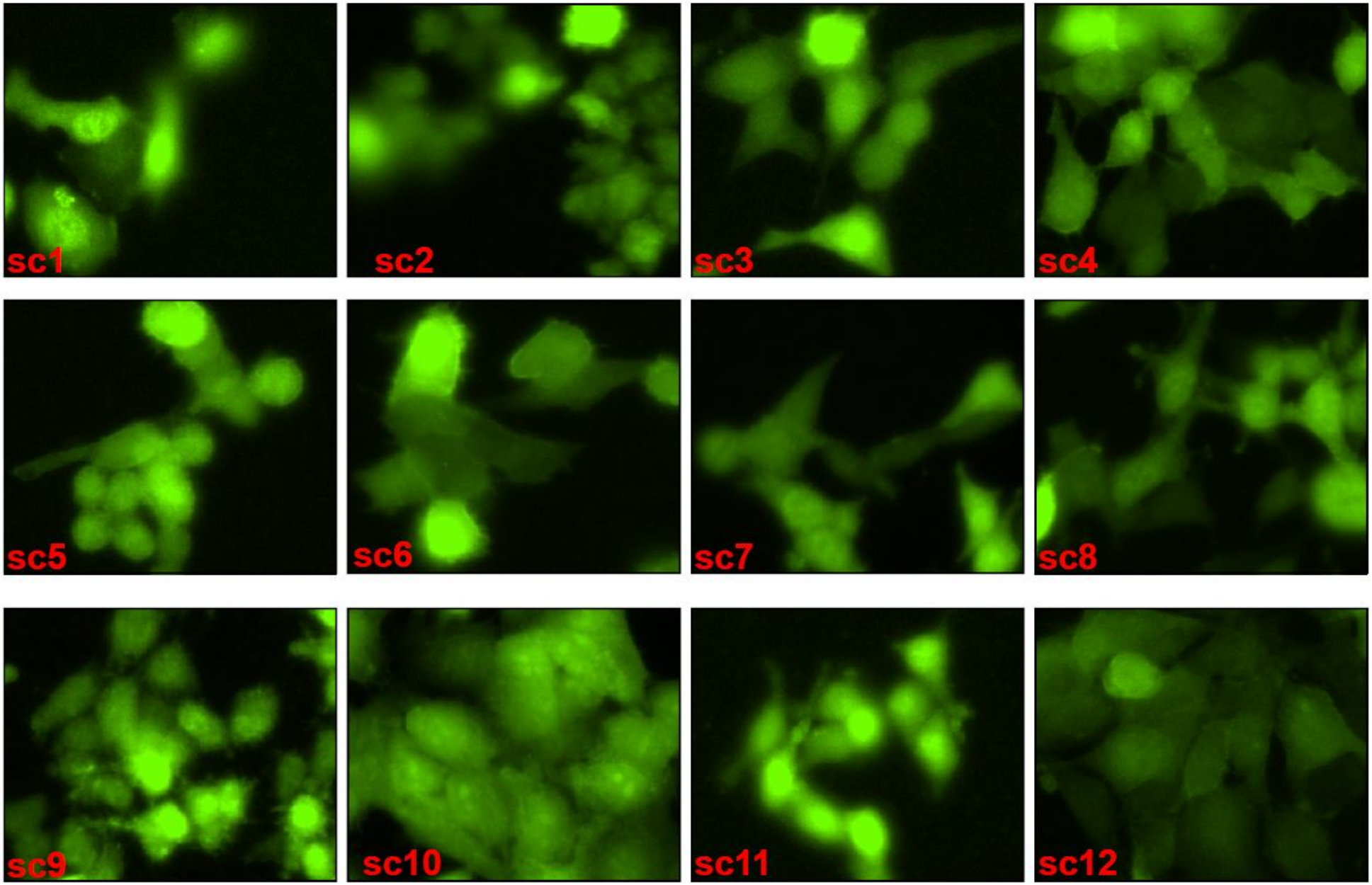
sc1
sc2
sc3
sc4
sc5
sc6
sc7
sc8
sc9
sc10
sc11
sc12

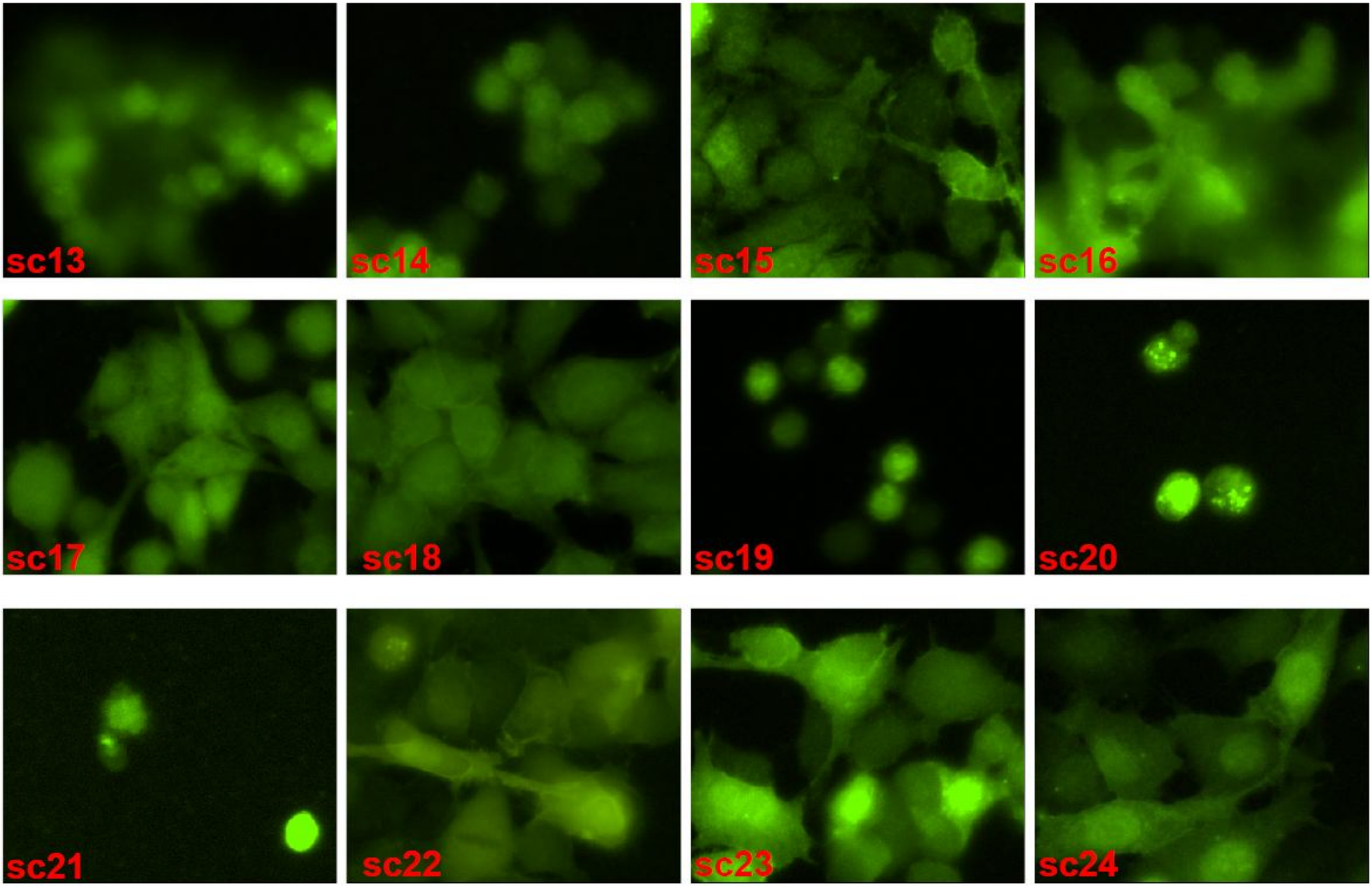
sc13
sc14
sc15
sc16
sc17
sc18
sc19
sc20
sc21
sc22
sc23
sc24

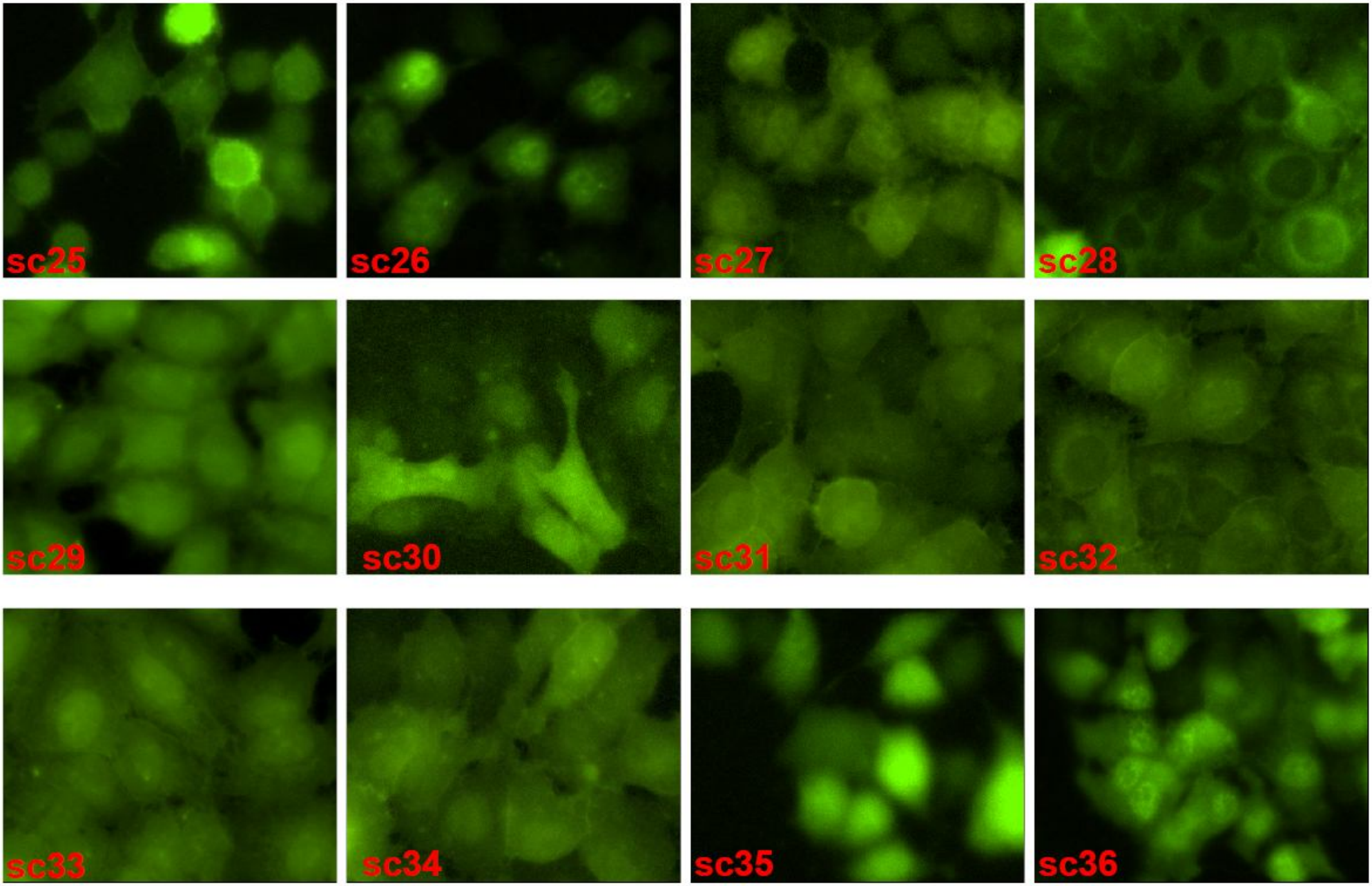
sc25
sc26
sc27
sc28
sc29
sc30
sc31
sc32
sc33
sc34
sc35
sc36

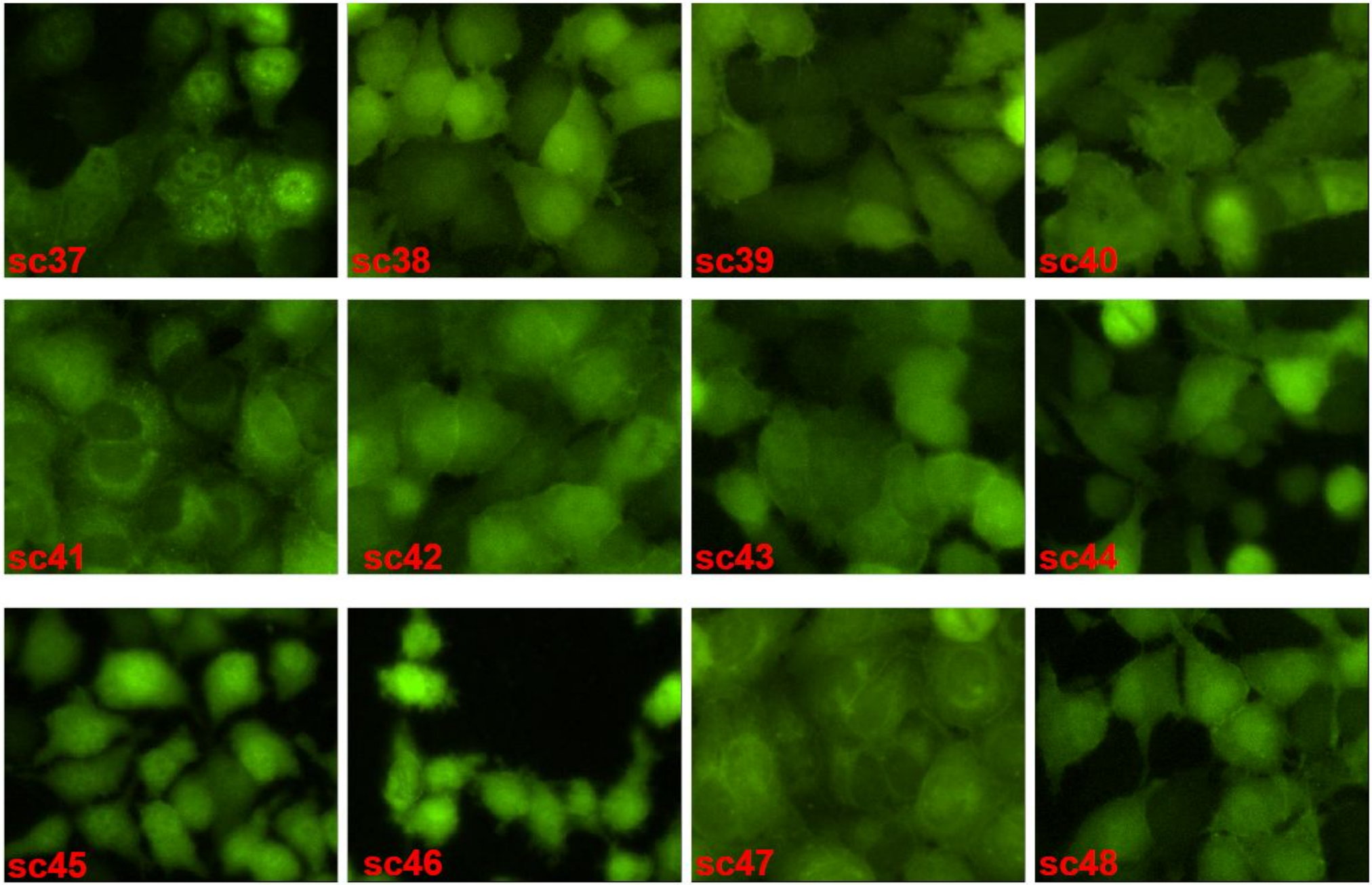
sc37
sc38
sc39
sc40
sc41
sc42
sc43
sc44
sc45
sc46
sc47
sc48

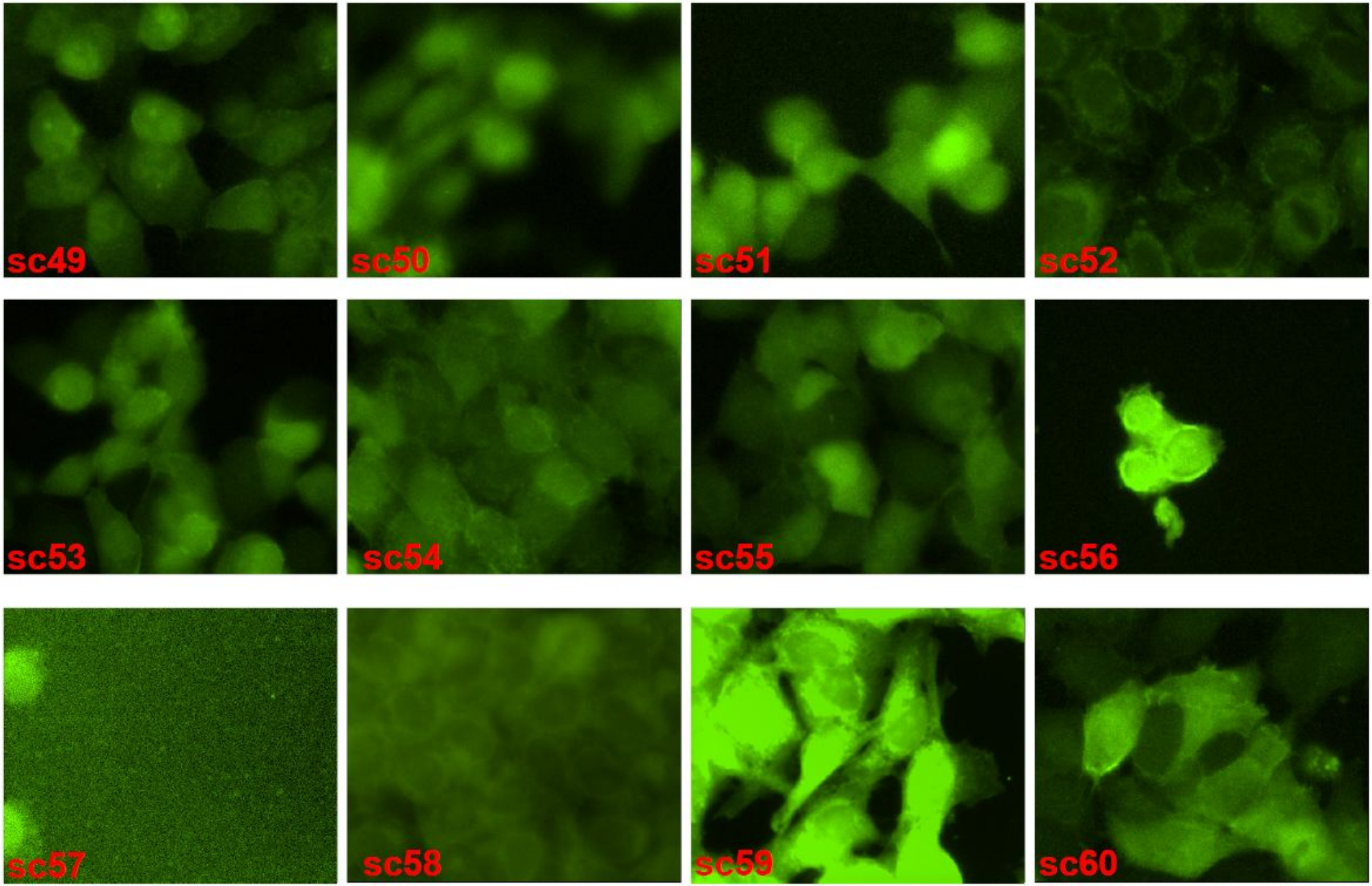
sc49
sc50
sc51
sc52
sc53
sc54
sc55
sc56
sc57
sc58
sc59
sc60

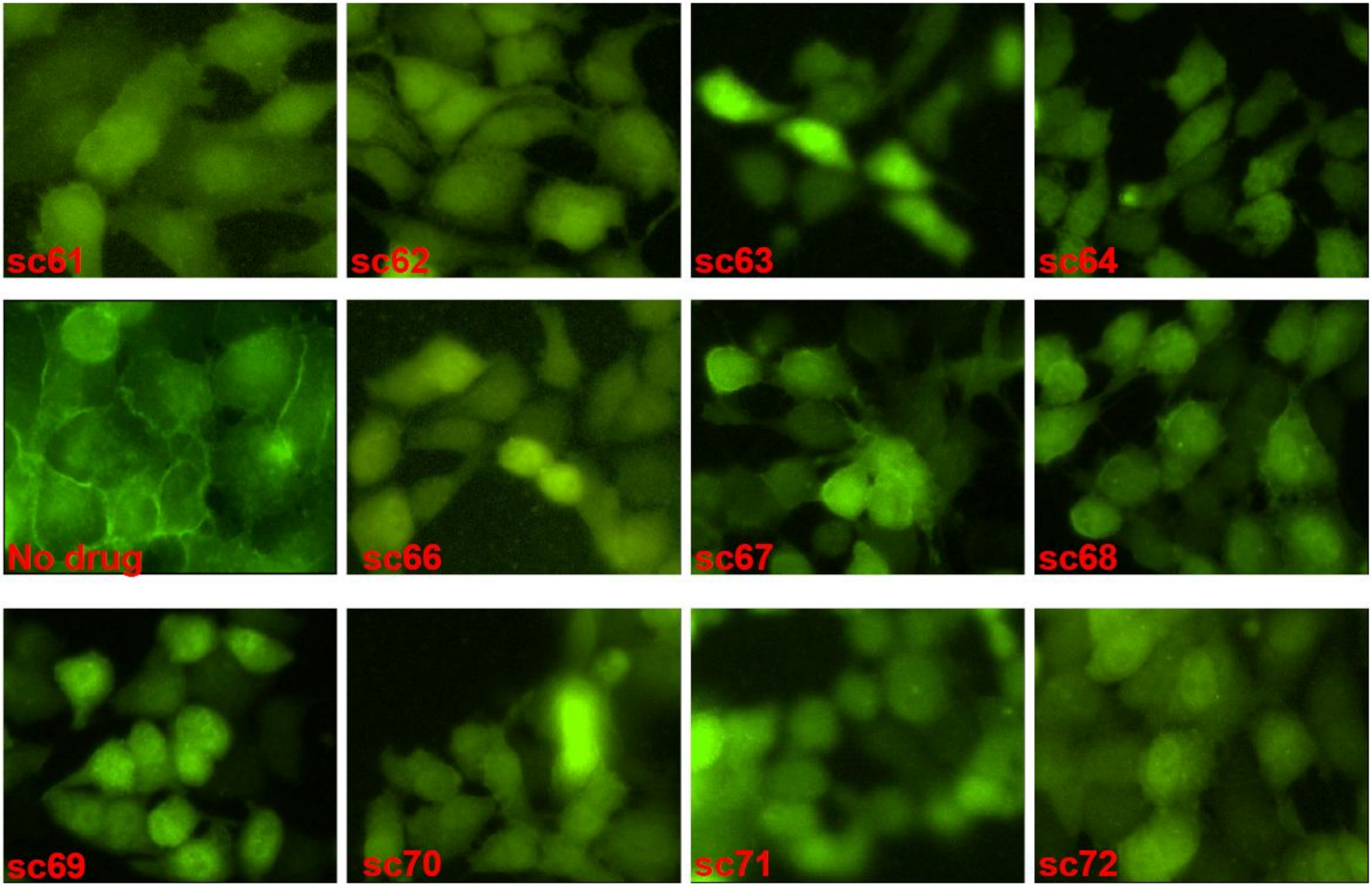
sc61
sc62
sc63
sc64
No drug
sc66
sc67
sc68
sc69
sc70
sc71
sc72

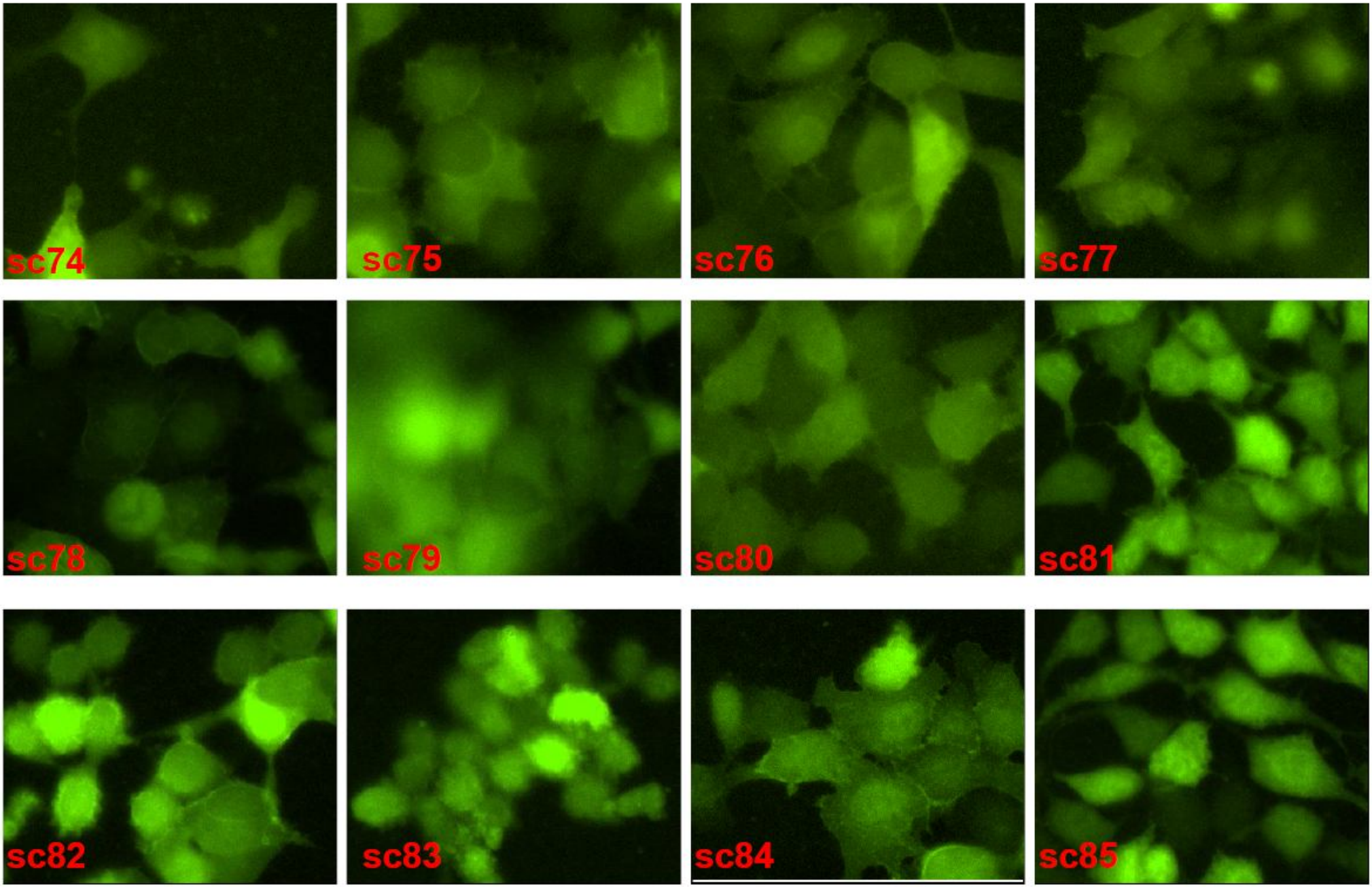
sc74
sc75
sc76
sc77
sc78
sc79
sc80
sc81
sc82
sc83
sc84
sc85

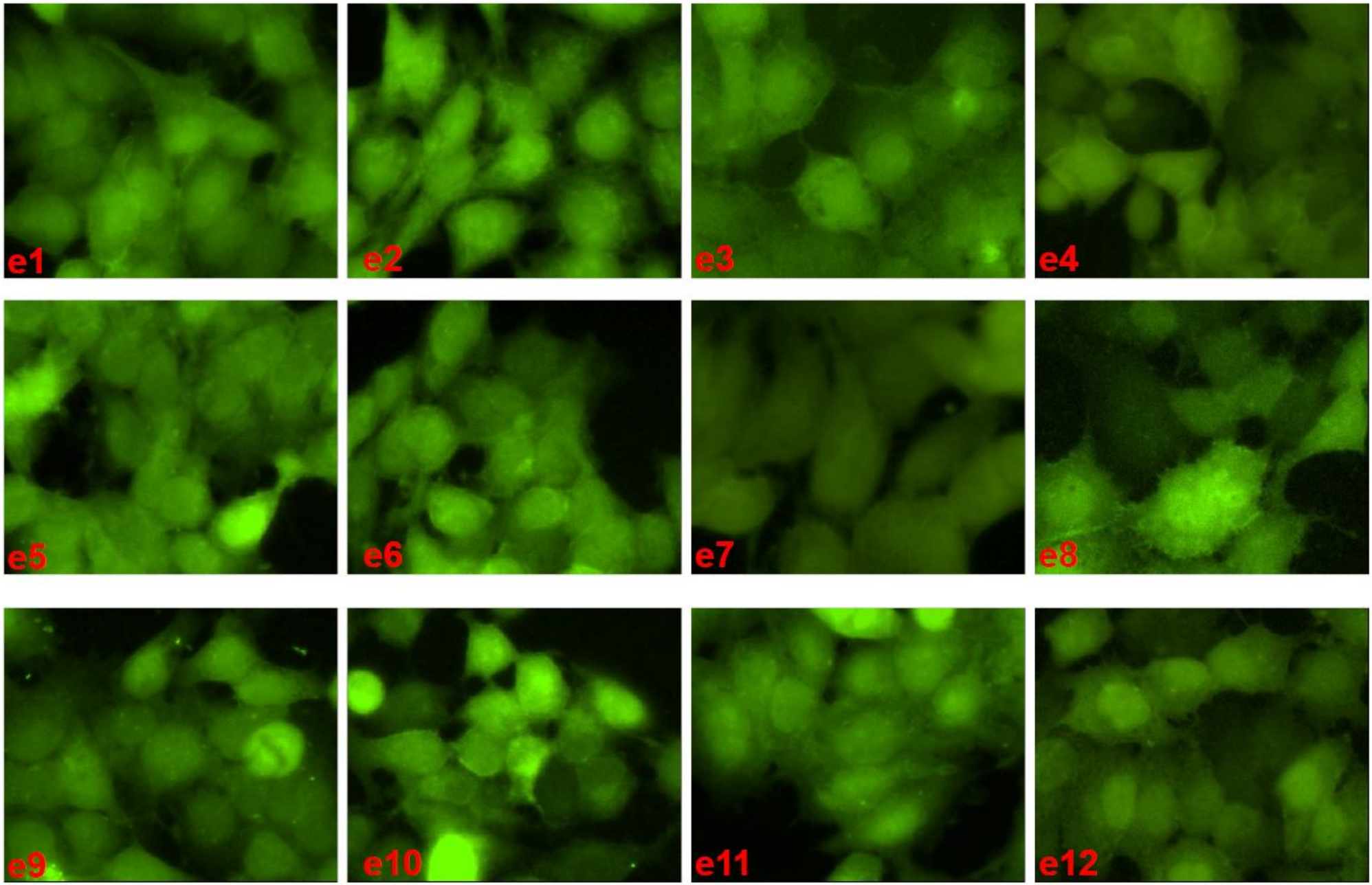
e1
e2
e3
e4
e5
e6
e7
e8
e9
e10
e11
e12

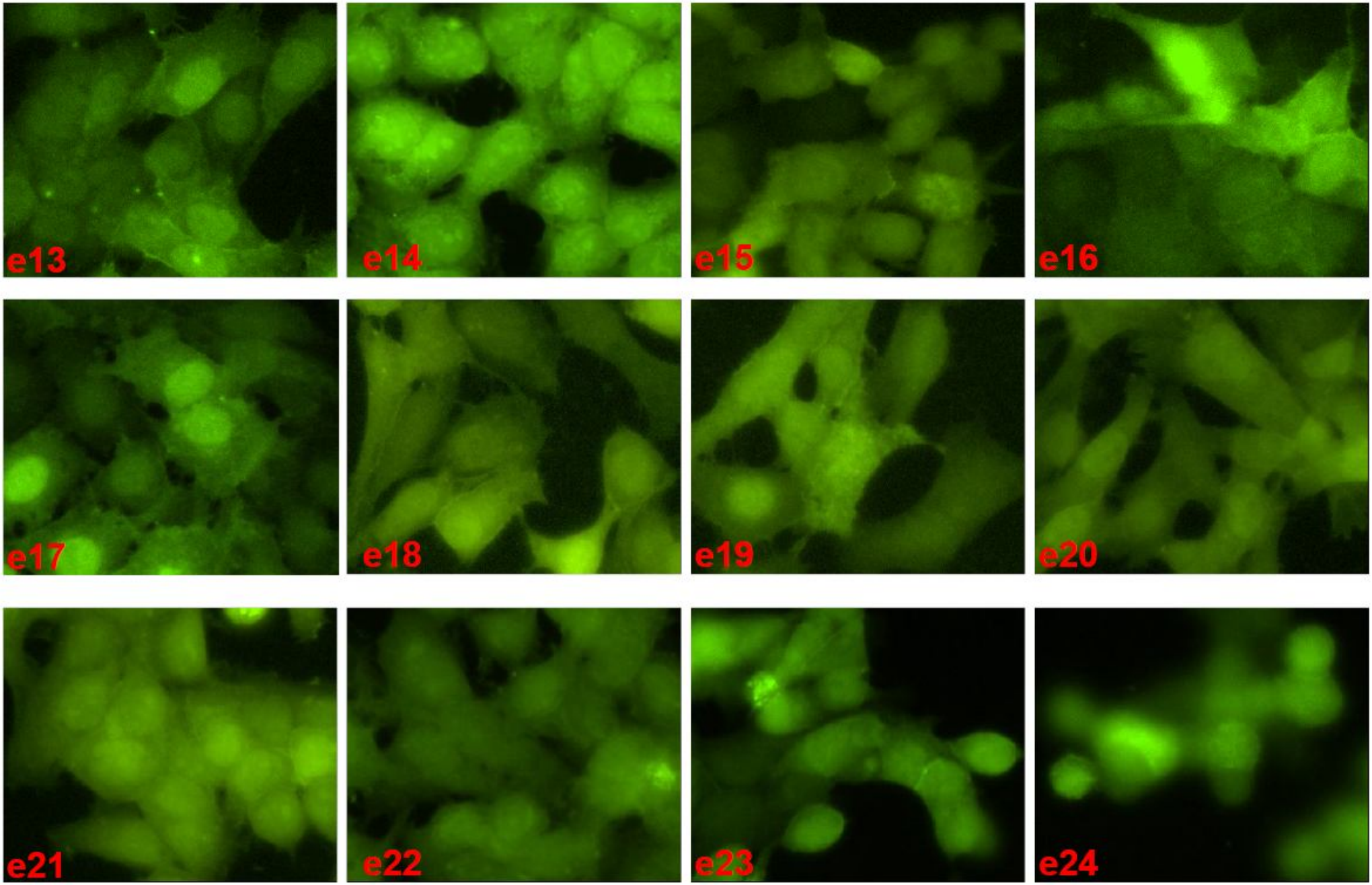
e13
e14
e15
e16
e17
e18
e19
e20
e21
e22
e23
e24

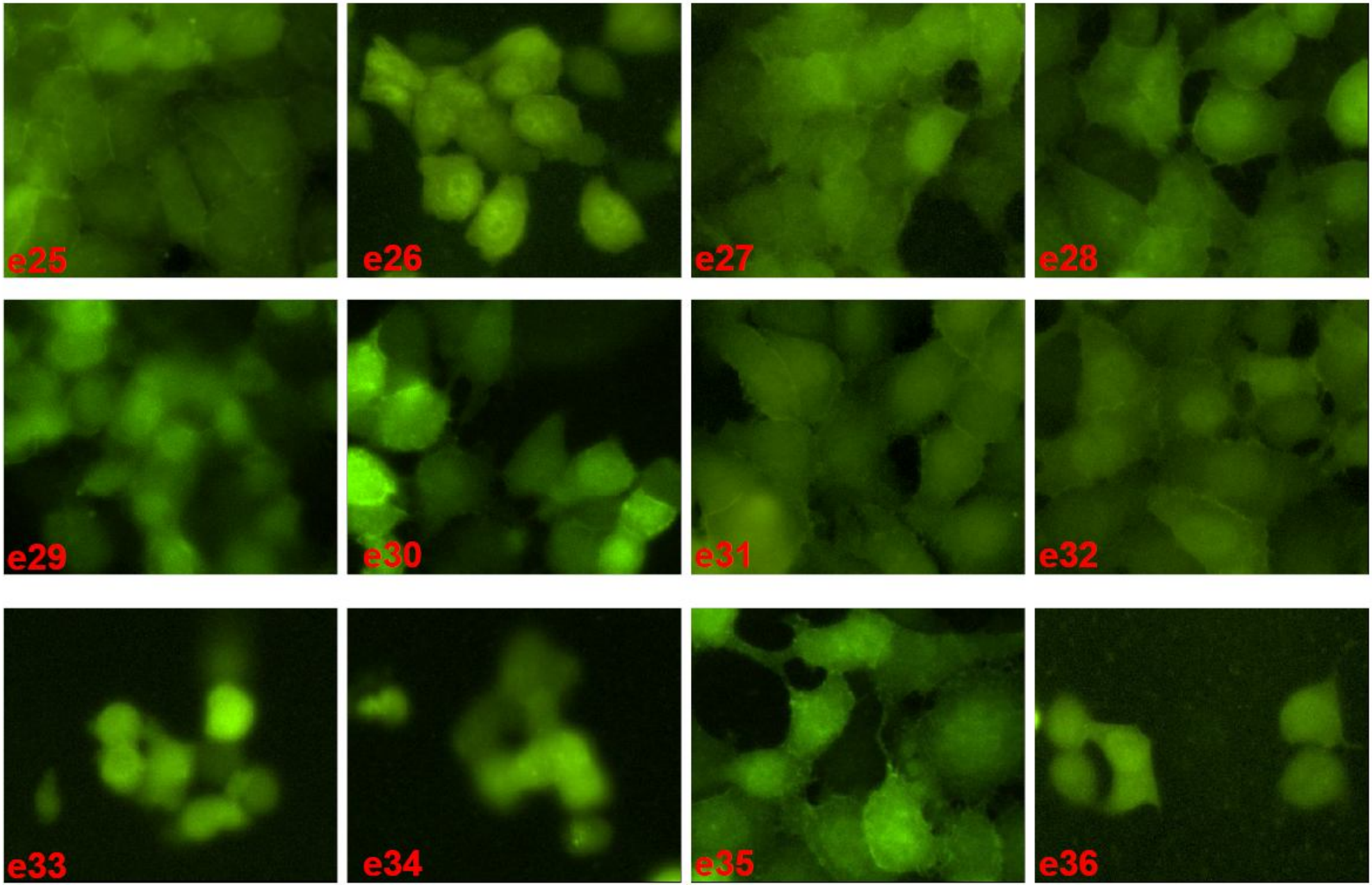
e25
e26
e27
e28
e29
e30
e31
e32
e33
e34
e35
e36

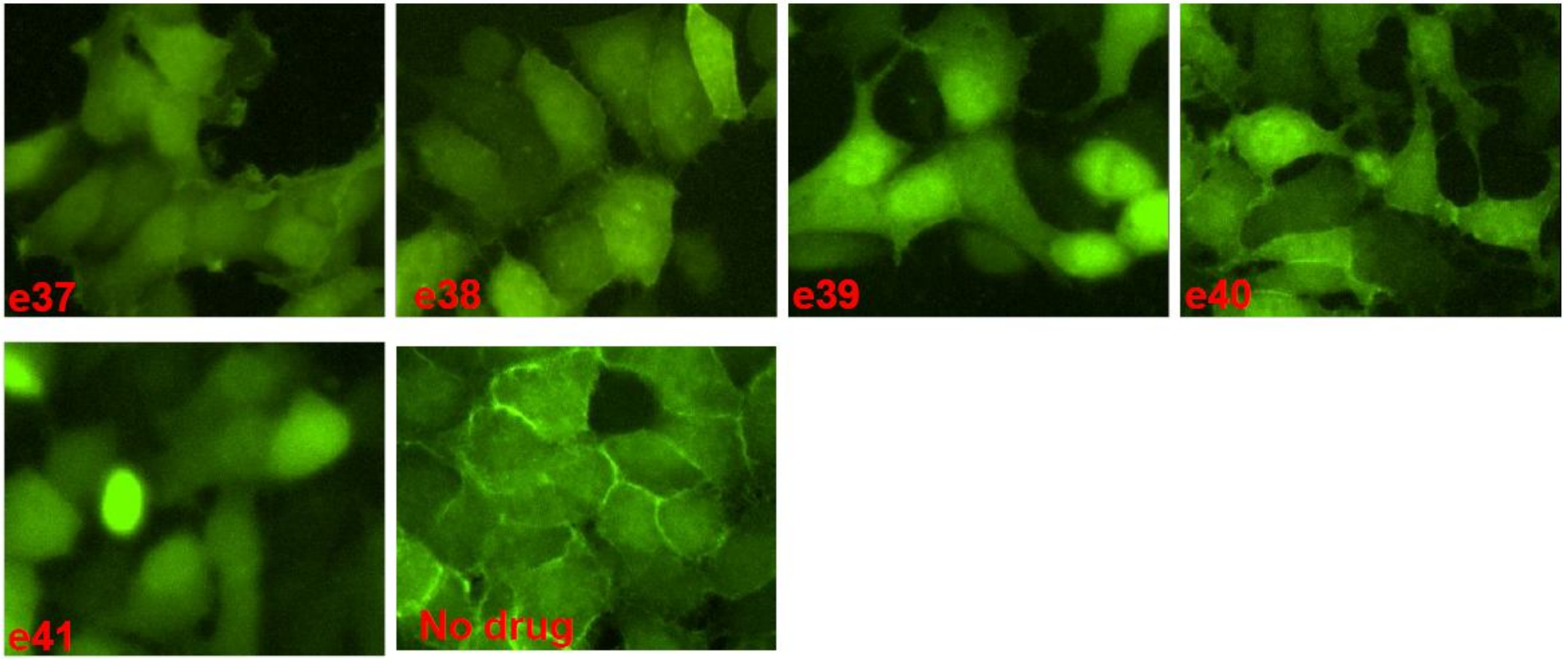

Figure S5. Positive hit compounds identified from the primary and secondary high throughput screenings.

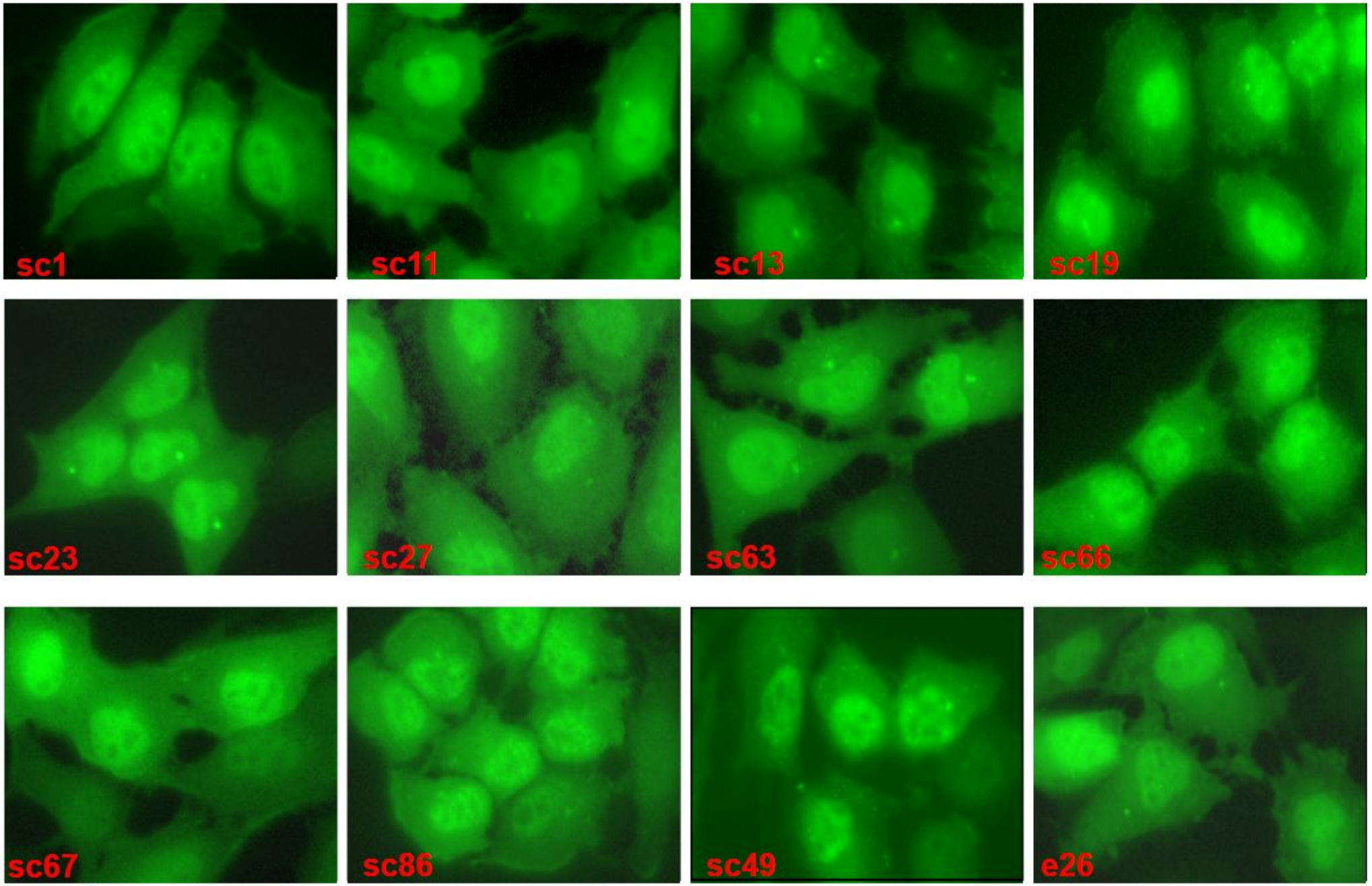
sc1
sc11
sc13
sc19
sc23
sc27
sc63
sc66
sc67
sc86
sc49
e26

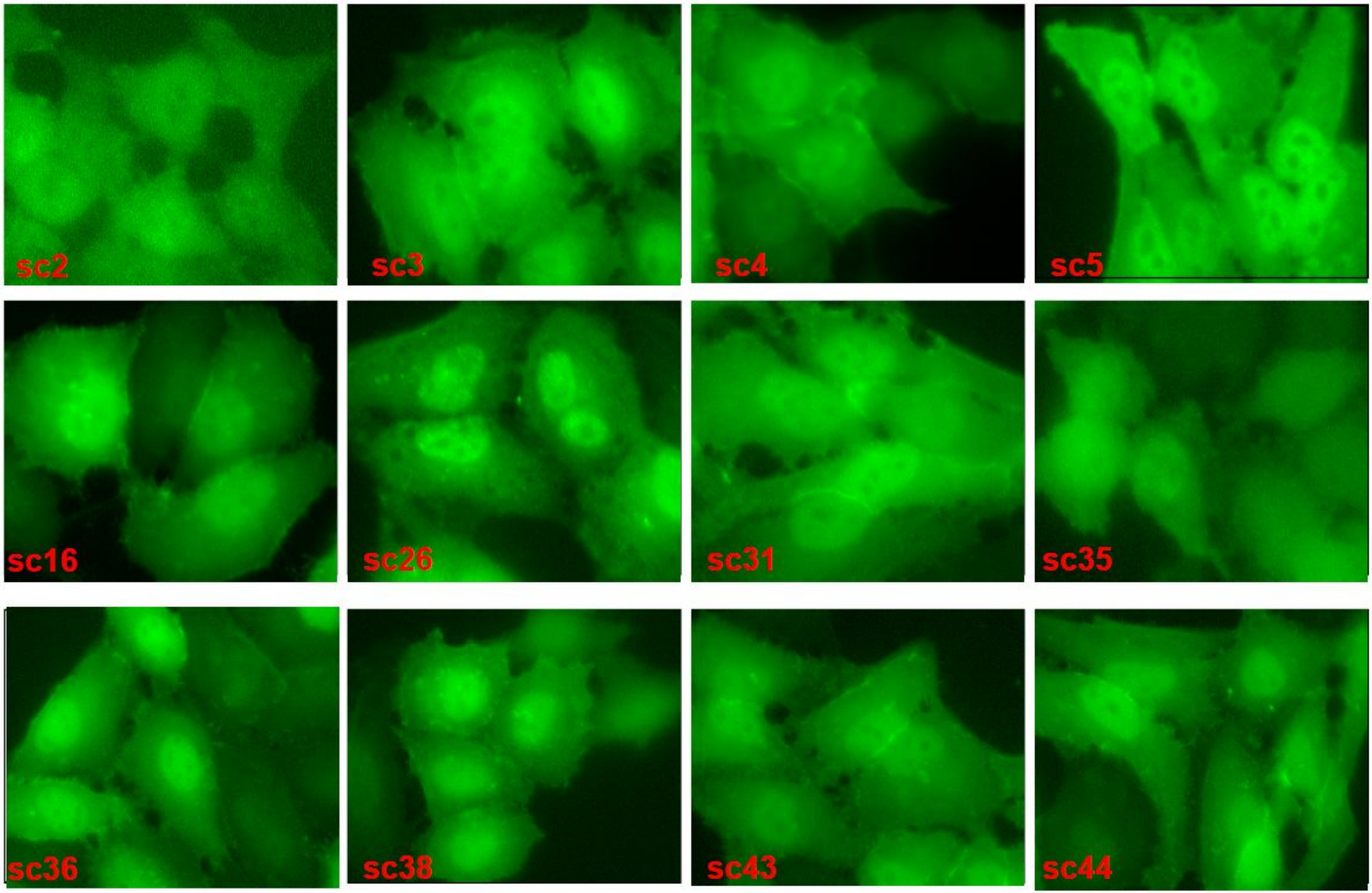
sc2
sc3
sc4
sc5
sc16
sc26
sc31
sc35
sc36
sc38
sc43
sc44

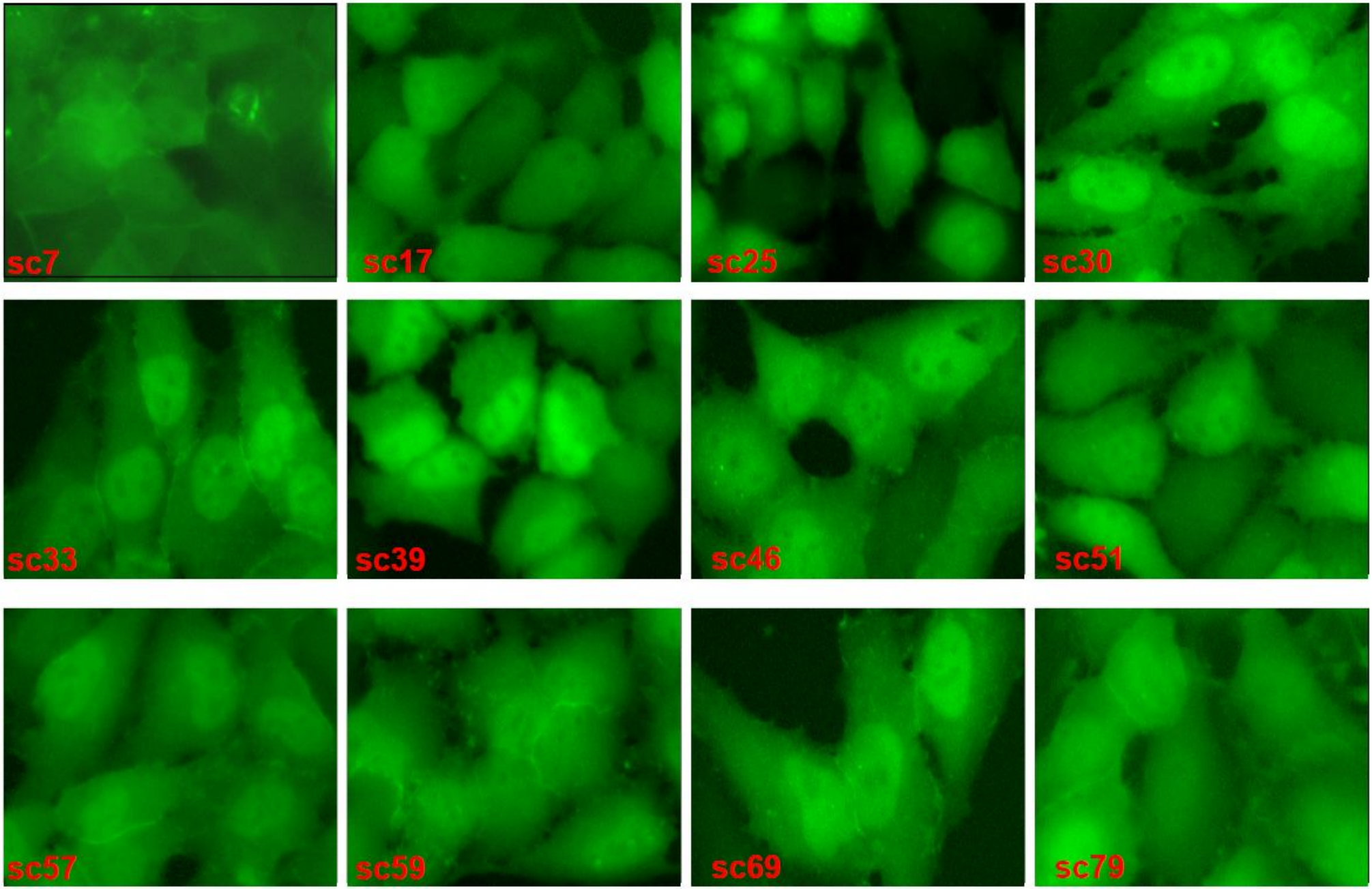
sc7
sc17
sc25
sc30
sc33
sc39
sc46
sc51
sc57
sc59
sc69
sc79

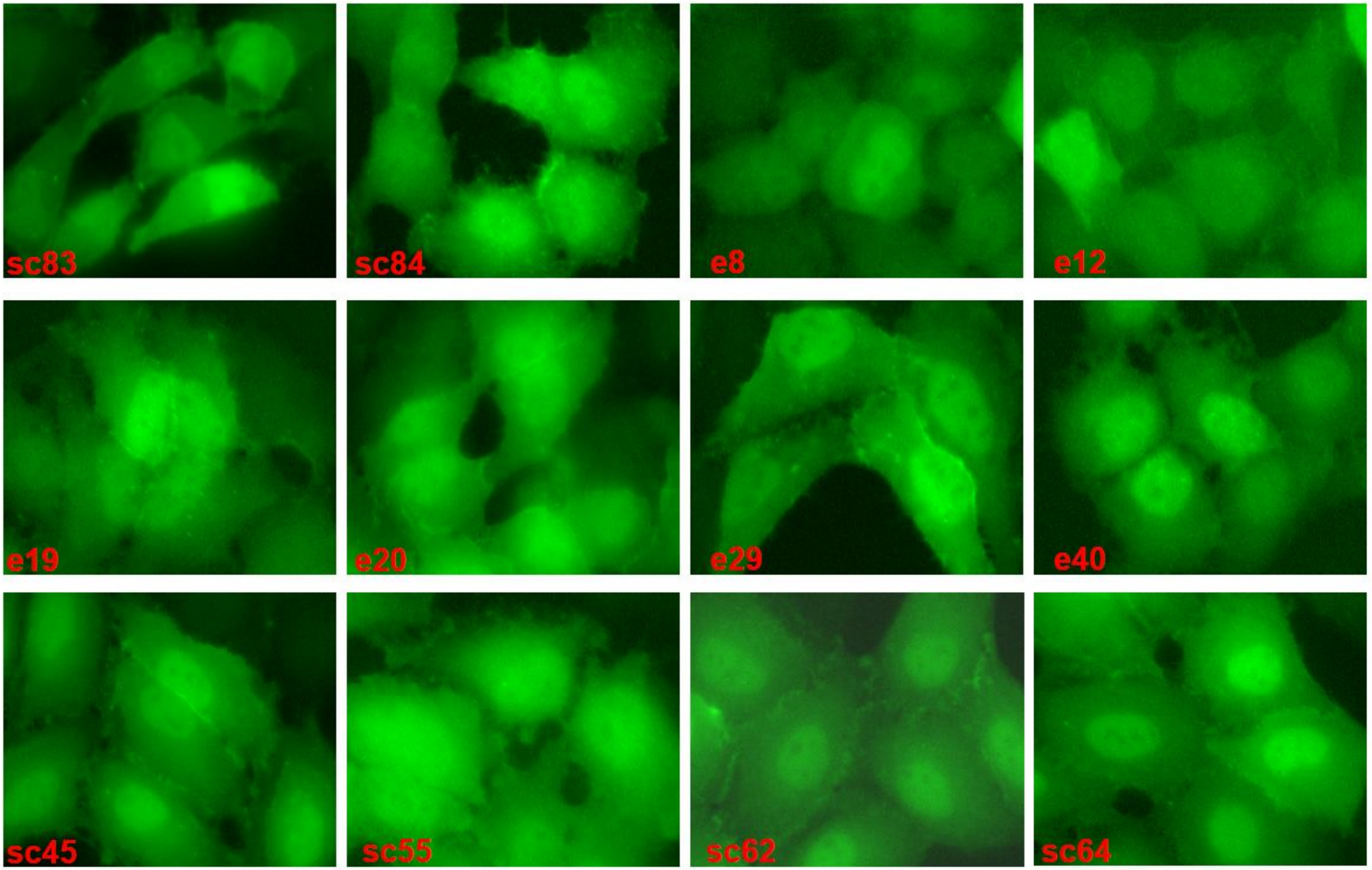
sc83
sc84
e8
e12
e19
e20
e29
e40
sc45
sc55
sc62
sc64

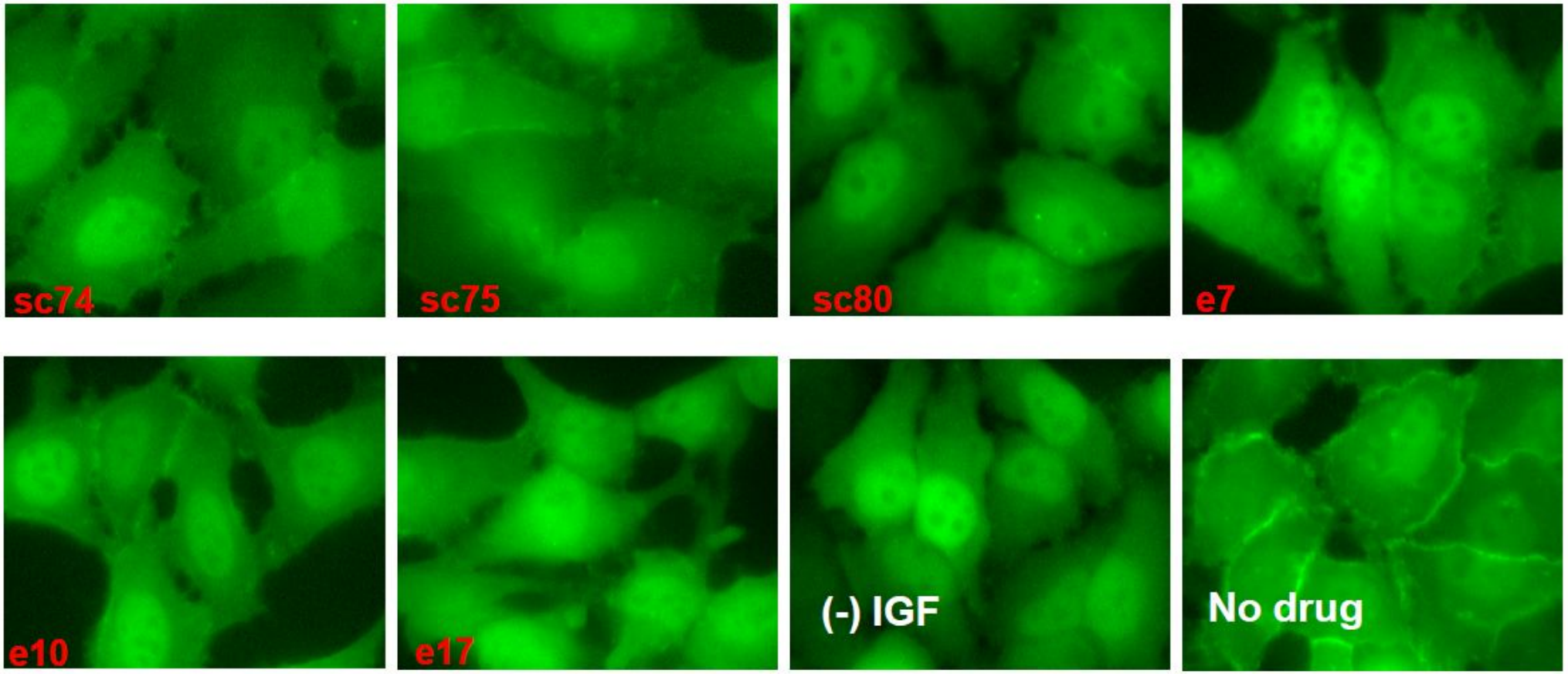

Figure S6. Positive hit compounds confirmed by live cell imaging.

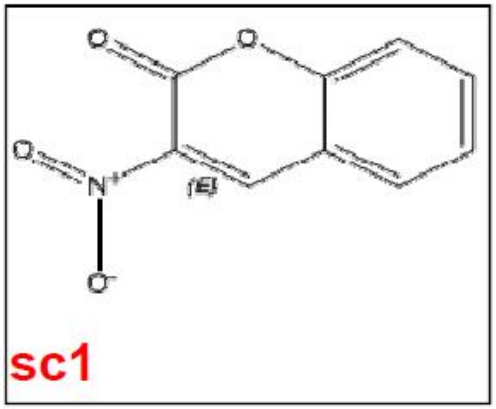
sc1

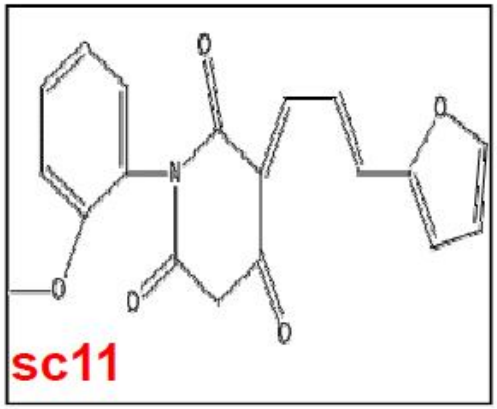
sc11

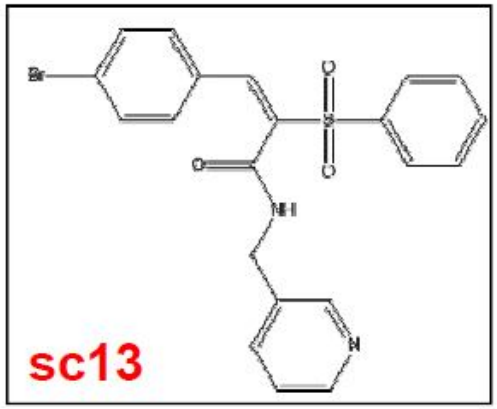
sc13

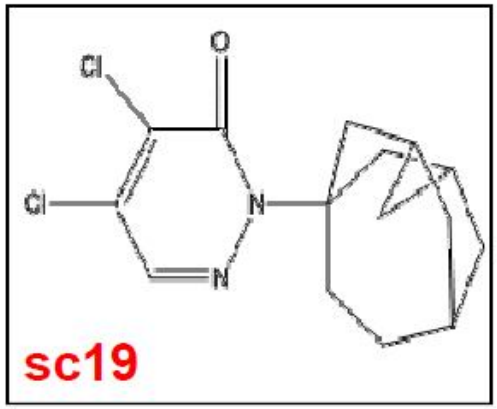
sc19

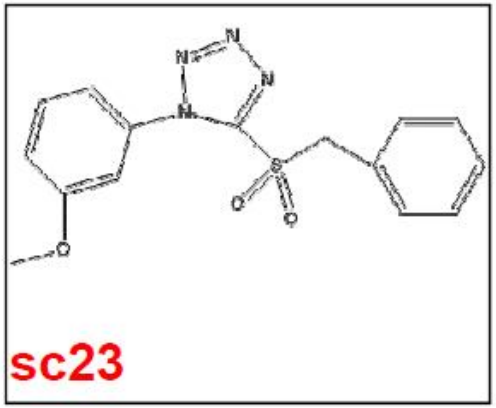
sc23

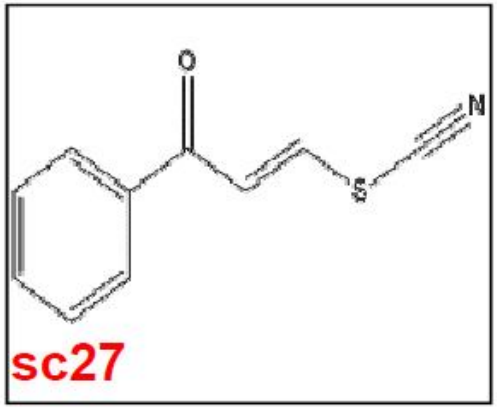
sc27

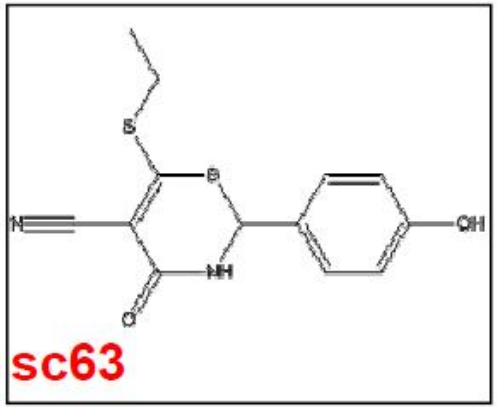
sc63

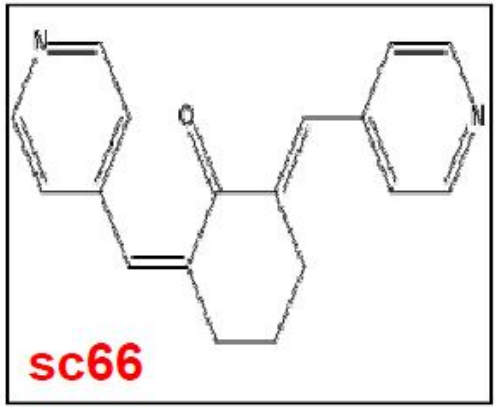
sc66

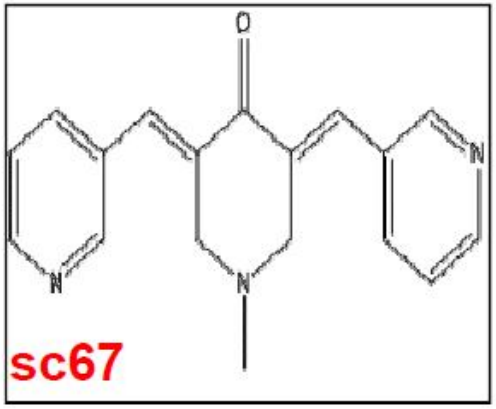
sc67

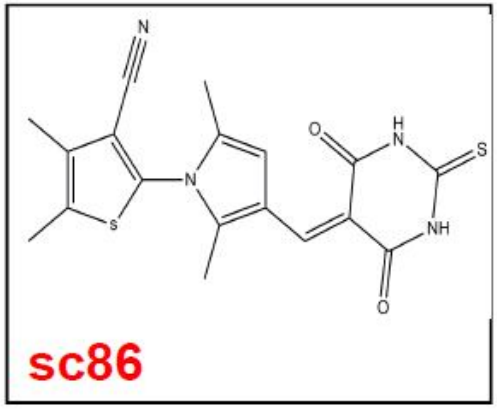
sc86

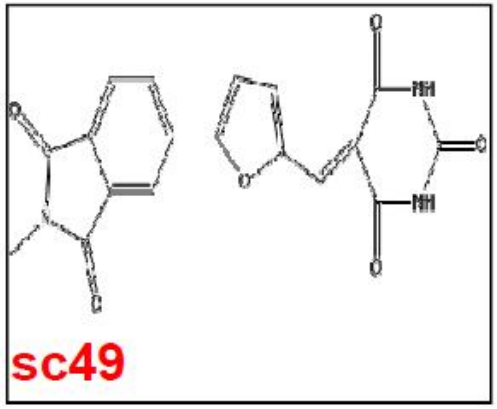
sc49

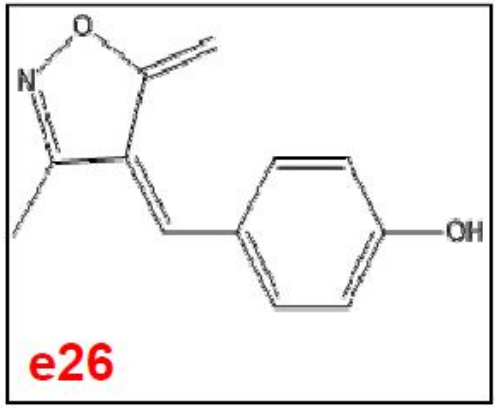
e26

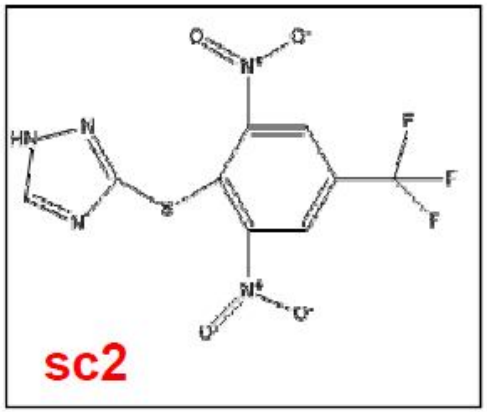
sc2

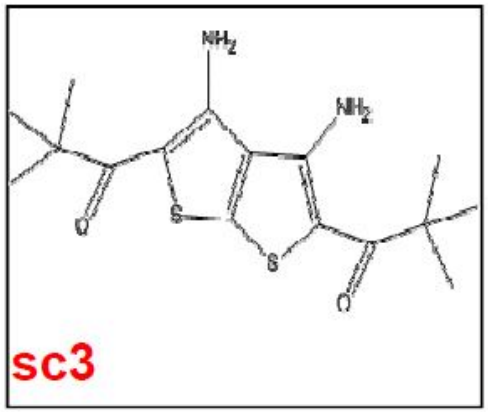
sc3

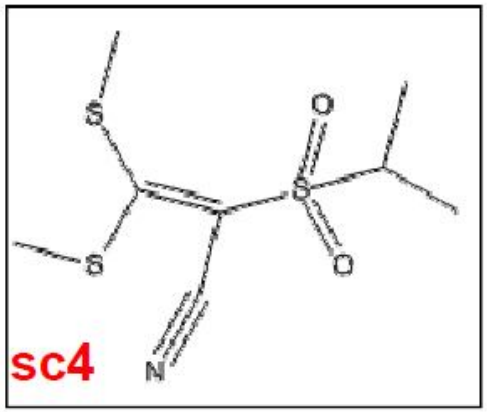
sc4

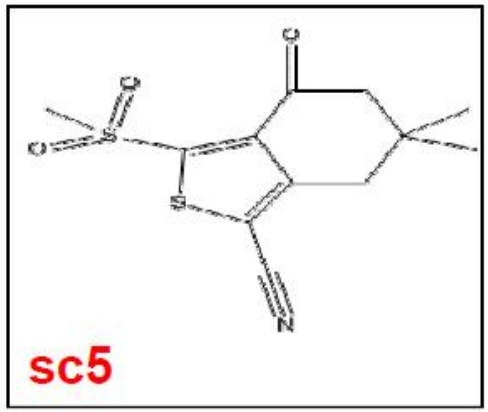
sc5

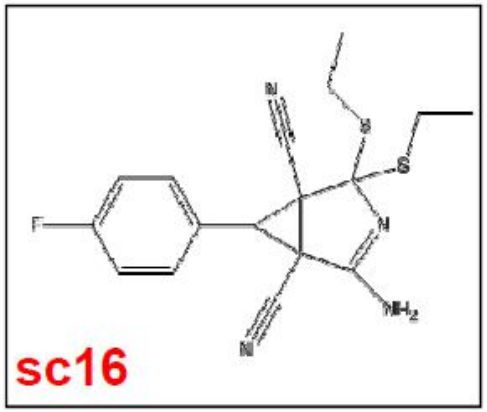
sc16

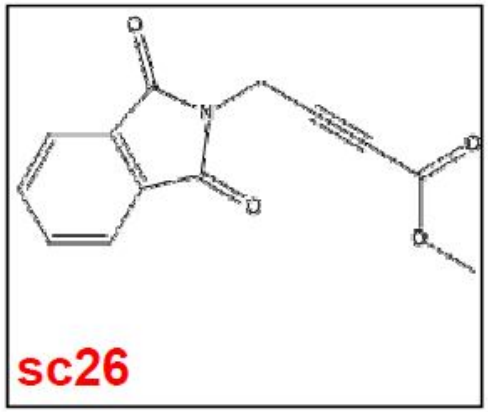
sc26

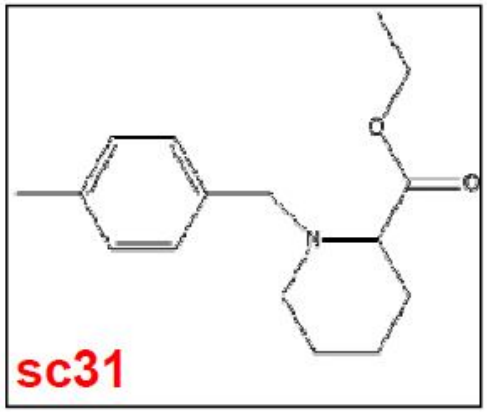
sc31

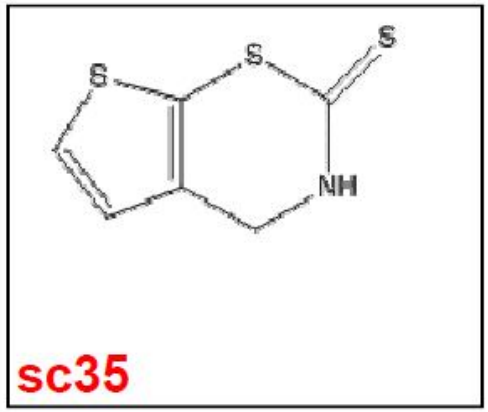
sc35

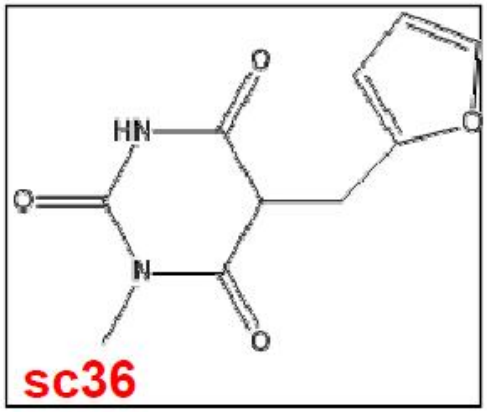
sc36

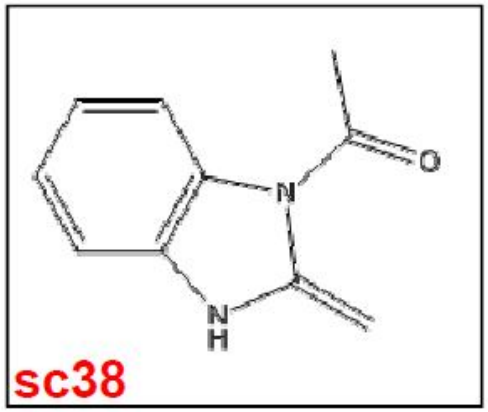
sc38

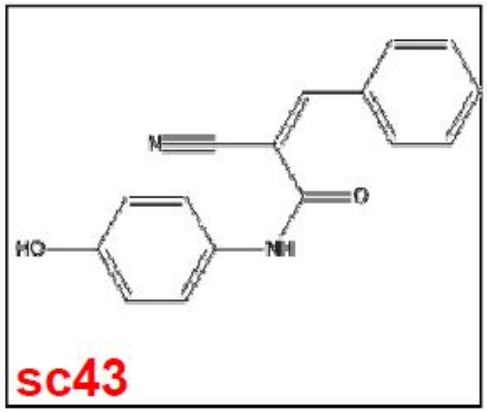
sc43

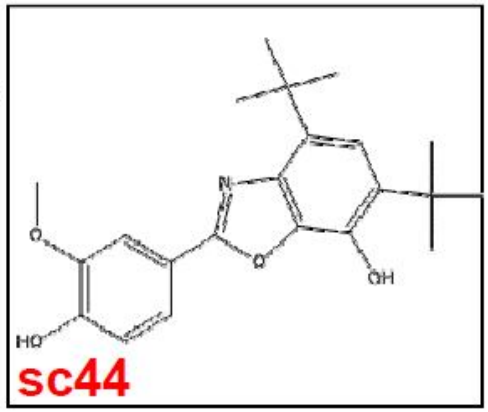
sc44

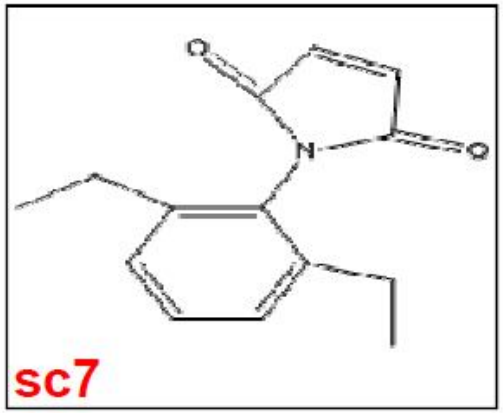
sc7

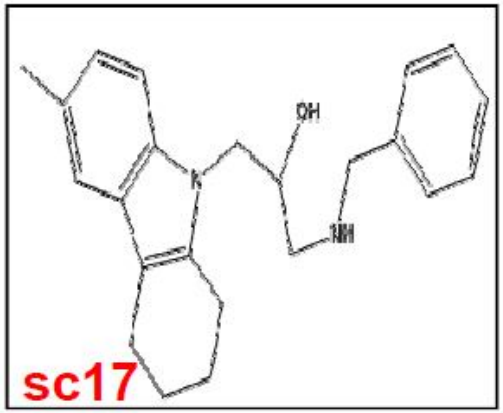
sc17

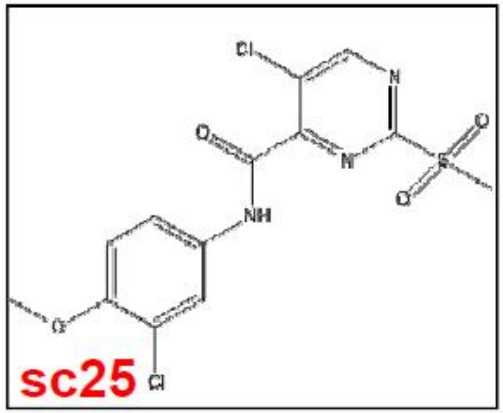
sc25

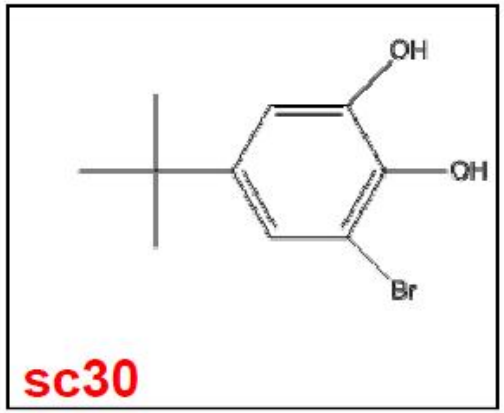
sc30

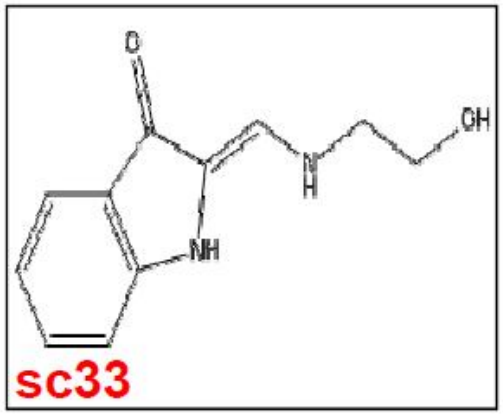
sc33

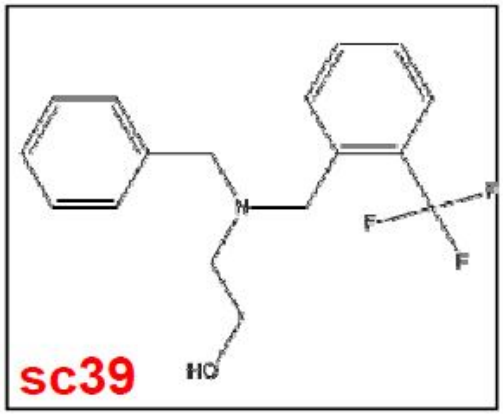
sc39

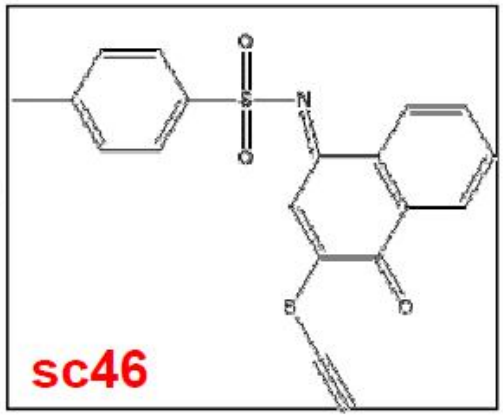
sc46

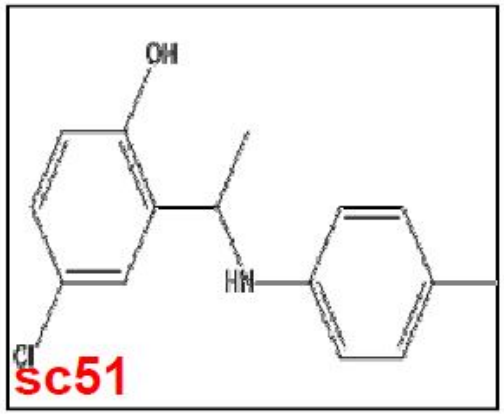
sc51

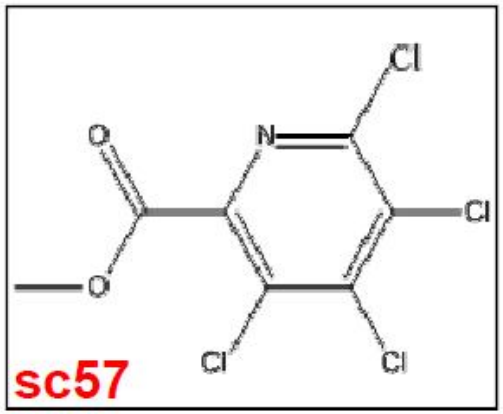
sc57

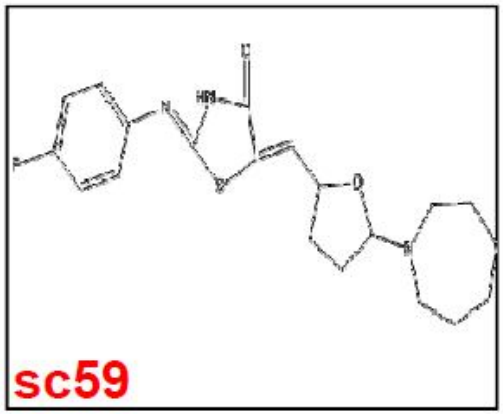
sc59

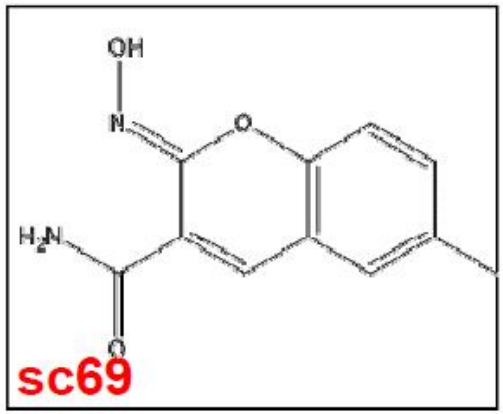
sc69

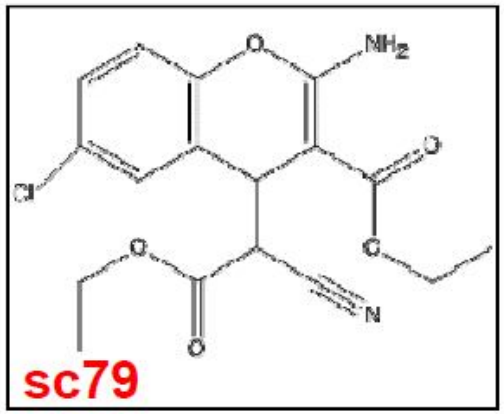
sc79

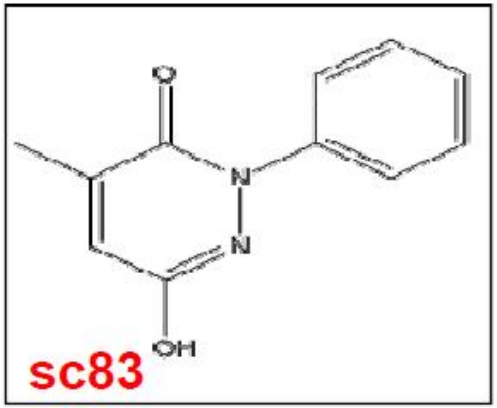
sc83

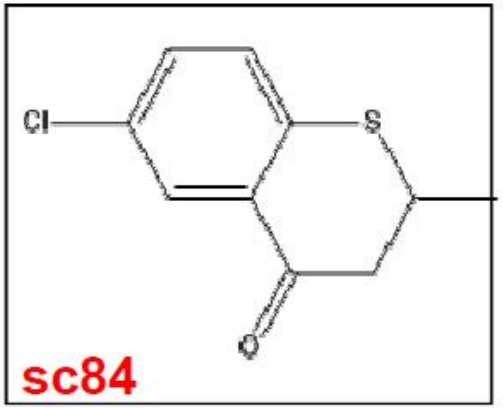
sc84

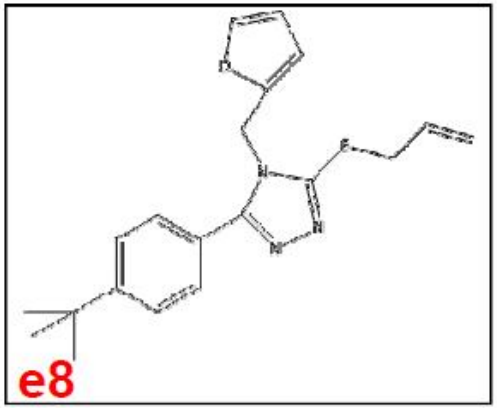
e8

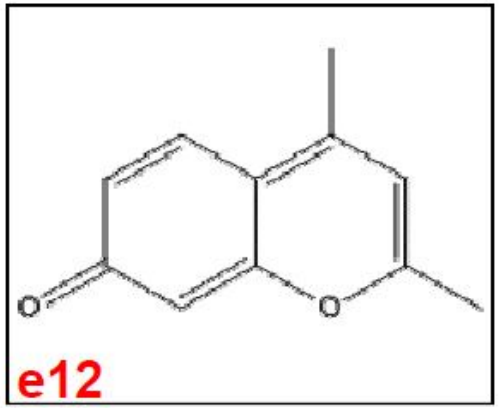
e12

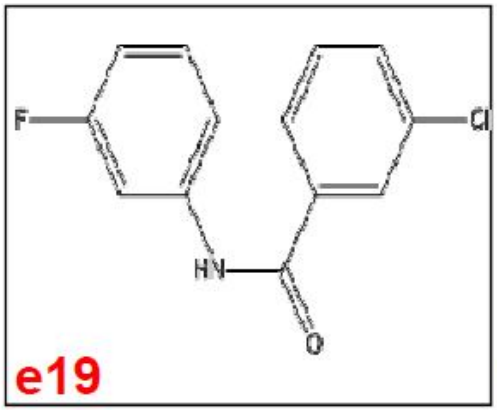
e19

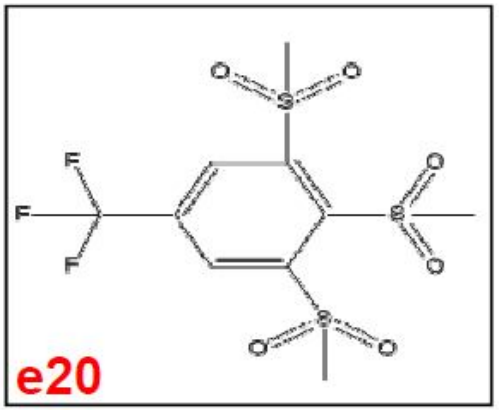
e20

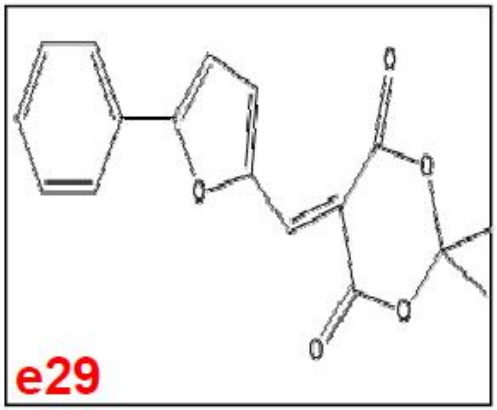
e29

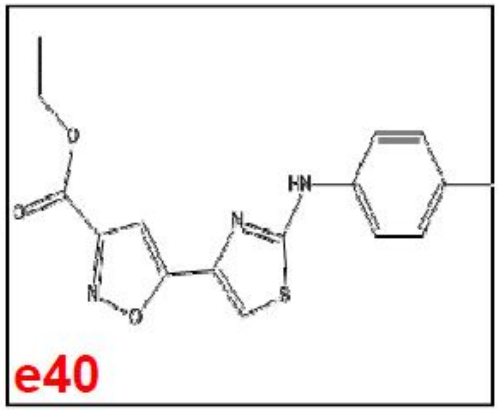
e40

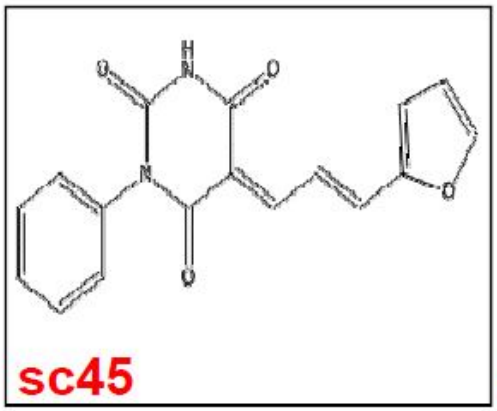
sc45

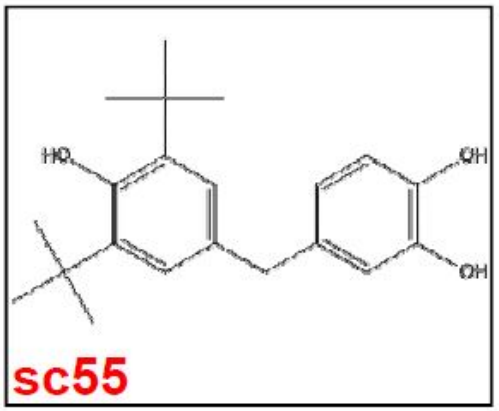
sc55

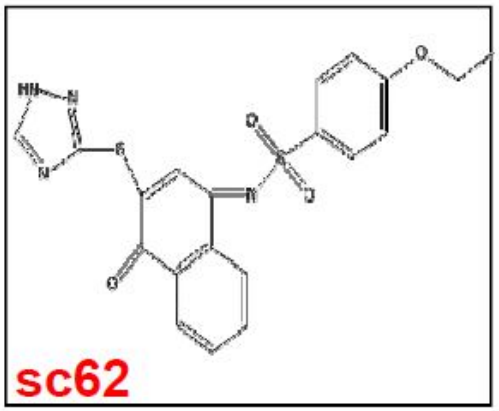
sc62

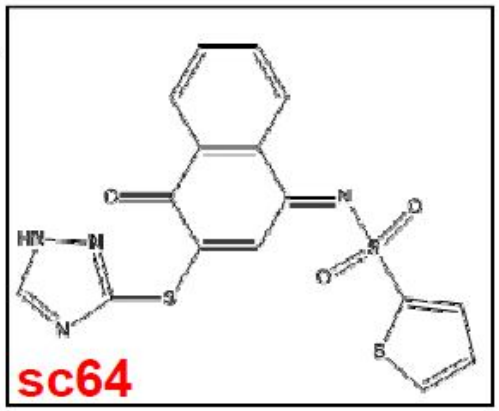
sc64

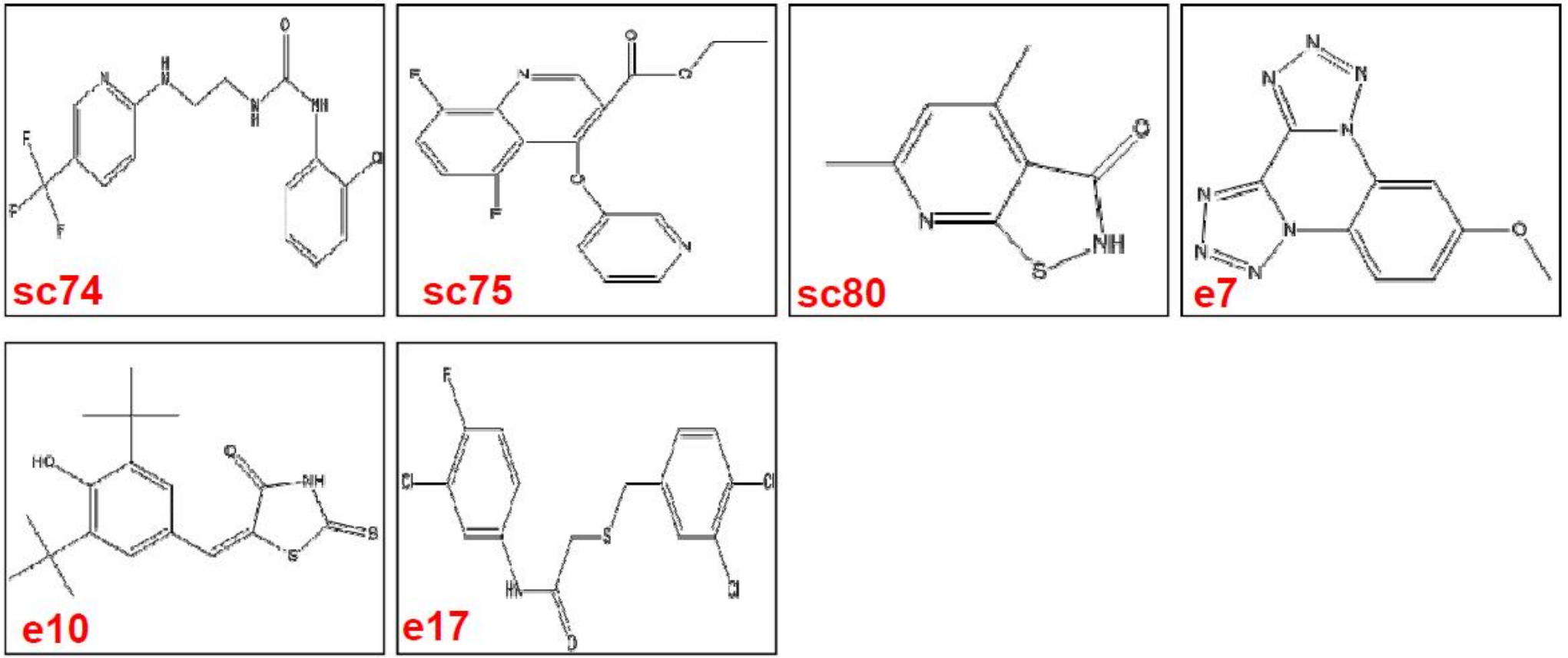

Figure S7. Chemical structure of confirmed positive hit compounds.

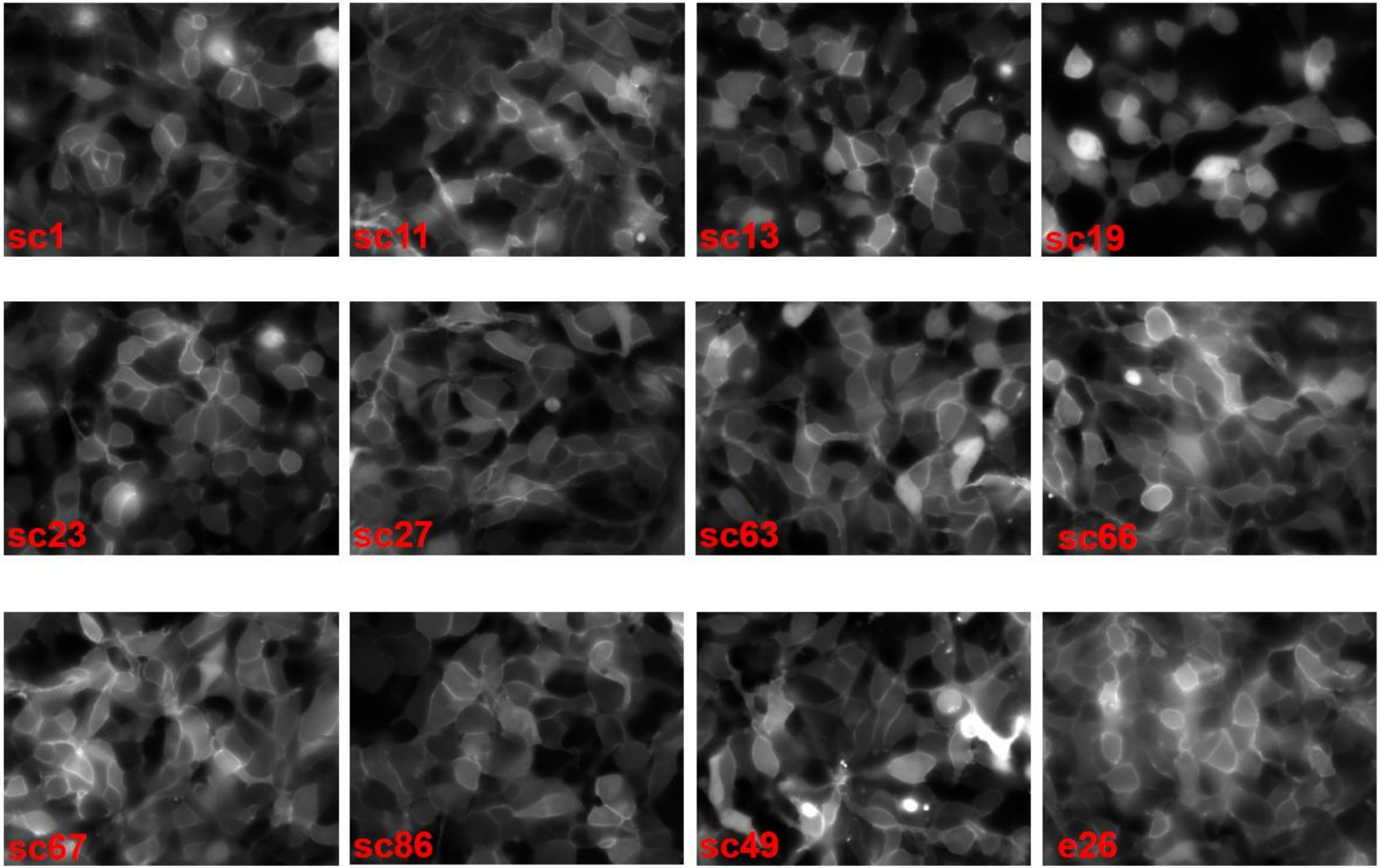
sc1
sc11
sc13
sc19
sc23
sc27
sc63
sc66
sc67
sc86
sc49
e26

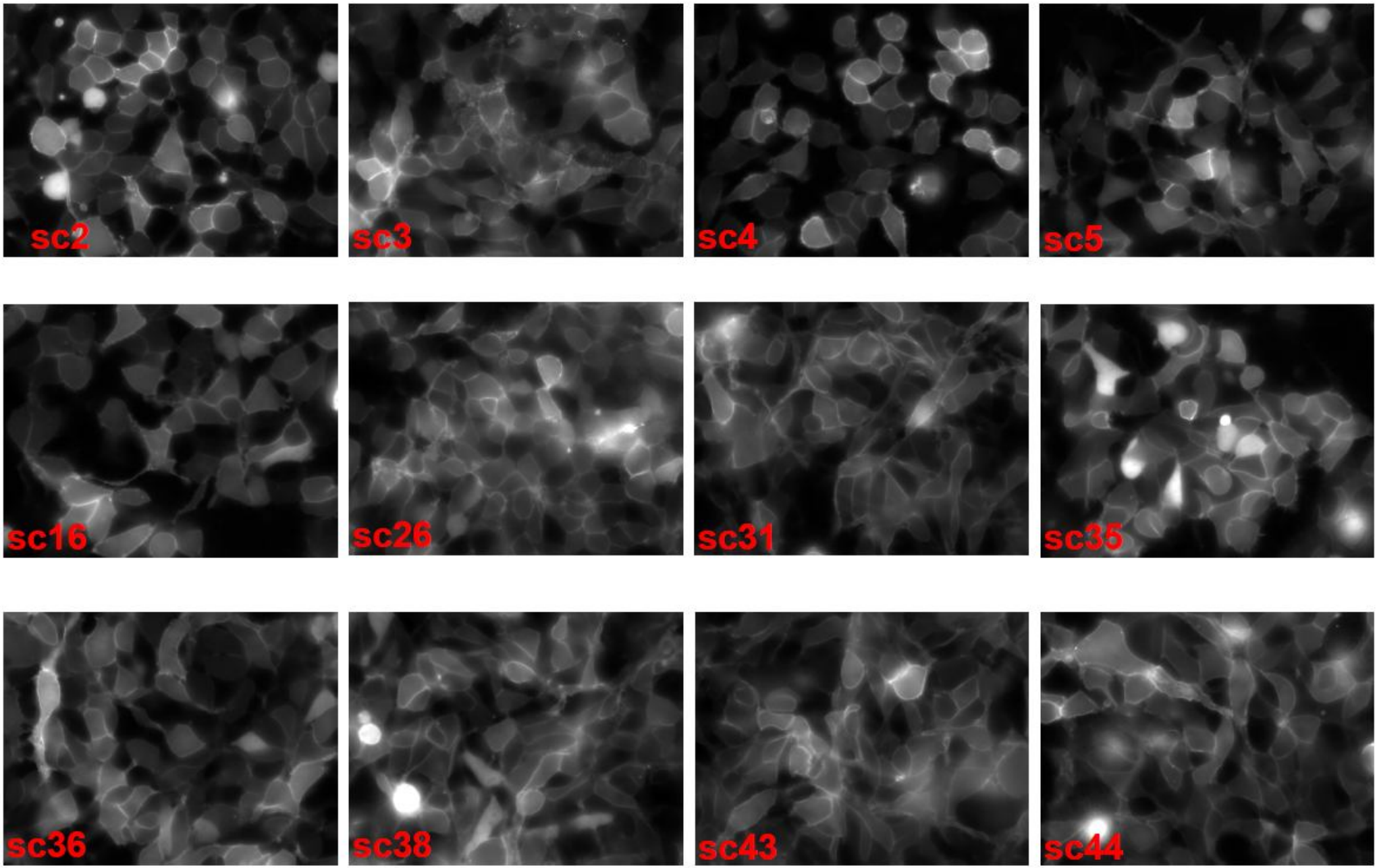
sc2
sc3
sc4
sc5
sc16
sc26
sc31
sc35
sc36
sc38
sc43
sc44

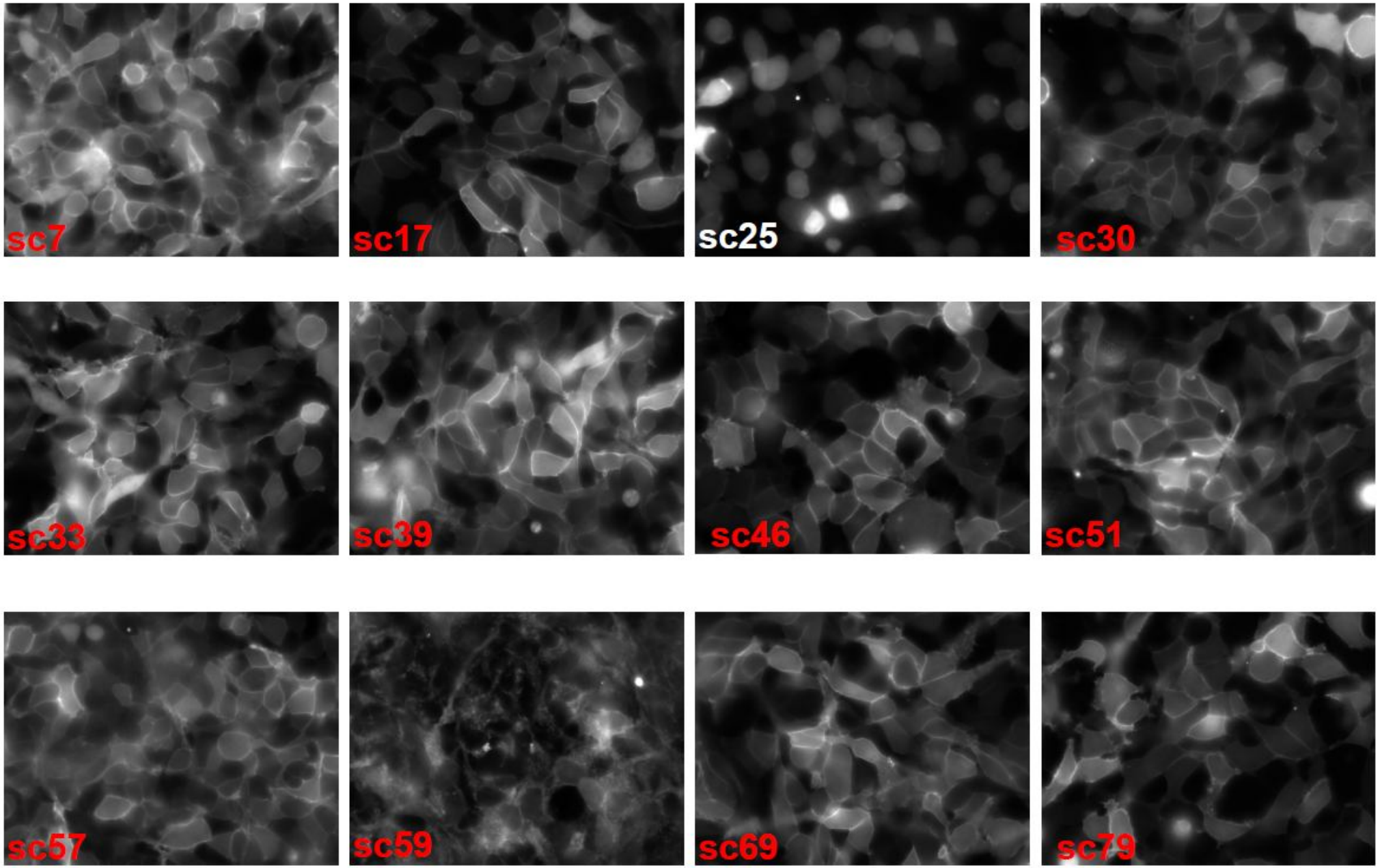
sc7
sc17
sc25
sc30
sc33
sc39
sc46
sc51
sc57
sc59
sc69
sc79

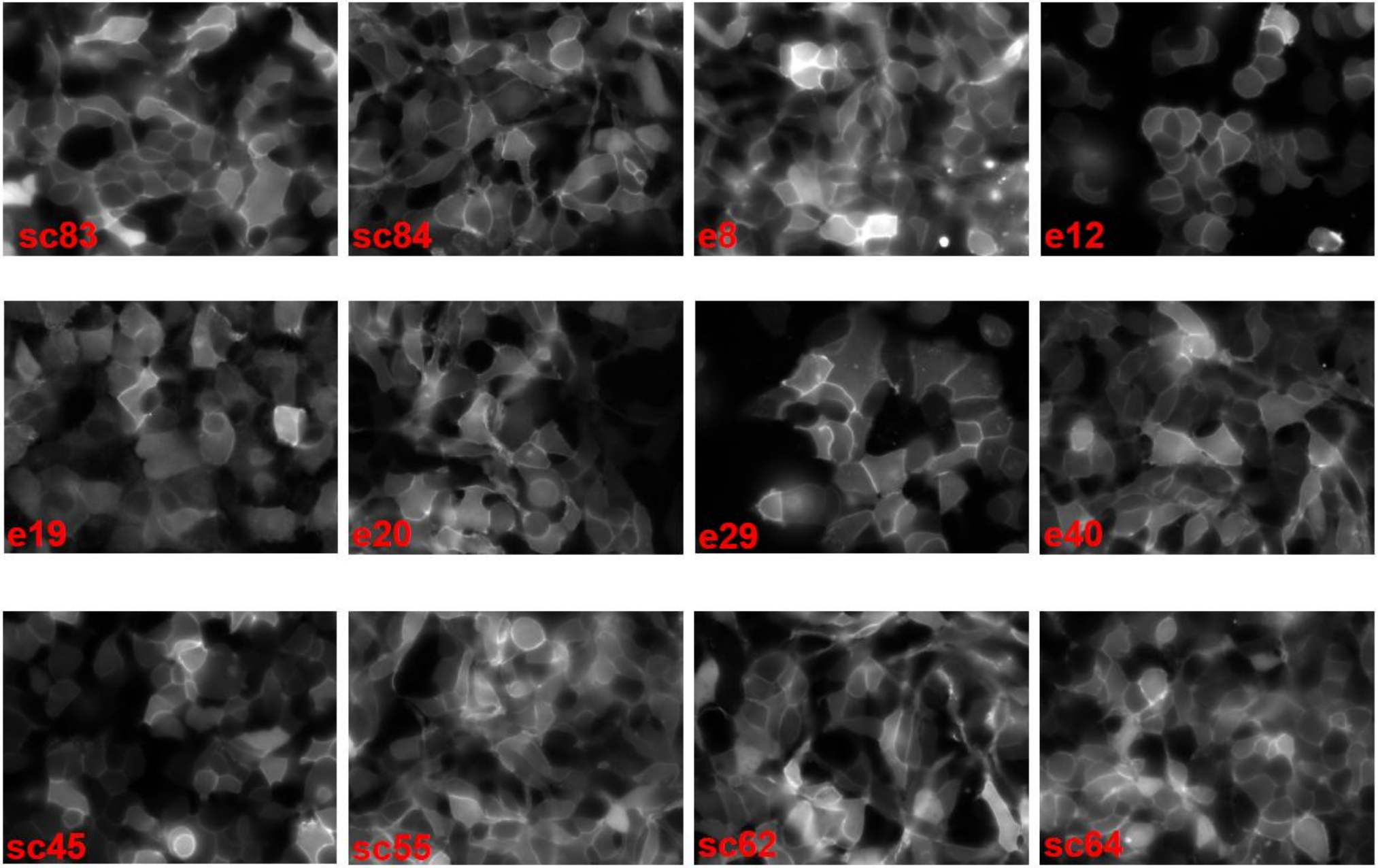
sc83
sc84
e8
e12
e19
e20
e29
e40
sc45
sc55
sc62
sc64

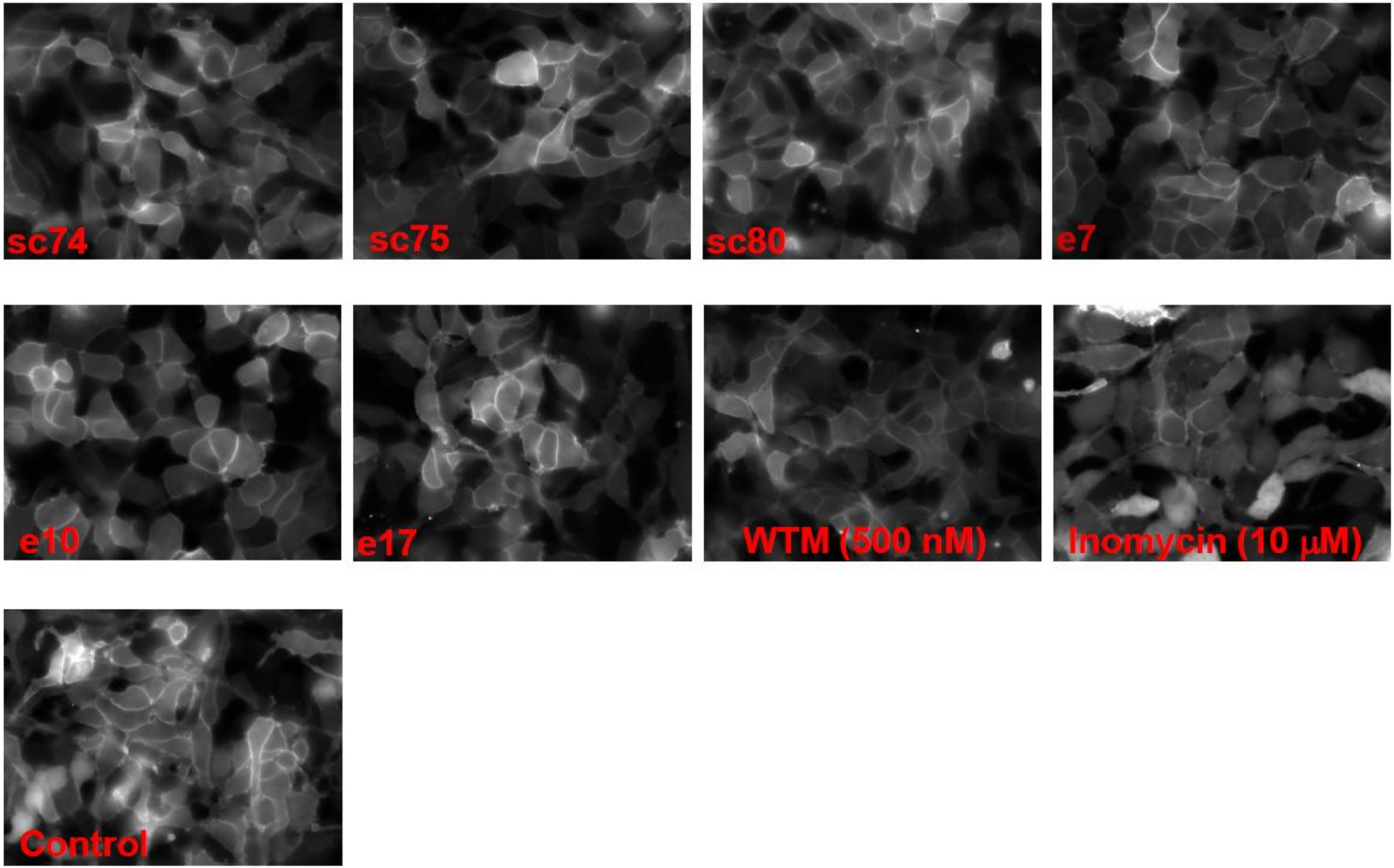

Figure S8. The effect of positive compounds on PtdIns(4,5)P2-mediated membrane localization of EGFP-PLC-delta1-PH. HEK293 cells stably expressing EGFP-PLC-delta-PH were treated with each compound (8 μg/ml) for 30 minutes before imaging.

HeLa-30min

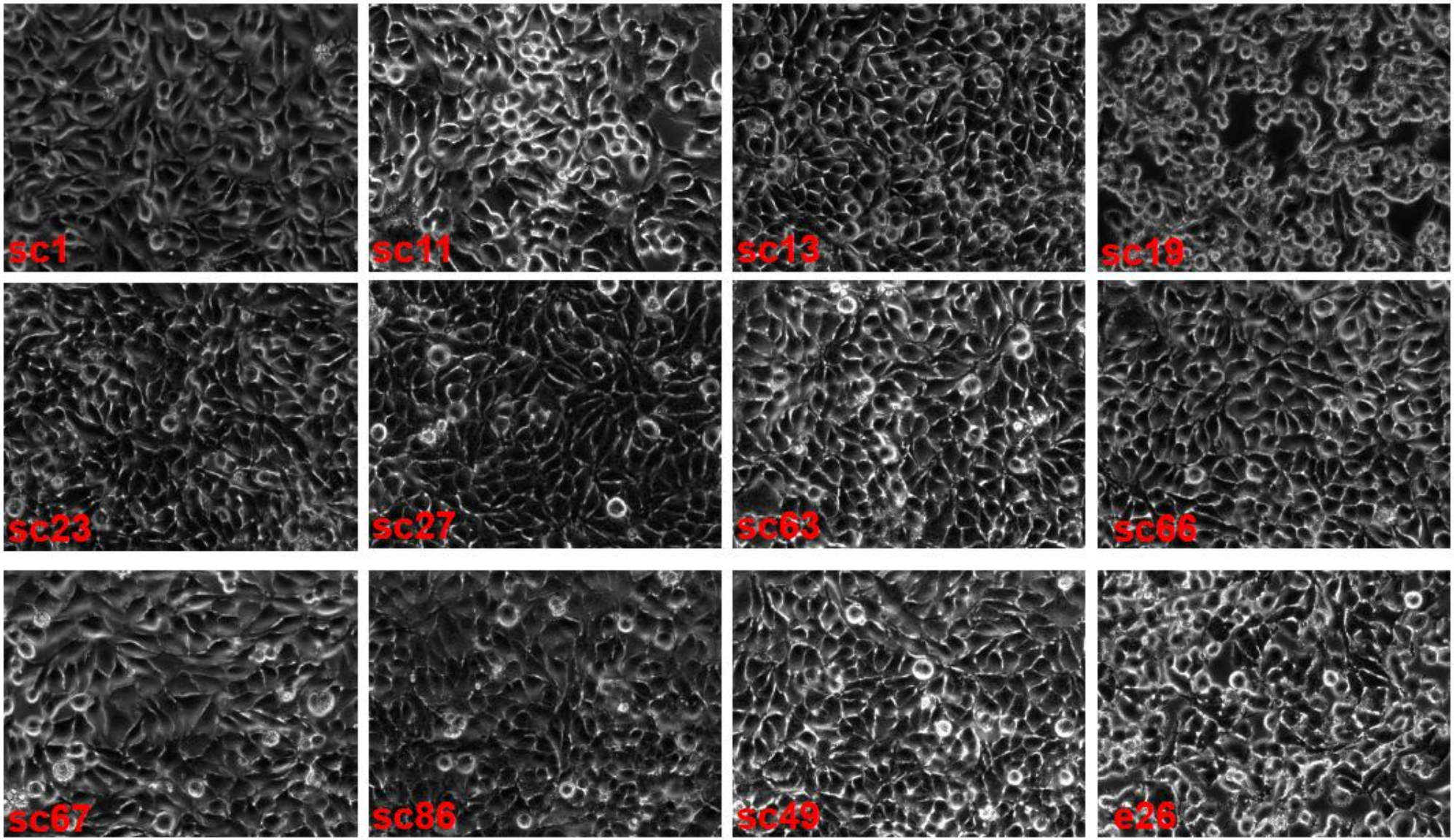

HeLa-30min

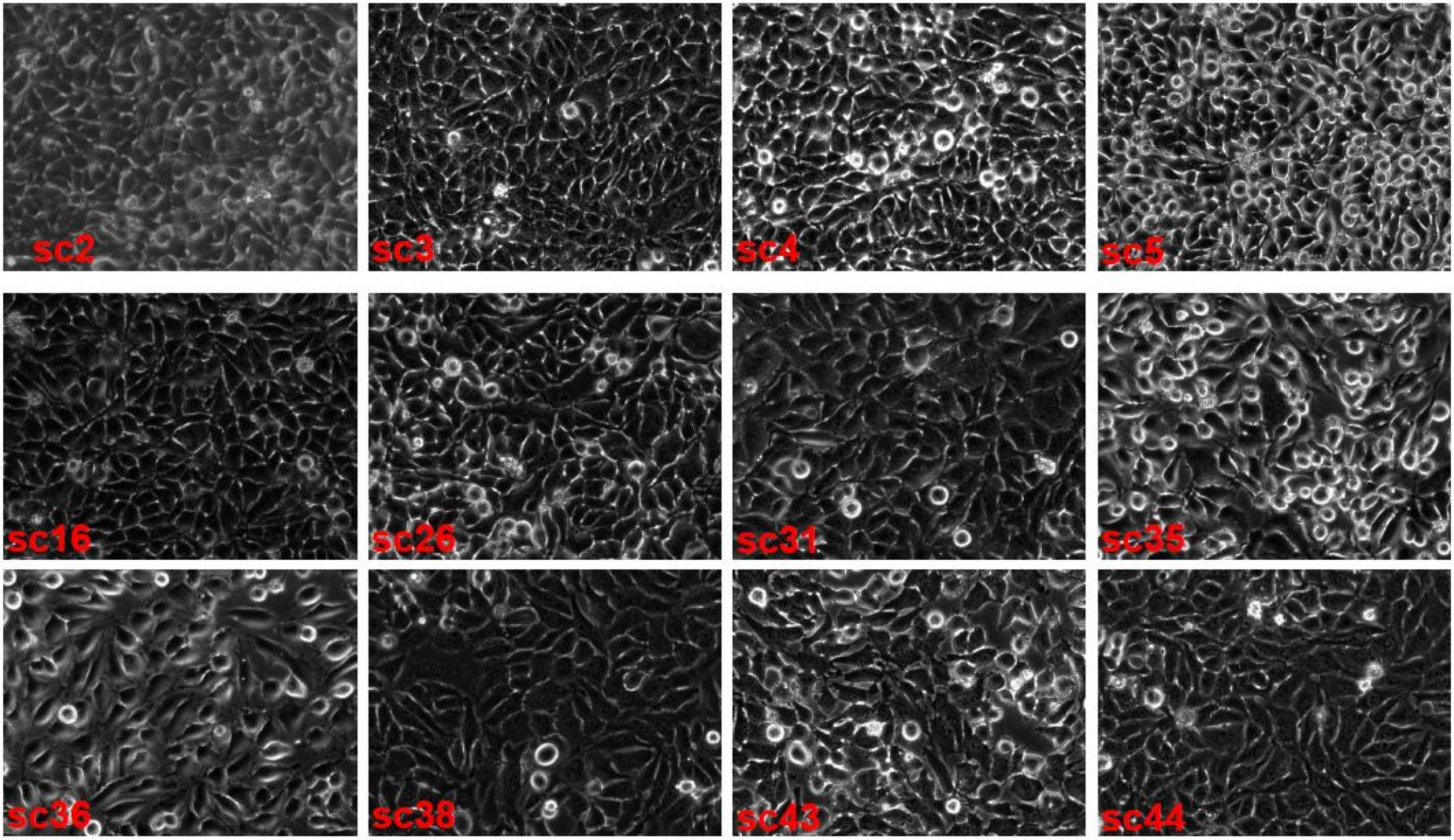

HeLa-30min

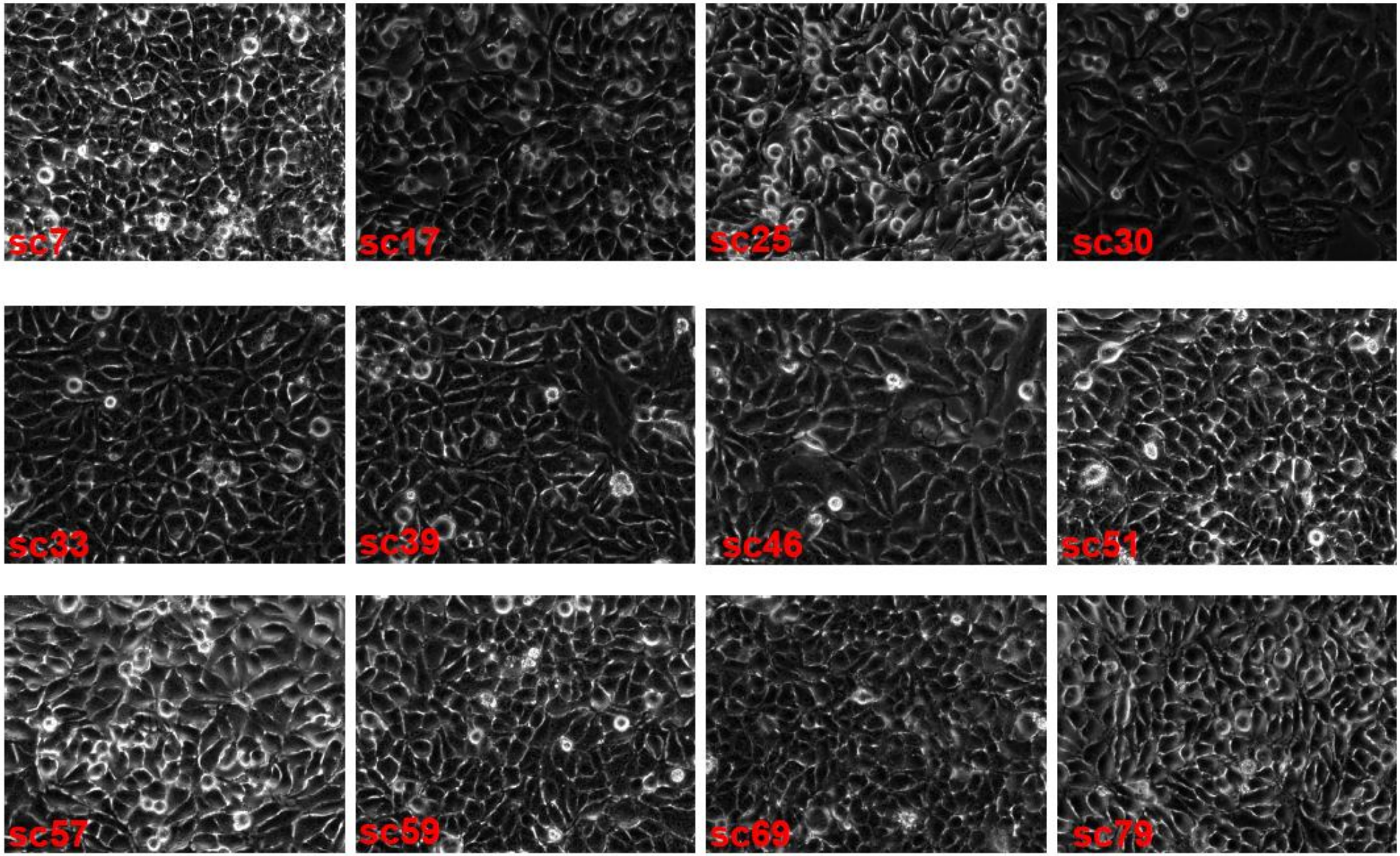

HeLa- 30min

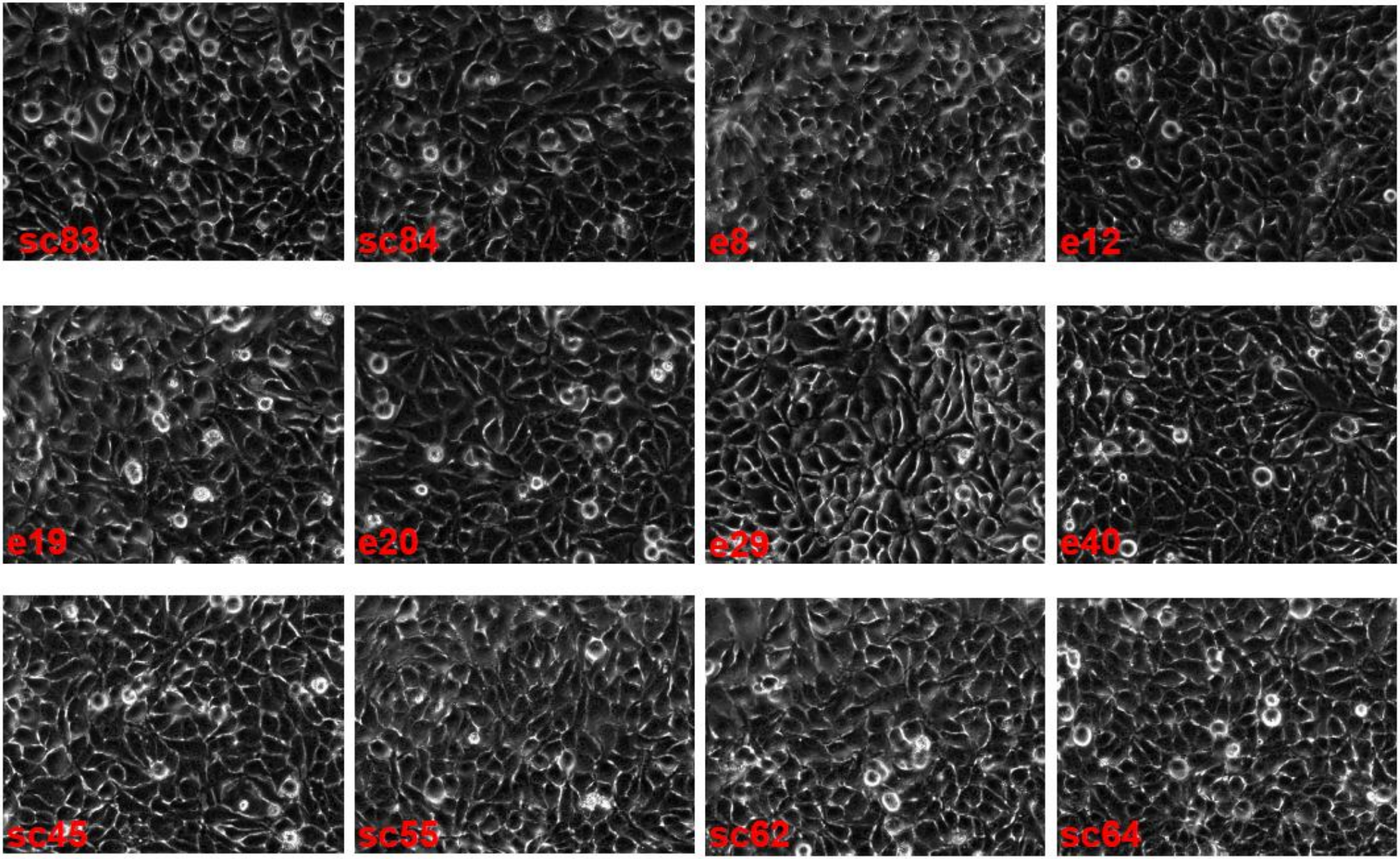

HeLa- 30min

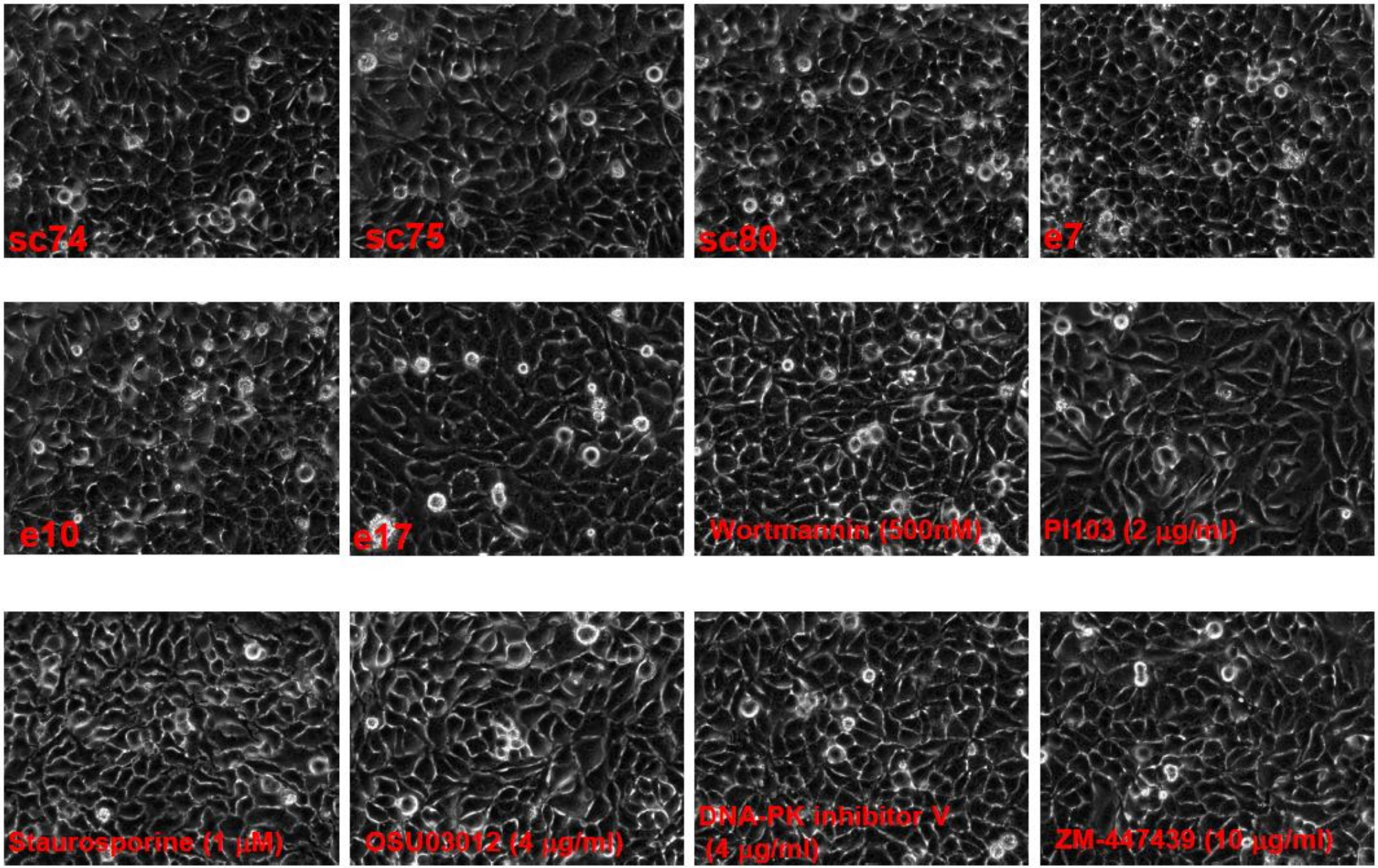
sc74
sc75
sc80
e7
e10
e17
Wortmannin (500nM)
PI103 (2 µg/ml)
Staurosporine (1 µM)
OSU03012 (4 µg/ml)
DNA-PK inhibitor V
(4 µg/ml)
ZM-447439 (10 µg/ml)

HeLa-6 hr

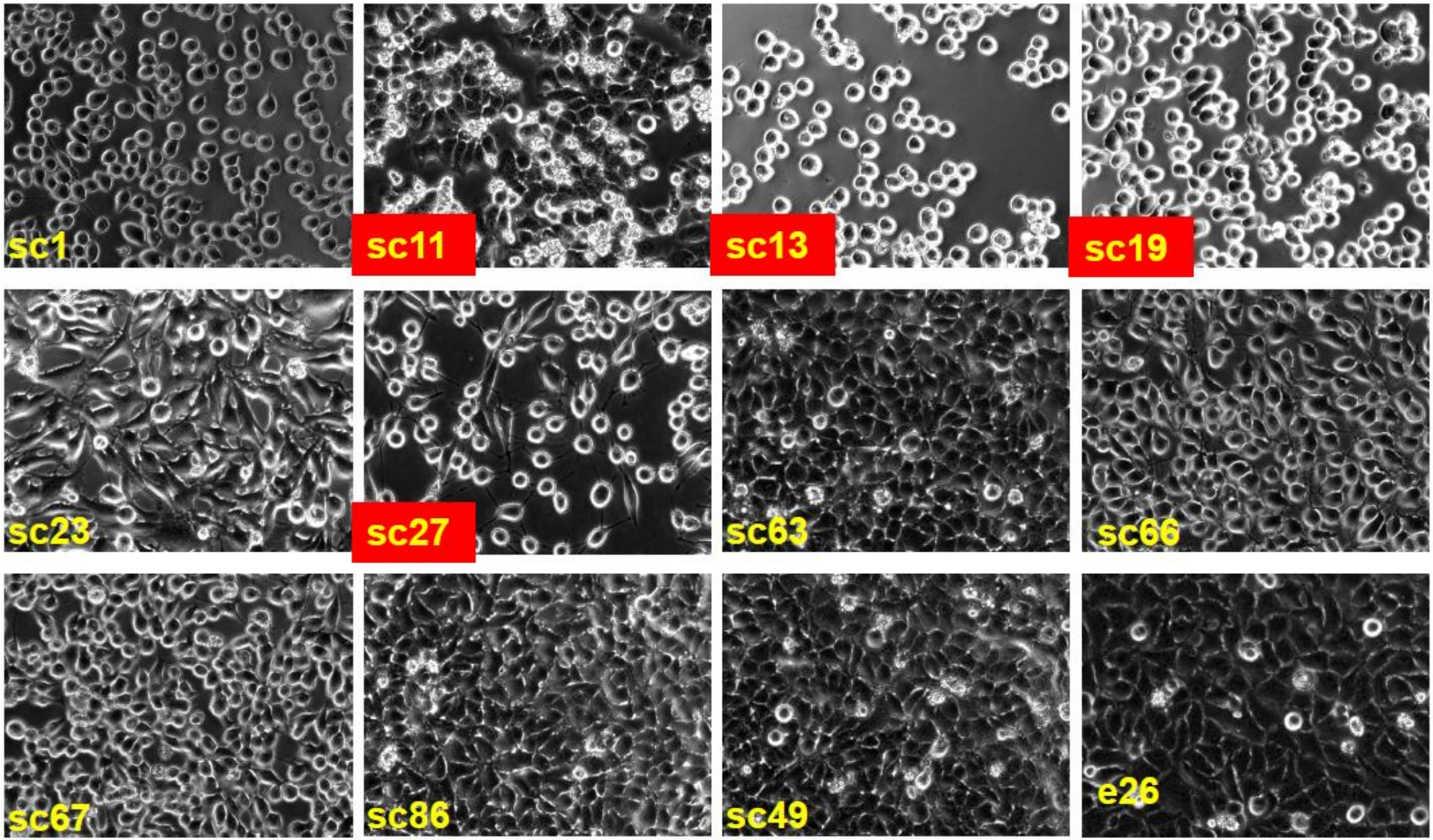

HeLa-6 hr

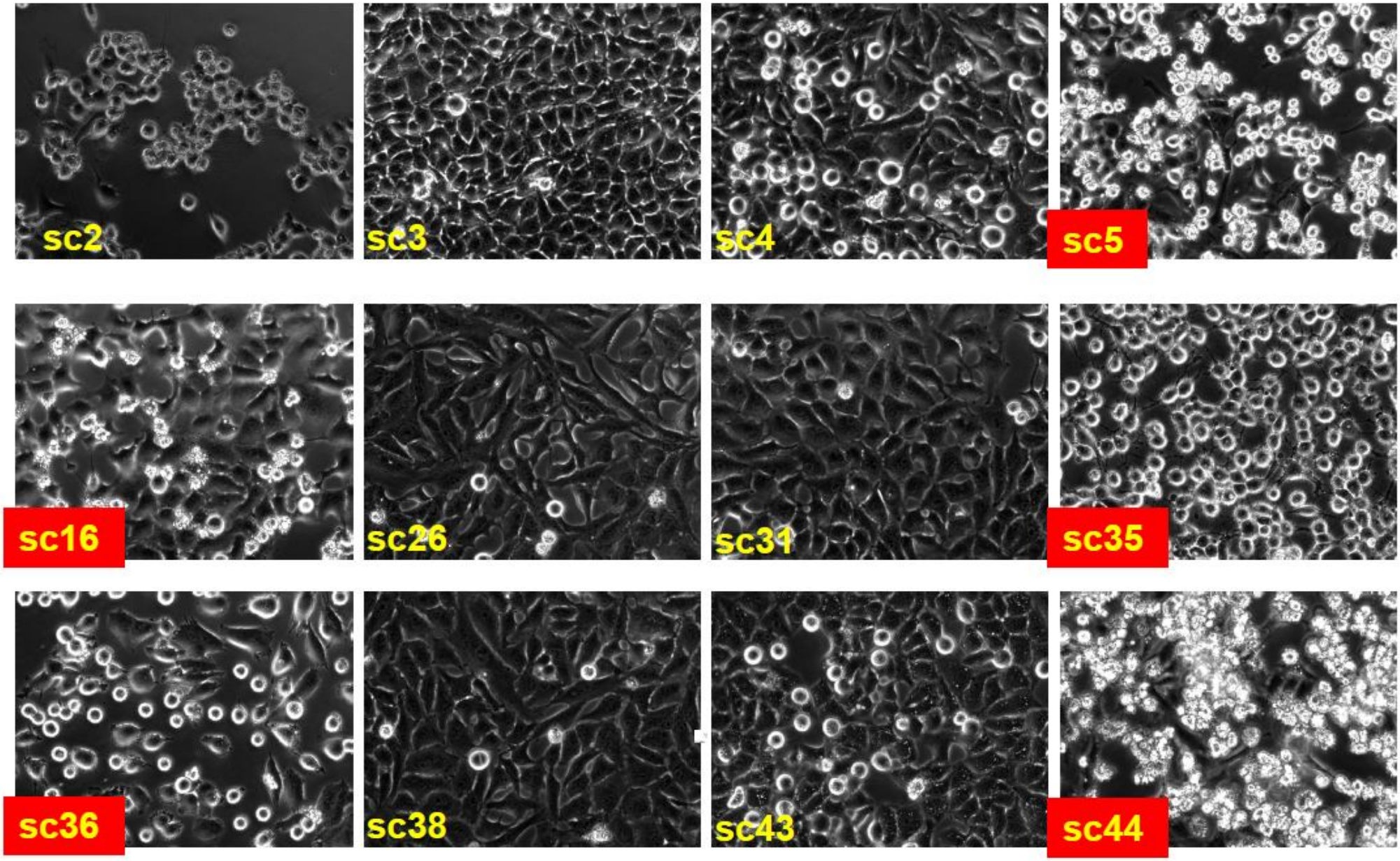

HeLa- 6 hr

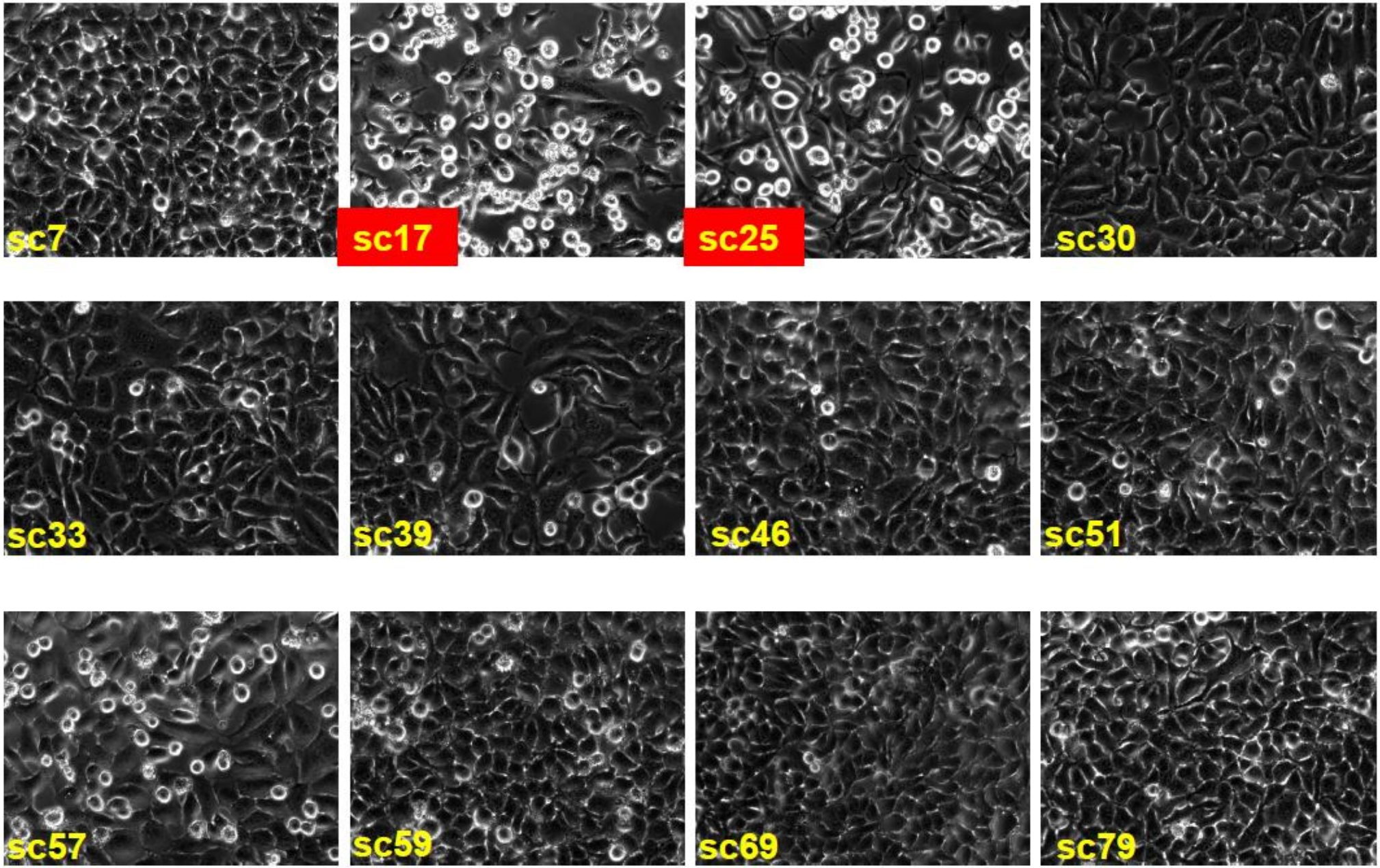

HeLa- 6 hr

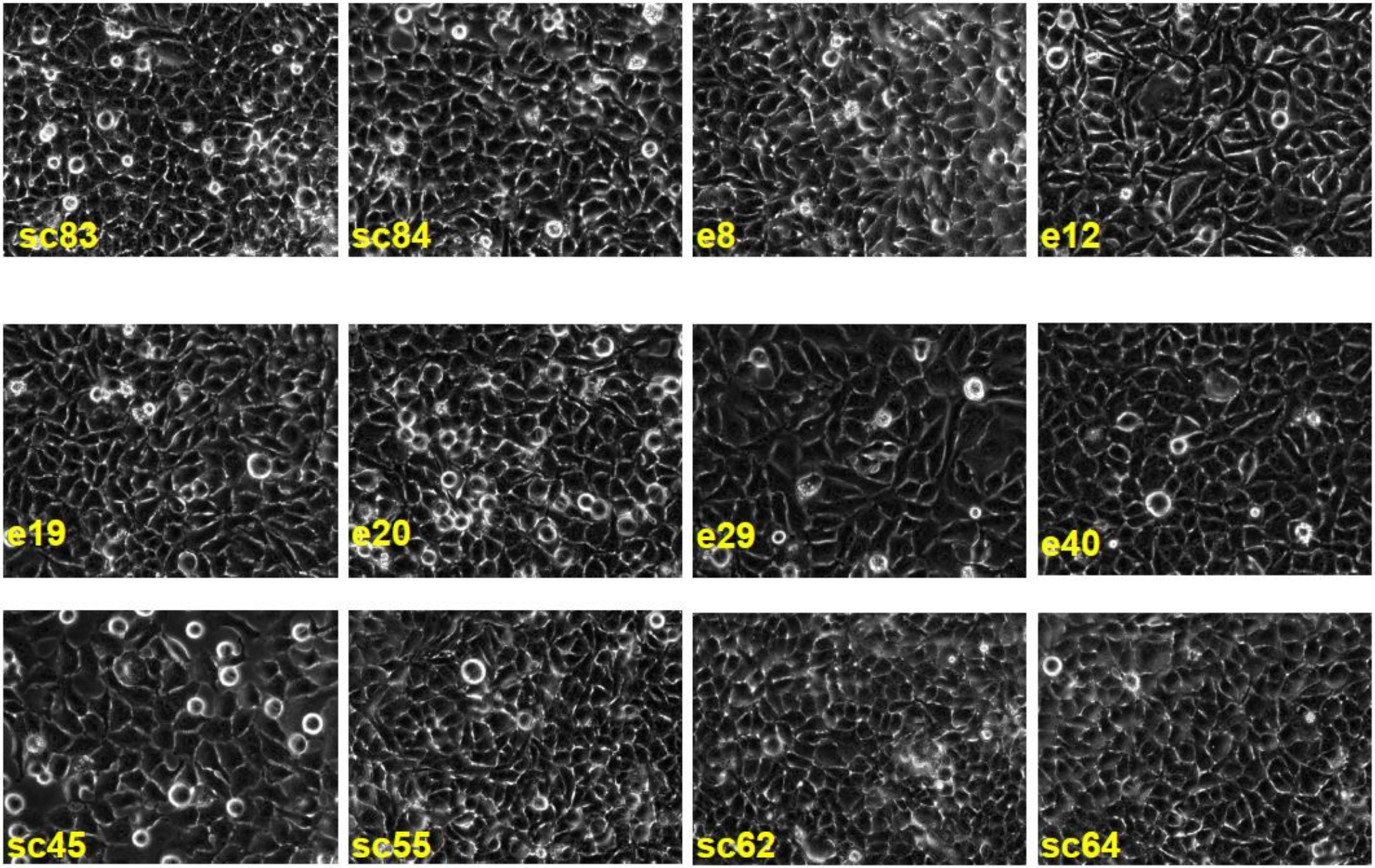

HeLa- 6 hr

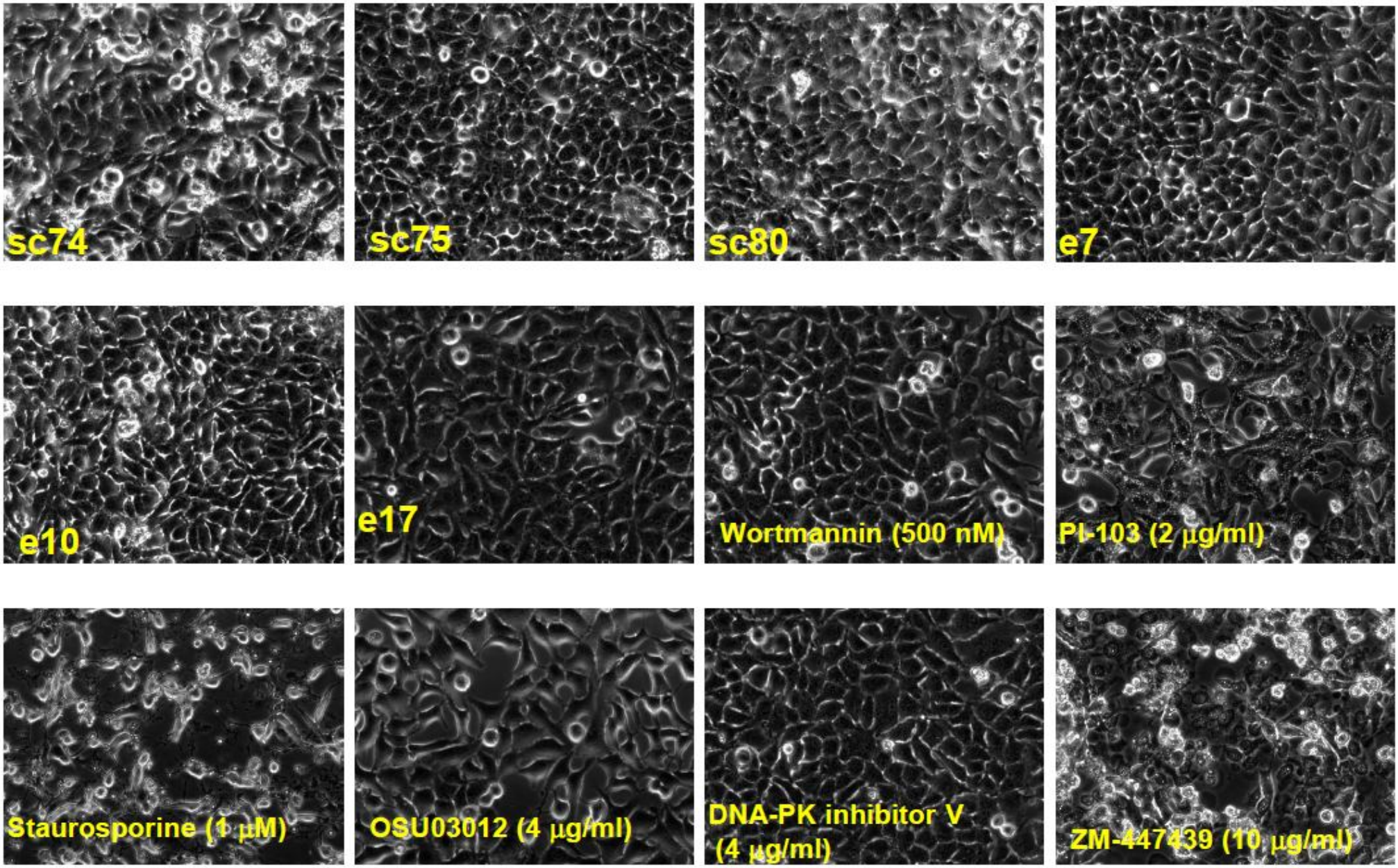
sc74
sc75
sc80
e7
e10
e17
Wortmannin (500 nM)
PI-103 (2 µg/ml)
Staurosporine (1 µM)
OSU03012 (4 µg/ml)
DNA-PK inhibitor V
(4 µg/ml)
ZM-447439 (10 µg/ml)

Figure S9. Morphological changes induced by identified positive hit compounds. HeLa cells were cultured in 24-well plate and treated with each compound (8 μg/ml) for indicated time. The bright field images were taken at each time points following chemical treatment. The compounds that induced significant morphological changes in 6 hrs are indicated in red. Cells were also treated with several known kinase inhibitors, including Wortmannin (PI3K inhibitor), PI-103 (PI3K and mTor kinase inhibitor), Staurosporine (broad-spectrum protein kinases inhibitor), OSU-0312 (Aurora kinase inhibitor), DNA-PK inhibitor V, and ZM447439 (PDK1 inhibitor) at the indicated concentrations.

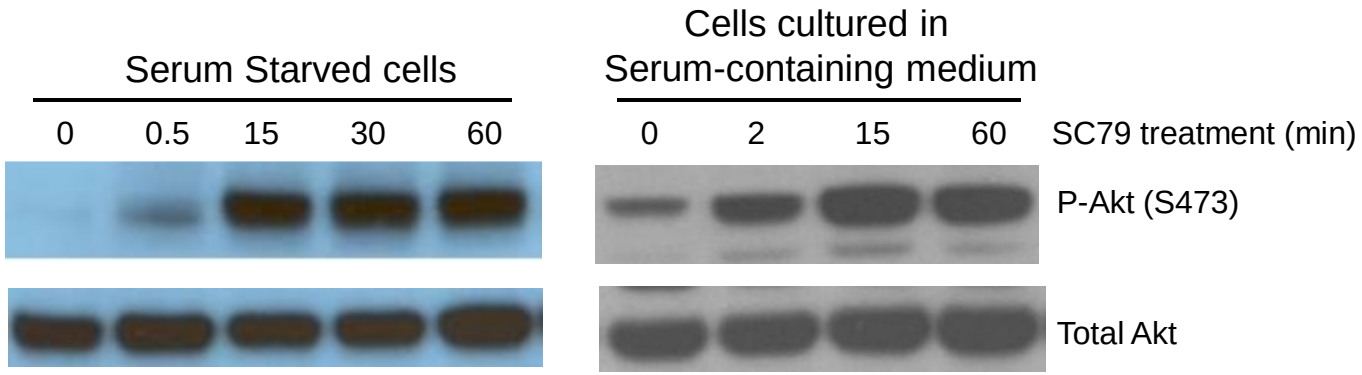

Figure S10. **Kinetics of Akt phosphorylation by SC79.** Serum-starved cells (overnight) or cells grown in serum-containing medium (1% FBS) were treated with SC79 (4㎎/ml) for indicated time. Total and phosphorylated Akt were detected by Western blot using anti-Akt and anti-Phospho-Akt (Ser473) antibodies, respectively.

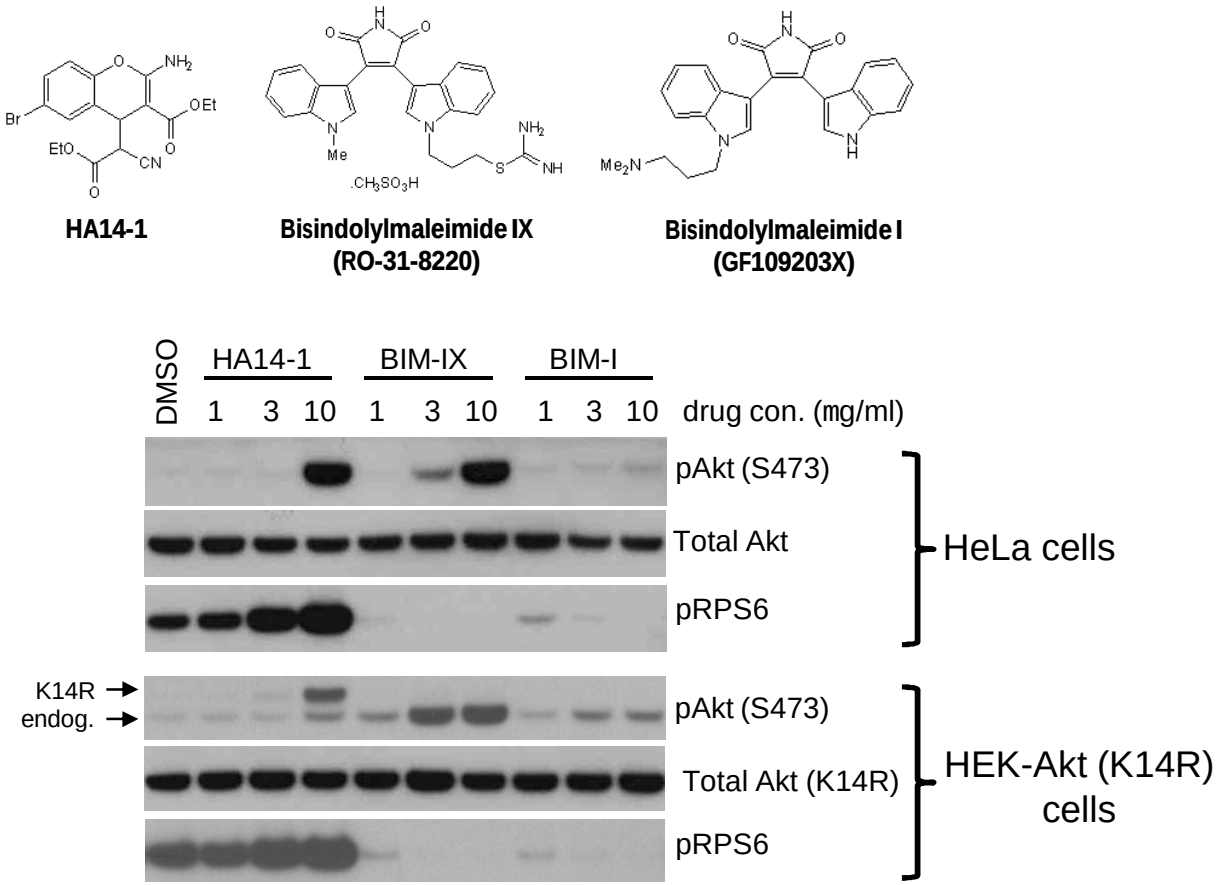

Figure S11. HA14-1, a structural analog of SC79, increases phosphorylation of both endogenous and mutant Akt (K14R) and enhances Akt signaling. In contrast, BIM-IX and BIM-I, two kinase inhibitors of PKC, enhance phosphorylation of endogenous Akt but inhibit its kinase activity. Both PKC and Akt belong to AGC family kinases with a similar kinase domain. HeLa or HEK-Akt (K14R) cells were treated with the indicated amounts of chemicals for 30 minutes. The levels of phosphorylation of Akt and RPS6 (riobosomal protein S6), a target of AGC family kinase, were analyzed by Western blot.

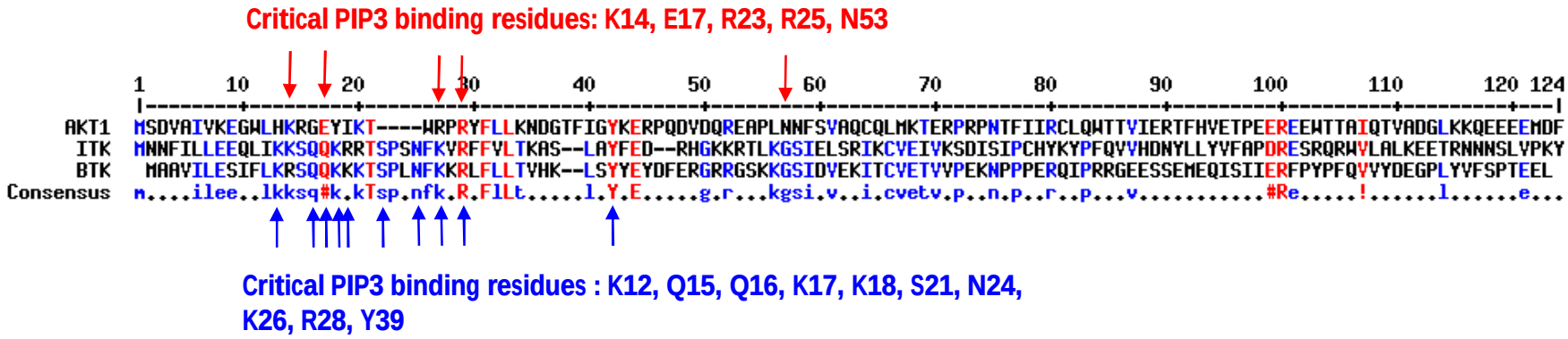

Figure S12. Alignment of PH domains of Akt and Tec family tyrosine kinase (Itk and Btk). The critical residues for PtdIns(3,4,5)P3 binding were indicated by arrows.

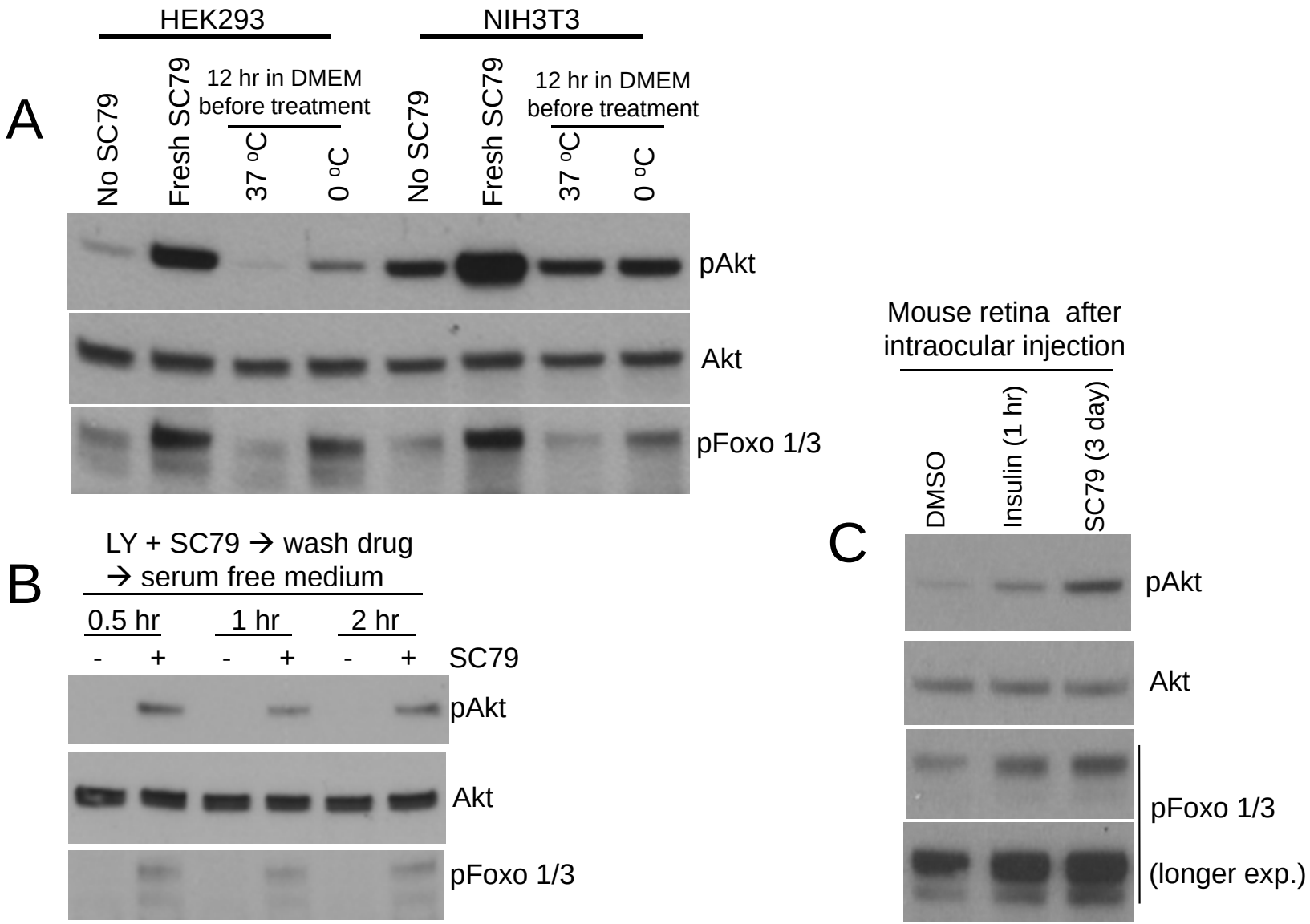

Figure S13. A sustained Akt activity after removal of SC79. (A) Serum-deprived HEK293 or NIH3T3 cells were treated with fresh SC79 (4 mg/ml) or SC79 pre-incubated in aqueous medium for 12 hr at 37°C or on ice. The levels of pAkt and pFoxo were analyzed after 30 min-drug treatment. **(B)** HeLa cells were treated with LY294002 (40 μM) and SC79 (4μg/ml) for 30 min. After removal of drug, cells were left in serum free medium and the levels of pAkt and pFoxo were analyzed in time course. **(C)** SC79 (100ng) was intravitreally injected into mouse eyes and the level of pAkt and pFoxo was analyzed in the retina on day 3. The retina from 1 hour after insulin (100 ng) injection serves as a positive control for Akt activation.

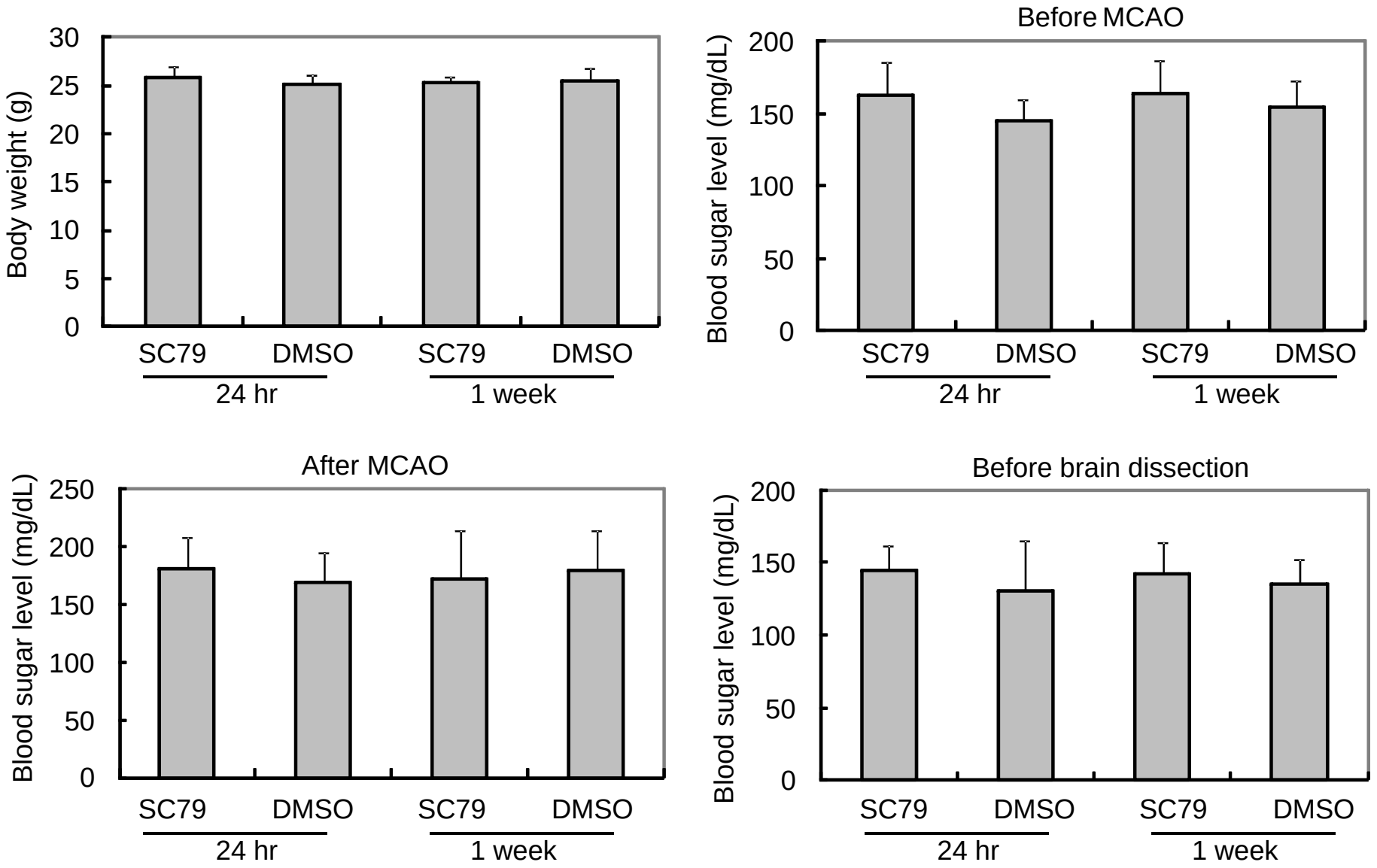

Figure S14. SC79 treatment does not alter the body weight and blood sugar level in experimental animals. SC79 was applied intravenously via tail vein injection at a concentration of 0.4 mg/g body weight. The body weight and blood sugar levels were measured at each indicated time points.